

**INVESTIGATION OF ANTIMICROBIAL AND NEMATICIDAL ACTIVITY OF
SECONDARY METABOLITES FROM *Armillaria* SPECIES**

JACKLYNE CHEPKEMOI

**A Thesis Submitted to the Graduate School in Partial Fulfilment of the Requirements for
the Master of Science Degree in Chemistry of Egerton University**


EGERTON UNIVERSITY

AUGUST, 2024

DECLARATION AND RECOMMENDATION

Declaration

This thesis is my original work and has not been presented in this University or any other for the award of a degree.


Signature  .Date.....05...08...2024.....

Jacklyne Chepkemoi

SM11/09076/20

Recommendation


This thesis has been submitted with our approval as university supervisors.

Signature ... Date...07...08...2024.....

Prof. J. C. Matasyoh, PhD.

Chemistry Department,

Egerton University, Njoro, Kenya

Signature... Date...07...08...2024.....

Prof. Dr. Marc Stadler, PhD.

Microbial Drugs Department,

Helmholtz Center for Infection Research, Braunschweig, Germany

COPYRIGHT

© 2024, Jacklyne Chepkemoi

All rights reserved. No part of this thesis may be produced, stored in a retrieval system or transmitted in any form or by any means, photocopying, scanning, recording or otherwise, without the permission of the author or Egerton University.

DEDICATION

This thesis is dedicated to my family and friends for their love and support throughout my study.

ACKNOWLEDGEMENTS

I thank the almighty God for His protection and blessings throughout my entire research period. I am thankful to Egerton University, especially chemistry department and Helmholtz Center for Infectious Research (HZI), Braunschweig, Germany for allowing me to use their facilities to achieve the objectives of my study. I sincerely thank my supervisors Prof. Josphat C. Matasyoh and Prof. Dr. Marc Stadler for the excellent supervision and guidance during my research. My heartfelt gratitude goes to Mr. Sebastian Pfutze and Ms. Winnie Chemutai Sum for their guidance in the laboratory work at HZI. Special thanks to Ms. Rita Toshe, Ms. Didsanutda Gonkhom, Ms. Divina Kwamboka, Ms. Winnie Maritim, Ms. Teresia Nduati, Ms. Lucy Wanga, Mr. David Muthama, Mr. Morris C. Waweru and Ms. Hellen Gathiru for their support towards some laboratory experiments. Finally, I sincerely thank my family for providing me their support and encouragement throughout my study.

ABSTRACT

Infectious diseases caused by pathogens are the leading cause of death for both adults and children. These diseases are responsible for 18.4 % fatalities worldwide. The widespread of the infectious diseases caused by these pathogens arises due to antimicrobial drug resistance. Plant-parasitic nematodes are responsible for approximately 80% of vegetable output loss in Kenya. They have also caused havoc on agriculture throughout the world, jeopardizing agriculture's long-term viability. Currently, control of nematodes relies on synthetic nematicides, which unfortunately causes environmental and ecological pollution and threatens human health. The development of antimicrobial drug resistance and the safety hazards of synthetic nematicides have triggered a great research effort towards natural products. In this study, antimicrobial and nematicidal activities of bioactive secondary metabolites from *Desarmillaria ectypa* (MUCL 31078), *A. gallica* (STMA 12242) and *A. mellea* (STMA 12328) were studied. The three fungal strains were obtained from Helmholtz Centre for infection research (HZI). Subculturing was done on YM 6.3 media and fermented on rice and Q6^{1/2} media. The metabolites from Q6^{1/2} media were extracted with Ethyl acetate solvent and ethyl acetate crude extract was obtained. The metabolites from rice media were extracted with methanol solvent and methanol crude extract was obtained. The methanol extract was subjected to liquid-liquid partitioning using hexane and ethyl acetate solvents where hexane and ethyl acetate crude extracts were obtained. The ethyl acetate crude extracts from rice and Q6^{1/2} media were then purified using Prep-high performance liquid chromatography. Nuclear magnetic resonance and high-resolution electrospray ionization mass spectrometry was used to obtain the structures of the pure compounds. One new compound, (**3**) alongside four known compounds, armillaridin (**1**), arnamiol (**2**), diatretol (**4**) and 3-chloro-6-hydroxy-4-methoxy-2-methylbenzoic acid (**5**) were isolated from *D. ectypa*. The known compounds, 5'-O-methylmelledonal (**6**), Melledonal C (**7**), 10 α -hydroxydihydromelleolide (**8**) and melledonal (**9**) were isolated from *A. mellea*. Lepistamide B (**10**), which is also a known compound was isolated from *A. gallica*. The compounds were tested for antimicrobial and nematicidal activity in which a weak activity was observed against *S. aureus* (ATCC 25923) and *E. coli* (ATCC 25922). The compounds did not show nematicidal activity. Armillaridin (**1**) was active against *Mucor hiemalis* (DSM 2656) at 33.3 μ g/mL and *Bacillus subtilis* (DSM 10) at 8.3 μ g/mL. The study provides potential leads of antimicrobials from *Armillaria* species.

TABLE OF CONTENTS

DECLARATION AND RECOMMENDATION	ii
COPYRIGHT	iii
DEDICATION.....	iv
ACKNOWLEDGEMENTS	v
ABSTRACT.....	vi
LIST OF FIGURES	xii
LIST OF TABLES	xiv
LIST OF ABBREVIATIONS AND ACRONYMS	xv
CHAPTER ONE	1
INTRODUCTION.....	1
1.1 Background information	1
1.2 Statement of the problem.....	2
1.3 Objectives	2
1.3.1 General objective	2
1.3.2 Specific objectives	2
1.4 Research questions.....	3
1.5 Justification.....	3
CHAPTER TWO	4
LITERATURE REVIEW	4
2.1 Introduction to fungi	4
2.2 Phylum Basidiomycota	4
2.3 Genus <i>Armillaria</i>	4
2.4 Species in the genus <i>Armillaria</i>	5
2.4.1 <i>Armillaria gallica</i>	5
2.4.2 <i>Desarmillaria ectypa</i>	6
2.4.3 <i>Armillaria mellea</i>	7

2.8 Secondary metabolites isolated from <i>Armillaria</i> species.....	8
2.9 Fungal pathogens in humans.....	10
2.10 Bacterial pathogens in humans	10
2.10 Plant parasitic nematodes and control.....	11
2.12 Life cycle of plant parasitic nematodes	12
2.13 Fungal secondary metabolites.....	12
CHAPTER THREE.....	14
MATERIALS AND METHODS	14
3.1 Sampling site and preparation of the fungal strains.....	14
3.2 Fermentation of fungal strains on solid media.....	14
3.3 Fermentation of fungal strain on liquid media.....	15
3.4 Extraction of secondary metabolites from rice media	15
3.5 Extraction of secondary metabolites from liquid media	15
3.6 Purification of fungal secondary metabolites	16
3.6.1 Purification of secondary metabolites of <i>D. ectypa</i> on rice media	16
3.6.2 Purification of secondary metabolites of <i>D. ectypa</i> on liquid media.....	16
3.6.3 Purification of secondary metabolites of <i>A. gallica</i> and on rice media	17
3.6.4 Purification of secondary metabolites of <i>A. mellea</i> on rice media	17
3.7 Antibacterial assay.....	17
3.8 Data analysis	18
CHAPTER FOUR.....	20
RESULTS AND DISCUSSION	20
4.1 Morphological characteristics of the fungal strains	20
4.2 Antibacterial and nematocidal activity of crude extracts and pure compounds	21
4.3 Chemical structures of the isolated compounds from the study	23
4.3 Structure elucidation of isolated compounds from <i>Desarmillaria ectypa</i>	24
4.3.1 Structure elucidation of compound 1	24

4.3.2 Structure elucidation of compound 2	29
4.3.3 Structure elucidation of compound 3	34
4.3.4 Structure elucidation of compound 4	39
4.3.5 Structure elucidation of compound 5	44
4.4 Structure elucidation of isolated compounds from <i>Armillaria mellea</i>	48
4.4.1 Structure elucidation of compound 6	48
4.4.2 Structure elucidation of compound 7	53
4.4.3 Structure elucidation of compound 8	58
4.4.4 Structure elucidation of compound 9	63
4.5 Structure elucidation of isolated compound(s) from <i>Armillaria gallica</i>	68
4.5.1 Structure elucidation of compound 10	68
4.6 Discussion.....	73
4.6.1 Characterization and bioactivity of the secondary metabolites.....	73
CHAPTER FIVE	76
CONCLUSIONS AND RECOMMENDATIONS	76
6.1 Conclusions.....	76
6.2 Recommendations.....	76
REFERENCES	77
APPENDICES	83
Appendix 1: ¹ H-NMR spectrum of compound 1	83
Appendix 2: ¹³ C-NMR spectrum of compound 1	83
Appendix 3: HMBC spectrum of compound 1	84
Appendix 4: HSQC spectrum of compound 1	84
Appendix 5: COSY spectrum of compound 1	85
Appendix 6: ¹ H-NMR spectrum of compound 2	85
Appendix 7: ¹³ C-NMR spectrum of compound 2	86
Appendix 8: HMBC spectrum of compound 2	86

Appendix 9: HSQC spectrum of compound 2	87
Appendix 10: COSY spectrum of compound 2	87
Appendix 11: ¹ H-NMR spectrum of compound 3	88
Appendix 12: ¹³ C- NMR spectrum of compound 3	88
Appendix 13: HMBC spectrum of compound 3	89
Appendix 14: HSQC spectrum of compound 3	89
Appendix 15: COSY spectrum of compound 3	90
Appendix 16: NOESY spectrum of compound 3	90
Appendix 17: ¹ H-NMR of compound 4	91
Appendix 18: ¹³ C-NMR spectrum of compound 4	91
Appendix 19: HMBC spectrum of compound 4	92
Appendix 20: HSQC spectrum of compound 4	92
Appendix 21: COSY spectrum of compound 4	93
Appendix 22: ¹ H-NMR spectrum of compound 5	93
Appendix 23: HSQC spectrum of compound 5	94
Appendix 24: HMBC spectrum of compound 5	94
Appendix 25: COSY spectrum of compound 5	95
Appendix 26: ¹ H-NMR spectrum of compound 6	95
Appendix 27: ¹³ C-NMR spectrum of compound 6	96
Appendix 28: HMBC spectrum of compound 6	96
Appendix 29: HSQC spectrum of compound 6	97
Appendix 30: COSY spectrum of compound 6	97
Appendix 31: ¹ H-NMR Spectrum of compound 7	98
Appendix 32: ¹³ C-NMR Spectrum of compound 7	98
Appendix 33: HMBC Spectrum of compound 7	99
Appendix 34: HSQC Spectrum of compound 7	99
Appendix 35: COSY Spectrum of compound 7	100

Appendix 36: ^1H -NMR spectrum of compound 8	100
Appendix 37: ^{13}C -NMR spectrum of compound 8	101
Appendix 38: HMBC spectrum of compound 8	101
Appendix 39: HSQC spectrum of compound 8	102
Appendix 40: ^1H -NMR Spectrum of compound 9	102
Appendix 41: ^{13}C -NMR Spectrum of Compound 9	103
Appendix 42: HMBC Spectrum of Compound 9	103
Appendix 43: HSQC spectrum of Compound 9	104
Appendix 44: COSY Spectrum of Compound 9	104
Appendix 45: ^1H -NMR Spectrum of Compound 10	105
Appendix 46: ^{13}C -NMR Spectrum of Compound 10	105
Appendix 47: HMBC Spectrum of Compound 10	106
Appendix 48: HSQC Spectrum of Compound 10	106
Appendix 49: COSY Spectrum of Compound 10	107
Appendix 50: A copy of research Permit	108
Appendix 51: Publication	109

LIST OF FIGURES

Figure 2.1: A photo of <i>Armillaria gallica</i>	6
Figure 2.2: A photo of <i>Desarmillaria ectypa</i>	7
Figure 2.3: A photo of <i>Armillaria mellea</i>	7
Figure 2.4: Secondary metabolites from <i>Armillaria</i> species.....	9
Figure 2.5: Life cycle of plant parasitic nematodes	12
Figure 3.1: A flow chart of the methodology summarising media preparation, subculturing, fermentation, extraction, purification of fungal secondary metabolites and bioassays ...	14
Figure 4.1: A photo of <i>Desarmillaria ectypa</i> on Y.M 6.3 media	20
Figure 4.2: A photo of <i>Armillaria gallica</i> on Y.M 6.3 media.....	20
Figure 4.3: A photo of <i>A. mellea</i> on YM media	21
Figure 4.4: Disc diffusion agar assay of pure compounds (1, 2, 4-10) against <i>E. coli</i> (ATCC 25922) and <i>S. aureus</i> (ATCC 25923). A and B shows the bioactivity of the pure compounds against test microorganisms and C shows the positive control (Chloramphenicol) against the test microorganisms.....	22
Figure 4.5: Chemical structures of the isolated compounds.....	23
Figure 4.6: Mass spectrum of compound 1 . A showing liquid (LC) chromatogram with the retention time. B showing the UV spectrum of the compound. C showing the molecular ion mass in positive mode and D showing the molecular on mass in the negative mode	24
Figure 4.7: Structure of compound 1 with and without HMBC, COSY correlations.....	28
Figure 4.8: Mass spectrum of compound 2 . A showing liquid (LC) chromatogram with the retention time. B showing the UV spectrum of the compound. C showing the molecular ion mass in positive mode and D showing the molecular on mass in the negative mode	29
Figure 4.9: Structure of compound 2 without and with HMBC, COSY correlations.....	33
Figure 4.10: Mass spectrum of compound 3 . A showing liquid (LC) chromatogram with the retention time. B showing the UV spectrum of the compound. C showing the molecular ion mass in positive mode and D also showing the molecular on mass in the positive mode	34
Figure 4.11: Structure of compound 3 with and without HMBC, COSY corrections.....	38
Figure 4.12: Mass spectrum of compound 4 . A showing liquid (LC) chromatogram with the retention time. B showing the UV spectrum of the compound. C showing the molecular	

ion mass in positive mode and D showing the molecular on mass in the negative mode.	39
Figure 4.13: Structure of compound 4 with and without HMBC, COSY corrections.....	43
Figure 4.14: Mass spectrum of compound 5 . A showing liquid (LC) chromatogram with the retention time. B showing the UV spectrum of the compound. C showing the molecular ion mass in positive mode and D showing the molecular on mass in the negative mode	44
Figure 4.15 : Structure of compound 5 with and without HMBC and COSY correlations....	47
Figure 4.16: Spectrum of compound 6 . A showing the UV spectrum and B showing the molecular ion mass in positive mode.....	48
Figure 4.17: Structure of compound 6 with and without HMBC, COSY corrections.....	52
Figure 4.18 : Spectrum of compound 7 . A showing the UV spectrum and B showing the molecular ion mass in positive mode.....	53
Figure 4.19: Structure of compound 7 with and without HMBC, COSY correlations.....	57
Figure 4.20: Spectrum of compound 8 . A showing the UV spectrum and B showing the molecular ion mass in positive mode.....	58
Figure 4.21: Structure of compound 8 with and without HMBC correlations	62
Figure 4.22: Spectrum of compound 9 . A showing the UV spectrum and B showing the molecular ion mass in positive mode.....	63
Figure 4.23: Structure of compound 9 with and without HMBC correlations	67
Figure 4.24: Mass spectrum of compound 10 . A showing liquid (LC) chromatogram with the retention time. B showing the UV spectrum of the compound. C showing the molecular ion mass in positive mode and D showing the molecular on mass in the negative mode.	68
Figure 4.25: Structure of compound 10 with and without HMBC, COSY correlations.....	72

LIST OF TABLES

Table 4.1: Minimum inhibitory concentrations (MIC in $\mu\text{g/mL}$) assays of compounds 1 , 6 and 7	21
Table 4.2: NMR data of compound 1	25
Table 4.3: NMR data of compound 2	30
Table 4.4 : NMR data table of compound 3	35
Table 4.5: NMR data of compound 4	40
Table 4.6: NMR data of compound 5	45
Table 4.7: NMR data of compound 6	49
Table 4.8 : NMR data of compound 7	54
Table 4.9: NMR data of compound 8	59
Table 4.10: NMR data of compound 9	64
Table 4.11: NMR data of compound 10	69

LIST OF ABBREVIATIONS AND ACRONYMS

COSY	Correlation Spectroscopy
DMSO	Dimethyl Sulfoxide
ESKAPE	<i>Enterococcus faecium</i> , <i>Staphylococcus aureus</i> , <i>Klebsiella pneumoniae</i> , <i>Acinetobacter baumannii</i> , <i>Pseudomonas aeruginosa</i> , and <i>Enterobacter</i> species
HMBC	Heteronuclear Multiple Bond Correlation
HRESIMS	High-Resolution Electrospray Ionization Mass Spectroscopy
HSQC	Heteronuclear Single Quantum Coherence
LCMS	Liquid- Chromatography Mass Spectrometry
LD	Lethal Dose
NMR	Nuclear Magnetic Resonance
NOESY	Nuclear Overhauser Effect Spectroscopy
PREP-HPLC	Preparative High-Performance Liquid Chromatography
YM	Yeast Malt

CHAPTER ONE

INTRODUCTION

1.1 Background information

Antimicrobial resistance is currently a major global public health concern despite the discovery of various natural and synthetic antimicrobial medications capable of eliminating hazardous microbes (Yamaç & Bilgili, 2006). The abuse and misuse of these therapies have been blamed for the antimicrobial resistance crisis. This situation is further exacerbated by a lack of new medication research due to limited economic incentives and difficult regulatory restrictions within the pharmaceutical industry. Due to this, microbial responses to conventional therapy have been ineffective, which may increase the risk of death, lengthen sickness, and increase medical costs (Alara & Alara, 2024). As a result, scientists are constantly looking for new antimicrobial drugs derived from various biological sources. Fungi have been found to contain antibiotics used in clinical treatment (order Actinomycetes). Although essential antibiotics such as penicillin are well established, the presence of antibiotics in mushrooms is less documented, making it more difficult to discover new antibiotics with various structural types (Wasser, 2011). Mushrooms require antifungal and antibacterial chemicals to thrive in their natural environment. As a result, antimicrobial chemicals isolated from various mushroom species may benefit humans (Yamaç & Bilgili, 2006).

Plant pathogenic nematodes have wreaked havoc on various commercially important crops. Agriculture suffers because of worm infestation. They are expected to cost the world \$78 billion in crop losses per year, with a 10-15% loss in crop productivity (Lima *et al.*, 2017). Stunted growth, enlarged roots that develop into root-knot galls, and roots that are two to three times the diameter of healthy roots are all symptoms of infection. Historically, pesticide drugs were the most common control method to manage parasitic nematodes that harm plants.

Chemical byproducts of these substances have also polluted soil and water, harming beneficial organisms such as soil worms (Castañeda-Ramírez *et al.*, 2020). Concerns about these pesticides have reignited interest in biological management as a more environmentally friendly method of preventing nematode damage. Because of their high nutritional content and non-poisonous nature, fungi have a long and well-documented history of being used for food and traditional medical reasons (Sośnicka *et al.*, 2018). Divisional fungi that produce mushroom Basidiomycota have long been recognized as prolific producers of structurally diverse and frequently beneficial secondary metabolites (Gressler *et al.*, 2021). Despite receiving far less attention in biologically active metabolites than the Ascomycota division,

several important lead compounds have already been discovered, leading to clinical development candidates and even marketed drugs and agrochemicals (Sandargo *et al.*, 2019). As a result, the proposed research seeks to identify metabolites found in *Armillaria* species of the Basidiomycota division as a potential source of novel and effective nematicidal and antibacterial compounds.

1.2 Statement of the problem

One of the most important health challenges of today is antimicrobial drug resistance. The prolonged usage and improper handling of the available antibiotics on the market are to blame for this issue. The spread of infectious diseases has increased because of antimicrobial medication resistance, which accounts for about 18.4% of all worldwide fatalities. Furthermore, it is not surprising that a sizable portion of people, particularly those in developing countries, are using naturally available bioactive alternatives for their primary healthcare given the numerous drawbacks and side effects associated with current antimicrobial drugs. Naturally available bioactive metabolites have attracted researchers to explore natural resources for alternatives. On the other hand, Nematodes have wreaked havoc on crops, resulting in lower agricultural output. According to research, nematodes can cause yield losses of up to 90% under ideal environmental conditions. Synthetic nematicides play a major role in the control of these parasitic nematodes. While synthetic nematicides can be useful in some situations, their widespread use has had a severe impact on the environment and human health. Because of this, over the past few years, their use has drastically decreased, and there is now a higher need for environmentally friendly alternatives. The threat to human health and food supply has piqued the interest of researchers, who are hoping to come up with practical solutions. Therefore, there is a need to put more effort in investigating new drugs to help reduce antimicrobial resistance and pollution of nematicides to the environment, to offset the losses caused by these nematodes and bacteria. Natural bioactive secondary metabolites offer intriguing drug development opportunities, even though they are yet to be fully explored.

1.3 Objectives

1.3.1 General objective

To explore the bioactive secondary metabolites from *Armillaria* species for antimicrobial and nematicidal activities

1.3.2 Specific objectives

- i. To characterize crude extracts from *Armillaria* species for nematicidal and antimicrobial activities

- ii. To determine the bioactivity of the pure compounds from *Armillaria* species for antimicrobial and nematicidal activities
- iii. To elucidate the chemical structures of the pure bioactive secondary metabolites from *Armillaria* species

1.4 Research questions

- i. How can the crude extracts from *Armillaria* species be characterized for nematicidal and antimicrobial activities?
- ii. Do the pure compounds from *Armillaria* species show antimicrobial and nematicidal activities?
- iii. Can the chemical structures of the bioactive secondary metabolites from *Armillaria* species be elucidated?

1.5 Justification

The increased infections caused by bacterial infections and the heavy losses incurred in agriculture summons the need for more effective drugs and nematicides. The production of secondary metabolites by fungi have been shown to be prolific, and several key lead compounds have already been found. These discoveries have produced clinical development candidates and even commercially available medications and agrochemicals. Therefore, the use of natural products in drug discovery is one promising alternative. This is because it has the potential to provide a reproducible source of bioactive compounds that are resilient to antimicrobial resistance as well as being environmentally friendly. To withstand the hostility of their natural environment, fungi accumulate antibacterial and antifungal secondary metabolites. They have thus been demonstrated to be a significant but unexplored source of new antibacterial drugs. Thus, compounds with strong antimicrobial and nematicidal activities can be isolated from fungi. Secondary metabolites from the fungi *Armillaria* species are a potential source of antimicrobial and nematicidal drug compounds. Therefore, this study aims to investigate more bioactive secondary metabolites from *Armillaria* species against selected human pathogens and nematodes to overcome the problem of antimicrobial drug resistance and nematicide pollution in the environment. The study also contributes to sustainable development goals (SDGs) which includes; a tight food security and a better health care system.

CHAPTER TWO

LITERATURE REVIEW

2.1 Introduction to fungi

Fungi are an excellent candidate for bioactive metabolite production because they are the most diverse, abundant group on the planet, and they resemble the animal system. Some fungi can accumulate a variety of secondary metabolites in their fruiting bodies, including organic acids, alkaloids, terpenoids, steroids, phenolic compounds, and (He *et al.*, 2022). These compounds have potential applications in a wide range of sectors, including food, medicine, and cosmetics. The current taxonomic classification of the kingdom fungi recognizes six phyla: Phylum Basidiomycota, Phylum Ascomycota, Phylum Glomeromycota, Phylum Blastocladiomycota, Phylum Chytridiomycota, and Phylum Neocallimastigomycota. Basidiomycota is one of the major phyla and more than 40,000 species have been described from the phyla (Naranjo-Ortiz & Gabaldón, 2019).

2.2 Phylum Basidiomycota

Basidiomycota is a large and diverse phylum of fungi, composed of filamentous hyphae. *Armillaria* species are classified under this phylum. Most species in this division reproduce sexually with a basidium that usually produces basidiospores. Both edible and wild mushrooms belong to this division (Liu *et al.*, 2022). Mushroom-forming fungus, jelly fungi, yeasts, rusts, and smuts are only a few of the 30,000 known species of Basidiomycota. Numerous ecological functions are performed by these fungi. By developing mycorrhizal symbioses with trees and shrubs, as well as by decomposing wood and leaf litter, many mushroom-forming species contribute to the ecology of forests (Dyshko *et al.*, 2024).

In relation to modern medicine, wild mushrooms, particularly basidiomycetes, constitute a significant and potential source of bioactive metabolites with a variety of pharmacological actions including immunostimulatory, anti-inflammatory, antiviral, antioxidant, fungicidal, and antitumoral. Fungal terpenoids such bisabolane sesquiterpenes cheimonophyllons from the culture of *Cheimonophyllum candidissimum* basidiomycete showed nematicidal activity against *C. elegans* (Li *et al.*, 2007). Therefore, the phylum Basidiomycota is a great potential source of bioactive antibacterial and nematicidal compounds.

2.3 Genus *Armillaria*

Many of the largest terrestrial species that cause enormous losses in a variety of habitats are found in the fungal genus *Armillaria*, which includes necrotrophic diseases. However, it is unclear how these organisms became pathogenic in a group that mostly consists of non-

pathogenic wood degraders (Sahu *et al.*, 2023). It descends from the Latin word *Armillaria* meaning a bracelet, a bangle, or an epaulette, which relates to a characteristic of most *Armillaria* species, a broad, persistent, skin-like ring attached to the upper part of the stipe (Sośnicka *et al.*, 2018). About 35 species of parasitic fungi belonging to the family Physalacriaceae (order Agaricales) are found in northern North America and Europe, mostly in hardwood or mixed coniferous forests. Members of this genus can live for hundreds of years under the right environmental circumstances, and some species have even been named among the largest and oldest living organisms (Coetzee *et al.*, 2018). *Armillaria* has been reported to cause root rot disease, which affects ornamental and natural trees and shrubs of several species. The literature shows that most of the *Armillaria* genus species tend to grow from a single fertilized spore and spread vegetatively in the forestry regions that contain great content of organic matter and are sufficient in humidity.

2.4 Species in the genus *Armillaria*

More than fifty *Armillaria* species have been described and the most virulent species that have been reported include *Armillaria mellea* and *A. ostoyae*. According to the research that has been conducted around the world, *Armillaria mellea* is virulent on forest trees, fruit and nut crops, and urban trees. Many cultivated and wild coniferous trees as well as fruit trees have been documented to die in North America and Europe due to *A. ostoyae* (Devkota & Hammerschmidt, 2020). A few *Armillaria* species that are present throughout the world were unintentionally introduced by humans when moving contaminated plant resources.

Several techniques can be employed by *Armillaria* species to get new food supplies. Additionally, they all demonstrate saprotrophic abilities and can take advantage of various types of dead wood (Heinzelmann *et al.*, 2019). *Armillaria* species are essential contributors to the ecosystem's carbon cycle since they are saprophytes. Some *Armillaria* species are also significant root and butt rot pathogens of woody plants worldwide, causing mortality and reduction in forests. The species have also been described to be constitutively luminescent in the dark, under environmental illumination. *Armillaria gallica* luminescence is enhanced, but luminescence in *Armillaria mellea* and *Desarmillaria tabescens* is reduced (Mihail & Bruhn, 2007). It is thought that bioluminescent fungi attract fungivorous invertebrates to aid spore dispersal.

2.4.1 *Armillaria gallica*

The fungus *Armillaria gallica* (Basidiomycota, Physalacriaceae) is a subterranean fungus that produces fruit bodies up to 10 cm in diameter, yellow-brown, and covered in tiny scales. The stem can grow to be up to 10 cm long, with a ring that divides the color of the stem

into pale orange to brown on top and a lighter color on the bottom. Gills that range from white to creamy or pale orange can be found on the underside of the caps.

The fungus can form a complex network of underground root-like structures (rhizomorphs) that aid in the decomposition of dead wood in temperate broadleaf and mixed forests. *Armillaria gallica* prefers warmer lowland habitats in the oak and alluvial forests and spreads to higher elevations along rivers and streams (Antonín *et al.*, 2009)



Figure 2.1: A photo of *Armillaria gallica*

Source: <https://www.dreamstime.com/photos-images/Armillaria-gallica.html>

2.4.2 *Desarmillaria ectypa*

The fungus *Desarmillaria ectypa*, also known as marsh honey fungus, is a saprotrophic species that grows on wet ground, peat, and in the presence of *Sphagnum* species and herbaceous plants as well as decaying sedge tufts like the *Carex rostrata* (Stasinska, 2015). Recently, the species was moved to the subgenus *Desarmillaria* in which it has been described to accommodate the exannulate mushroom forming armillarioid species (Koch *et al.*, 2017).

The cap can grow to be 10 cm in diameter and is initially convex before flattening and developing a depressed center with age. The cap has a slightly curved margin and is frequently striated, allowing the gills to be seen through the thin structure. The gills are narrow and decurrent, beginning whitish and progressing to cream, buff, or pinkish. Dark brown and scaly in the center. The remainder of the cap is yellowish-brown to brown, paler when dry, and darker when wet. The stem can grow up to 10 cm tall, cylindrical, and swollen at the base. It matches the cap in color. Marsh honey fungus grows in wet habitats such as actively raised bogs, alkaline fens, and transitional and low Aapa mires. The species is distinguished by the absence of a ring on the stipe (Stasinska, 2015).



Figure 2.2: A photo of *Desarmillaria ectypa*

Source: <https://www.dreamstime.com/photos-images/Armillaria-ectypa.html>

2.4.3 *Armillaria mellea*

Commonly known as a honey mushroom, *Armillaria mellea* belongs to a diverse taxonomic group that includes the kingdom Fungi, division Basidiomycota, class Agaricomycetes, order Agaricales, and genus *Armillaria*. There are several ways to prepare the species (young fruiting bodies), which is deemed edible when properly cooked. Major caution should be exercised when preparing and consuming the honey mushroom because incidents of allergy to it have been documented, and some people may have digestive issues. (Sośnicka *et al.*, 2018). The species has medicinal properties and numerous studies have demonstrated its curative properties. The species has long been used to cure a wide range of ailments in Chinese herbal medicine, including headaches, hypertension, epilepsy, sleeplessness, neurasthenia, and many others. Its antihyperglycemic effects have also been demonstrated (Kostić *et al.*, 2017).



Figure 2.3: A photo of *Armillaria mellea*

Source: <https://www.dreamstime.com/photos-images/Armillaria-mellea.html>

2.8 Secondary metabolites isolated from *Armillaria* species

The species in the genus *Armillaria* have been known to produce compounds normally referred to as melleolides (**Figure 2.4**). This class of compounds consist of an orsellinic acid moiety esterified within a sesquiterpene protoilludene alcohol (Bohnert *et al.*, 2014). Based on where the double bond is located within the protoilludene backbone, melleolides can be categorized into three classes. Armillyl orsellinates are Δ^{2-4} -unsaturated, whereas melleolides are Δ^{2-3} -unsaturated. Armillanes are distinguished by the absence of a double bond within the six-membered ring (Pfütze *et al.*, 2023). Some of the compounds extracted from *A. mellea* with bioactivity include Armillyl orsellinate (**i**), Judeol (**ii**), Armillyl everniate (**iii**), Melleolide I (**iv**), Armillaribin (**v**), and Armillaricin (**vi**). Both compound (**i**) and compound (**ii**) exhibited antimicrobial activity against *Bacillus subtilis*, *Candida albicans*, *Escherichia coli* and *Staphylococcus aureus* on bioautographic assays (Cadelis *et al.*, 2020). Compound **iv** was shown to have an activity against *Cladosporium cucumerinum* and also active against gram positive bacterium (Midland *et al.*, 1982). The species *A. gallica* can produce sesquiterpenoid aryl esters (cyclobutene-containing metabolites) that are thought to inhibit the growth of antagonistic bacteria or fungi. Armillaritin (**vii**), Armillarillin (**viii**), Armimelleolide B (**ix**), and Armimelleolide A (**x**). All compounds were discovered to have antitumor activity (Lou *et al.*, 2022). The bioactivity of the compounds isolated from *Armillaria* suggests that they are a potential source of antimicrobials.

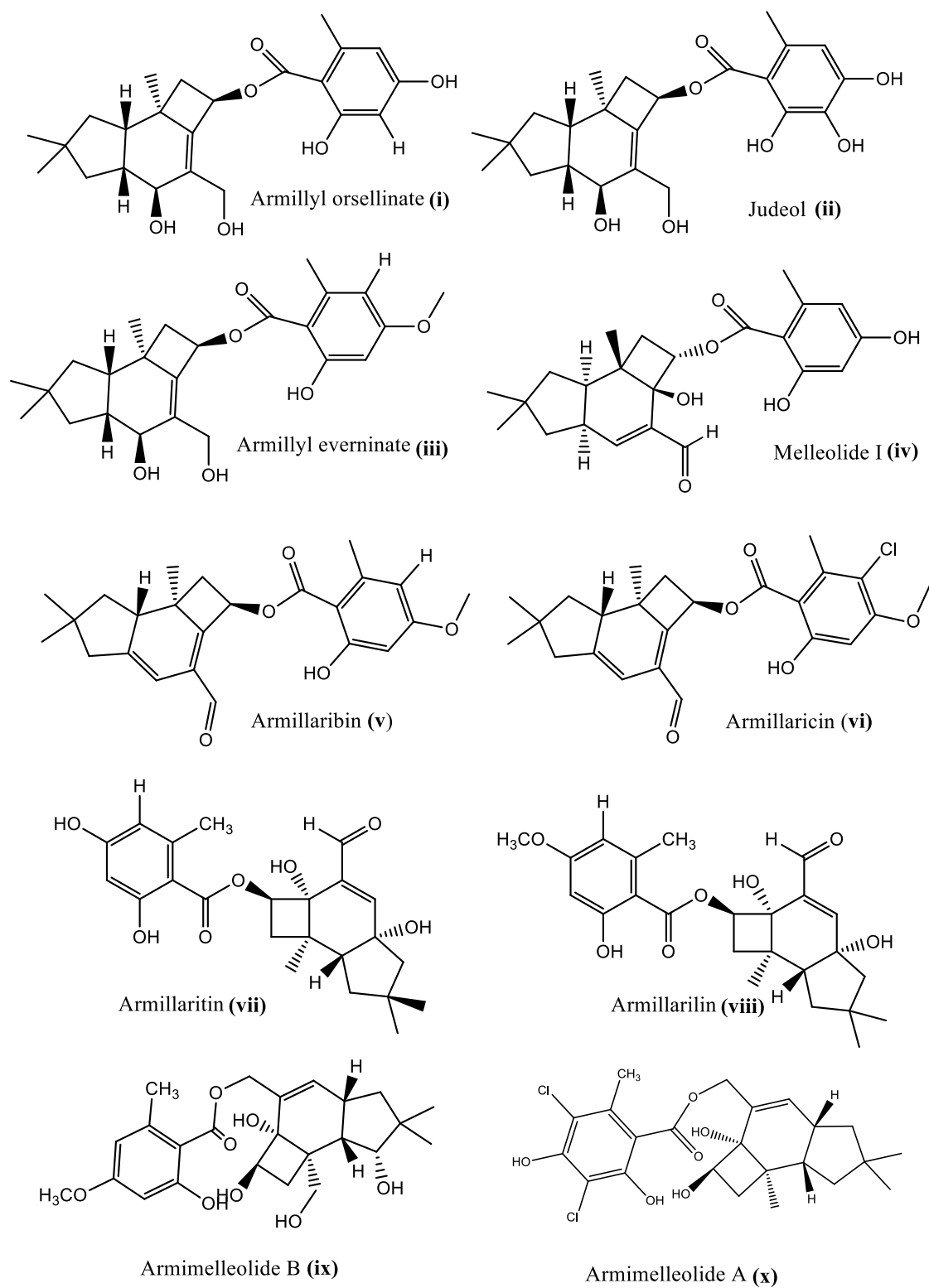


Figure 2.4: Secondary metabolites from *Armillaria* species

2.9 Fungal pathogens in humans

Fungal pathogens can cause life-threatening infections in both immunocompetent and immunocompromised people. Their devastating effects on human health worldwide go primarily unnoticed (Xie *et al.*, 2014). Pathogenic fungi infect billions of people every year, with over 1.5 million infections resulting in death. *Candida albicans*, *Cryptococcus neoformans*, and *Aspergillus fumigatus* are the three most common fungal pathogens, with *C. albicans* being the most common invasive fungal pathogen in humans (Xie *et al.*, 2017).

Candida albicans are a naturally occurring member of the human microbiota. However, it is capable of causing severe systemic infections in immunocompromised individuals, with mortality rates approaching 40% (Ciurea *et al.*, 2020). Despite currently available treatment options, estimated mortality rates for these invasive infections range from 20 to 95%, depending on the pathogen and patient population. Because fungi, like their human hosts, are eukaryotes, only a few drug targets can be used to selectively kill the pathogen while causing minimal host toxicity (Xie *et al.*, 2014).

2.10 Bacterial pathogens in humans

Protozoans, fungi, viruses, and mycobacteria play a minor role than bacteria in causing illnesses, which account for around 90% of all infections (Khan *et al.*, 2015). *Pseudomonas aeruginosa* is a gram-negative aerobic bacterium found in normal intestinal flora that is also a powerful pathogen classified as an ESKAPE (*Enterococcus faecium*, *Staphylococcus aureus*, *Klebsiella pneumoniae*, *Acinetobacter baumannii*, *Pseudomonas aeruginosa*, and *Enterobacter* species) organism that causes Intensive Care Unit (ICU)-acquired infections in critically ill patients. *Pseudomonas aeruginosa* is difficult to treat due to a variety of mechanisms that can contribute to its antibiotic resistance, including innate mechanisms like the over-expression of efflux pumps and decreased outer membrane permeability, as well as acquired mechanisms like the acquisition of resistance genes or mutation in genes encoding for porins and other proteins (Breijyeh *et al.*, 2020). *Pseudomonas aeruginosa* is responsible for 11% of all nosocomial infections, with high mortality and morbidity rates. Specifically, in immune-compromised individuals, *P. aeruginosa* is a gram-negative, non-fermenter bacterium that causes illnesses (Khan *et al.*, 2015).

Escherichia coli is a typical microbe that lives in the human gastrointestinal tract. However, some *E. coli* strains can lead to severe sickness in people, which results in a sizable number of fatalities each year. In Kenya, group B *Streptococci* and *Escherichia coli* strains were the main causes of bacteremia in children (Sum *et al.*, 2019).

2.10 Plant parasitic nematodes and control

Nematodes are among the world's most complex and numerous organisms (Ntalli *et al.*, 2020). They are a group of multicellular, translucent, thread-like, pseudocoelomate organisms that can live freely or as parasites on other living things (Shah & Mahamood, 2017). They belong to the phylum Nematoda, the second-largest group of Metazoa after arthropods, and the kingdom Animalia. Due to their inner and outer morphology, which allows them to adapt fast, they are widely distributed on Earth. Nematodes can attack and kill a wide range of organisms including animals, microorganisms, and plants. Plants with major agricultural and forestry importance have likely drawn the most interest among the species vulnerable to parasite infestations. They inflict an estimated \$78 billion in crop losses annually and, on average, crop production losses of 10 to 15 % (Carneiro *et al.*, 2017). This puts a strain on the sustainability of world food production. More than 5000 plant species are severely harmed by root-knot nematodes (*Meloidogyne* species), which feed with their styles on the roots of the plants. They thus represent one of the major obstacles to increased agricultural output worldwide. *Meloidogyne incognita*, *M. javanica*, and *M. arenaria* are some of the most economically harmful root-knot nematodes that infect a variety of plants, including those in the Solanaceae and Malvaceae families (Ntalli *et al.*, 2020). They are difficult to manage because root-knot nematodes are polyphagous, have a high reproductive capacity, and practically all their life cycle is contained within the host plant (Subedi *et al.*, 2020). Infected plants grow more slowly than healthy ones and have roots that are two to three times greater in diameter. These swollen roots eventually form the typical root-knot galls (Lu *et al.*, 2020).

Utilizing synthetic chemical compounds has become the most well-liked strategy for controlling plant parasitic nematodes in recent years. Despite being helpful in some circumstances, the extensive use of synthetic chemical nematicides has had negative effects on the environment and human health. As a result, their use for pest management in forestry and agriculture has significantly declined during the past few years. Due to the decline in the usage of synthetic chemical nematicides, there are now greater demands for environmentally benign alternatives. Biological control is a possible strategy for the management of nematode parasites. Biological agents include both living things and the waste products of their metabolism. Fungi, which are known to have a wide variety of metabolic pathways, have produced many key classes of industrial compounds, including many antibiotics used in medicine. About 60% of the described nematicidal chemicals from fungi were discovered and characterized for the first time. Such a high ratio implied that natural, unstudied fungal species and strains should contain a significant quantity of nematicidal chemicals. Because of their new

structures and nematicidal properties, secondary metabolites in fungi could hold great promise (Li *et al.*, 2007). There have been several fascinating discoveries of nematicidal chemicals from fungi, but no commercial product based on these compounds has yet been produced. However, several compounds that have been discovered from fungi are in trials. For instance, from the studies of Li *et al.* (2007), it has been demonstrated that omphalotin from the fungus *Omphalotus olearius* has nematicidal activity comparable to that of the widely used nematicide ivermectin. Therefore, compounds from fungi are a potential candidate for nematicidal drugs.

2.12 Life cycle of plant parasitic nematodes

Nematodes undergo six stages in their life cycle. These stages include the eggs, four juveniles and the adults (Figure 2.5) and they can overwinter at any of the stages (Kumar & Yadav, 2020). Depending on the type of nematode and the habitat, the majority of species lay between 50 and 500 eggs per female, however some can lay as many as 1,000 (Lima *et al.*, 2017). The second juvenile stage is an important stage because the plants infected begins to show signs of infection such as root gall developments (Kyndt *et al.*, 2013).

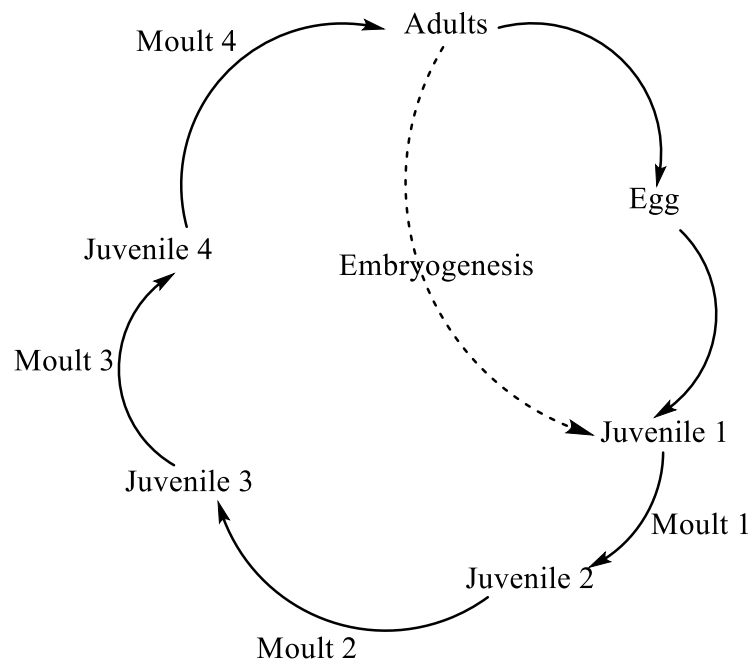


Figure 2.5: Life cycle of plant parasitic nematodes

2.13 Fungal secondary metabolites

Various secondary metabolites with varying structural compositions are produced by fungi. The antibacterial, anticancer, antioxidant and nematicidal capabilities of these secondary metabolites are inhibited. Due to their abundance of diverse classes of compounds, including sesquiterpenes, oxalic acid, epipolythiopiperazine-2,5 diones, quinolines, benzoic acid derivatives, terpenes, anthraquinones, cyclic peptides, steroids, and polysaccharides, fungi

from the divisions Basidiomycota and Ascomycota have undergone extensive study (Vallavan *et al.*, 2020). Fungal terpenoids have been reported to inhibit nematicidal activity. Examples of these terpenoids are the bisabolene sesquiterpenoids, cheimonophyllons from the cultures of *Cheimonophyllum candidissimum*. They showed activity against *C. elegans* with LD₅₀ between 10 and 100 µg (Li *et al.*, 2007). Therefore, fungal metabolites are a potential source of nematicidal compounds. Marasmane sesquiterpene isovelleral, is a key component of the chemical defense system against nematodes in the mushroom species, *Lactarius vellereus*. Isovelleral was shown to be active against *M. incognita* with LD₃₀ at 100 µg mL⁻¹ and against *C. elegans* at LD₅₀ at 50 µg mL⁻¹.

Sesquiterpenoids are the major constituents of the genus *Armillaria* fruiting bodies and mycelium in the literature. The sesquiterpenoids found in this species are members of the protoilludane derivatives group, including several compounds (Muszynska *et al.*, 2011). The strength of antimicrobial activity is determined by the number of carbon atoms in the molecule and the type of substituent. Melleolide was the first isolated sesquiterpene aryl ester from *A. mellea* that demonstrated antibiotic activity (Sośnicka *et al.*, 2018). Later, armillarin and armillaridin were isolated, and since then, more than 50 different sesquiterpenoids, including armillaricin, armillaribin, armillaririgin, and judeol, have been isolated (Cadelis *et al.*, 2020). Small-molecule natural compounds from *Armillaria* species have also been described aside from sesquiterpenoids. For instance, Diatretol, a modified diketopiperazine reported from *D. ectypa*, exhibits some effectiveness against the bacterium *Bacillus*. Another compound that was discovered in the basidiocarps of a Chinese *A. mellea* isolate is Armillaramide, a new sphingolipid (Baumgartner *et al.*, 2011).

CHAPTER THREE

MATERIALS AND METHODS

3.1 Sampling site and preparation of the fungal strains

The fungal strains were obtained from fungal collection unit in Helmholtz Centre for Infection research (HZI). The fungal strains were identified as *Desarmillaria ectypa* (MUCL 31078), *A. mellea* (STMA 12328) and *Armillaria gallica* (STMA 12242). The three fungal strains were subcultured on YM 6.3 media (malt extract 10 g/L, D-glucose 4 g/L, yeast extract 4 g/L and pH 6.3). The media was autoclaved and dispensed into petri dishes and allowed to cool under sterile conditions. Thereafter, the fungi were inoculated in triplicates into the petri dishes containing YM 6.3 media and incubated at room temperature. The pure cultures that were fully grown were fermented on solid and liquid media. The strain *D. ectypa* was fermented on both solid and liquid media while *A. gallica* and *A. mellea* was fermented only on solid media. Media preparation, Subculturing, fermentation, extraction, purification of secondary metabolites and bioassays are summarised in **figure 3.1**.

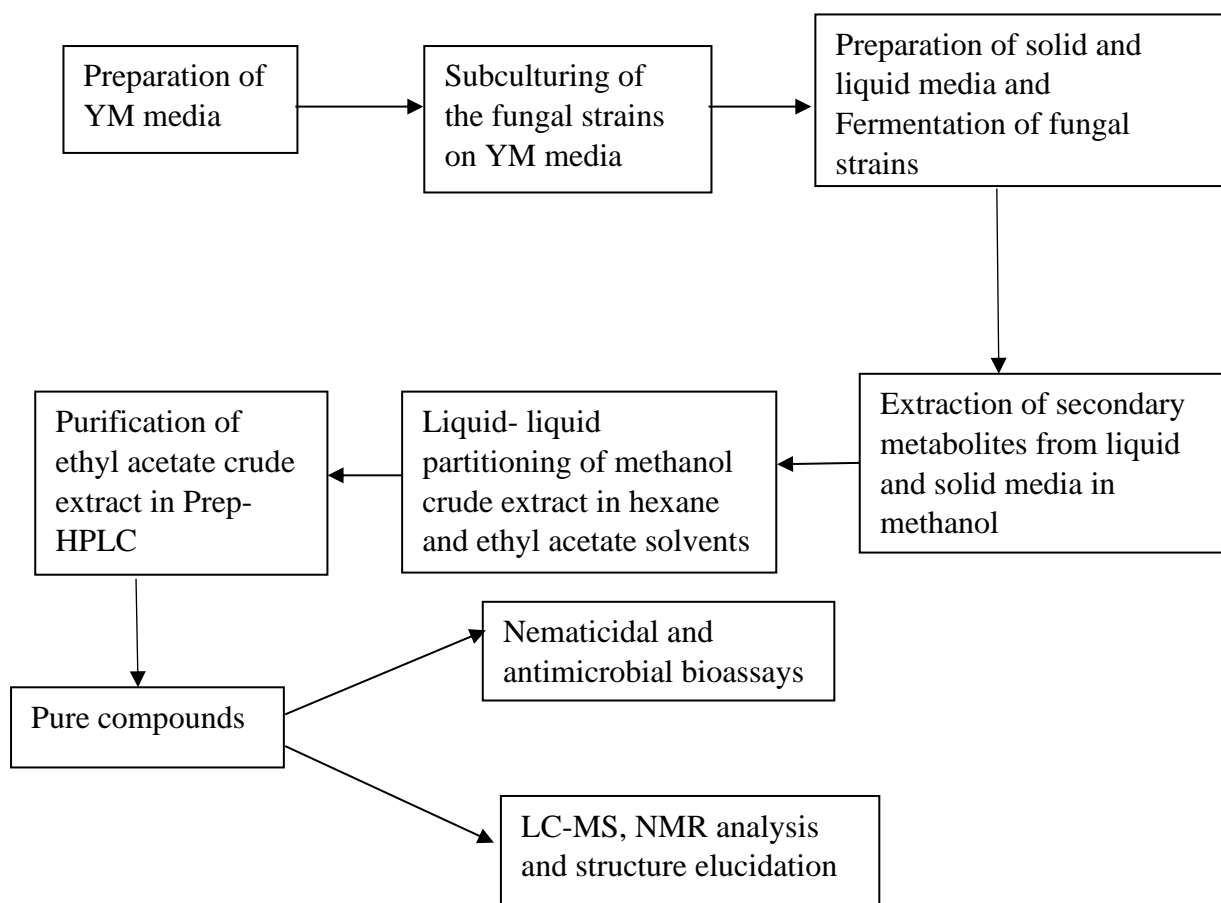


Figure 3.1: A flow chart of the methodology summarising media preparation, subculturing, fermentation, extraction, purification of fungal secondary metabolites and bioassays

3.2 Fermentation of fungal strains on solid media

Rice media was used in solid fermentation of the fungal strains. Fermentation was done in twenty 500 mL Erlenmeyer flasks. 90 g of rice was weighed and added into each flask containing 90 mL of distilled water and autoclaved twice at 121 °C for 20 mins and allowed to cool. Petri dishes containing the fully grown pure fungal cultures were selected for fermentation. On sterile conditions, a cork-borer of 7 mm was used to cut the fungal culture into several pieces and five plugs were inoculated into each flask containing sterile rice and incubated at 21 °C for 28 days. During the fermentation period the fungi was monitored, and fermentation was terminated after the fungi was fully grown on the media.

3.3 Fermentation of fungal strain on liquid media

The media that was used in liquid fermentation was Q6^{1/2} media. The media was prepared by weighing 5 g of D-glucose, 20 g of glycerine and 10 g of cottonseed flour. All the ingredients were stirred in 2 L of distilled water and pH was then adjusted to 7.2. The media was then autoclaved at 121 °C for 20 min. About 200 mL of the media was poured into twelve, 500 mL Erlenmeyer flasks. On sterile conditions, the petri dishes containing the pure cultures of *D. ectypa* were selected for fermentation. A cork borer of 5 mm was used to cut the fungal plugs into several pieces. Into each of the flask containing sterile liquid media, 5 plugs were inoculated and incubated in the shaker at 141 rpm at 23 °C for 21 days. During the fermentation period, glucose levels were regularly checked using Fehling's strips. Fermentation was terminated after 21 days, that is, when the glucose test was negative.

3.4 Extraction of secondary metabolites from rice media

The fermented fungal cultures in the flasks were crushed into small pieces and soaked in distilled methanol and ultrasonicated for two hours. Thereafter, the methanol extract was filtered and evaporated under a reduced pressure using the rotary evaporator to obtain the methanol crude extract. The crude extract was suspended in distilled water followed by sequential partitioning between hexane and ethyl acetate solvents. The extracts were evaporated to obtain hexane and ethyl acetate crude extracts respectively. The ethyl acetate crude extract proceeded to purification.

3.5 Extraction of secondary metabolites from liquid media

Three days after completion of glucose, mycelium was separated from the supernatant by filtering under a vacuum. The mycelium was extracted twice with acetone under an ultrasonic bath for 30 minutes. The acetone was evaporated, and the remaining aqueous extract was partitioned on a separating funnel with ethyl acetate at a 1:1 ratio with that of the aqueous phase. The ethyl acetate extract was dried by passing through anhydrous sodium sulphate and

evaporated. The supernatant was also partitioned using ethyl acetate at a 1:1 ratio with the aqueous phase. The organic portion of ethyl acetate was dried over anhydrous sodium sulphate and evaporated under a reduced pressure to obtain ethyl acetate crude extract that proceeded to purification.

3.6 Purification of fungal secondary metabolites

The ethyl acetate crude extracts of the fungal strains were purified in prep-HPLC using different methods of purification. The pure compounds that were obtained were subjected to liquid chromatography-mass spectroscopy (LC-MS) and Nuclear magnetic resonance (NMR) and their structures were thereafter elucidated.

3.6.1 Purification of secondary metabolites of *D. ectypa* on rice media

The ethyl acetate crude extract that was obtained after partitioning was further purified using preparative High-Performance Liquid Chromatography (prep-HPLC). The crude extract was first weighed and dissolved in acetone before injecting to the HPLC column. Gradient mode of separation was applied in the purification process. The column that was used was nucleodur C18 Htec, 250 mm × 40 mm, 10 µm and a flow rate of 40 mL/min. Acetonitrile and water were used as the mobile phases. These solvents were first filtered before running it in the HPLC column to prevent any particles present in the solvents from blocking the column. The solvents were prepared by adding 0.1% of Formic acid to 1 L of acetonitrile and 0.1% of Formic acid to 1 L of deionized distilled water. The gradient method that was used to purify the compounds was 5% ACN at 10 min intervals, 35% ACN at 35 min, 65% ACN at 45 min, 90% ACN at 70 min and 100% ACN at 75 min. The method of purification yielded four fractions of pure compounds namely Rn1F2, Rn1F11, Rn2F13, and Rn2F8F4. These pure compounds were dried and weighed and thereafter they were subjected to LCMS to obtain their masses and nuclear magnetic resonance (NMR). The NMR data was analysed using Mestre nova software and the structures of the pure compounds were elucidated.

3.6.2 Purification of secondary metabolites of *D. ectypa* on liquid media

The ethyl acetate crude extract from the supernatant was further purified using prep-HPLC. The crude extract was first weighed and dissolved in acetone before injecting into the HPLC column. Gradient mode of separation was applied during the purification process. The column that was used was Gemini C18, 250 mm × 10 mm, 10 µm and at a flow rate of 30 mL/min. Acetonitrile (ACN) and water (H₂O) were used as the mobile phases. The solvents were prepared by adding 0.1% of Formic acid to 1 L of acetonitrile and 0.1% of Formic acid to 1 L of deionized distilled water. The method that was used to purify the compounds was 15% ACN at 5 mins interval, 60% ACN at 50 min, and 100% ACN at 100 min. During

purification process, solvents were monitored, and the peaks were collected into the test tubes. The method of separation yielded four fractions in which only fraction three was pure. This fraction was dried and weighed. The pure compound was thereafter subjected to nuclear magnetic resonance (NMR) and LCMS. The NMR data was analysed, and the chemical structure of the pure compound was elucidated.

3.6.3 Purification of secondary metabolites of *A. gallica* and on rice media

The ethyl acetate crude extract that was obtained in liquid-liquid partitioning was further purified Prep-HPLC. The column that was used was Gemini C18 250×10 mm. The mobile phases were Methanol and water and the method of separation of the compounds used was gradient mode; 15% methanol at 0 mins, 65% methanol at 22 min, 100% methanol at 22.50 min, maintained at 100 % methanol for 10 min, and sharply decreasing to 15% methanol at in one min. Gradient method yielded five fractions (F1, F2, F3, F4 and F5). F5 was further subjected purification using isocratic method on a smaller column (Nucleodur polar Tec, 5 µm). One pure compound was obtained from this method of purification.

3.6.4 Purification of secondary metabolites of *A. mellea* on rice media

The ethyl acetate crude extract was purified using Prep-HPLC. The column that was used was Luna C18 250×21.2 mm, 5 µm. The solvents used were Acetonitrile as B and deionized water as A and the method of separation of the compounds used was gradient mode; 5% in 0 mins increasing to 100% B in 19 min and maintaining at 100 % B for 10 min and decreasing to 5% B in 16 min; flow rate 8 mL/min. The retention times and the UV patterns were monitored during purification. Gradient method yielded ten fractions (F1 to F10). Due to the amounts obtained F5 and F6 and F9 were further purified on isocratic method using the same column. From isocratic method, F5 (85 % Methanol) yielded one pure compound namely, AMF5A. F6 (75 % methanol) yielded three pure compounds namely AMF6B3, AMF6B4 and AMF6B5. F9 (50 % methanol) yielded one pure compound namely AM9.1. These pure compounds were thereafter subjected to LC-MS and NMR.

3.7 Antibacterial assay

Disc Agar diffusion assay method (Kajaria *et al.*, 2012) and serial dilution assay employed by method was used in testing the activity of the compounds against gram negative and gram positive bacteria and also against filamentous fungi. In disc agar diffusion assay, the ethyl acetate crude extracts and the pure compounds were tested against *E. coli* (ATCC 25922) and *S. aureus* (ATCC 25923). The compounds were prepared by dissolving in methanol and prepared to a concentration of 1 mg/mL. The bacterial cultures were prepared by first preparing the nutrient broth media. Nutrient broth was weighed to 0.65 g and dissolved in 50 mL of

distilled water and thereafter autoclaved at 121 °C for 15 minutes. The media was allowed to cool to room temperature and under sterile conditions, *E. coli* and *S. aureus* were inoculated into the broth using a sterile wire loop. The prepared cultures of *E. coli* and *S. aureus* were then incubated at 37 °C for 24 hrs. Muller Hinton Agar was weighed to 38 g and dissolved in 1 L of distilled water and thereafter autoclaved at 121 °C for 15 minutes. The media was thereafter dispensed into the sterile petri dishes under sterile conditions and allowed to cool. Sterile swabs were then dipped into the 24-hr old bacterial cultures and swabbed onto the Muller Hinton Agar. The sterile discs were then soaked in 40 µL of the pure compounds. The soaked discs were thereafter placed on the petri dishes of Muller Hinton Agar containing bacteria using sterile forceps. Chloramphenicol disc was used as a positive control and the sterile disc soaked in methanol as used as a negative control. The plates were refrigerated overnight to allow the extracts and the pure compounds to diffuse into the agar. They were later incubated at 37 °C for 24 hrs after which the diameter of the zones of inhibition were measured in millimetres using a ruler.

Minimum inhibitory concentrations (MICs) were determined against *B. subtilis* and *M. hiemalis* on serial dilution assay in 96-well microtiter plates according to the method described by Harms *et al.* (2021). Nystatin was used as positive control for *M. hiemalis* while Oxytetracycline was used as a positive control for *B. subtilis*. The compounds were prepared in acetone to a concentration of 1 mg/mL.

3.8 Data analysis

Mass spectrometry and NMR were used to identify pure compounds. The measurements of mass spectrometry and NMR were done in HZI. In mass spectrometry, HRESIMS (High-Resolution Electrospray Ionization Mass Spectroscopy) was used to obtain the molecular ion masses, adducts and molecular formula of the pure compounds. Deuterated methanol (CD₃OD), chloroform (CDCl₃) and acetone (CD₃)₂CO) was used in NMR spectroscopy. The internal standard used was tetramethyl silane (TMS), and the chemical shifts was given as parts per million (ppm). 1D and 2D NMR was used to show correlations between carbons and protons in the molecule. ¹H, ¹³C, HSQC, COSY and HMBC NMR spectra was obtained from NMR. ¹H NMR was used to determine the multiplicities of protons and the type of protons in the compounds. The ¹³C NMR spectrum was used to determine the total number of carbon atoms in the compound and to reveal the type of carbon in the compound. The Heteronuclear Single Quantum Coherence (HSQC) was used to determine the connectivity of hydrogen to their respective carbon atoms. ¹H-¹H COSY (Correlation spectroscopy) was used to identify spin-spin coupling interactions and provide information on protons attached to

adjacent carbons. The Heteronuclear Multiple Bond Correlation (HMBC) was used to identify proton-carbon connectivity up to three bonds away.

CHAPTER FOUR

RESULTS AND DISCUSSION

4.1 Morphological characteristics of the fungal strains

The fungal strains that were obtained from Helmholtz Centre for Infection research were subcultured on PDA and YM 6.3 media and the growth of the fungal strains were monitored. The two fungal strains differed on growth rate, color, mycelial features, and rhizomorphs. *Armillaria gallica* (STMA12242) was noted that the mycelia were pale brown in color and had short rhizomorphs that penetrated the media. The strain *Desarmillaria ectypa* (MUCL31078) was a fast-growing strain and had long rhizomorphs that penetrated the media and white mycelia that developed brown patches as it grew old. A deep red color was observed in the media in which *A. mellea* (STMA12328) was cultured. The mycelia appeared whitish with deep brown patches on it. **Figures 4.1-4.3** shows the morphological characteristics of the fungal strains grown on media.



Figure 4.1: A photo of *Desarmillaria ectypa* on Y.M 6.3 media



Figure 4.2: A photo of *Armillaria gallica* on Y.M 6.3 media.

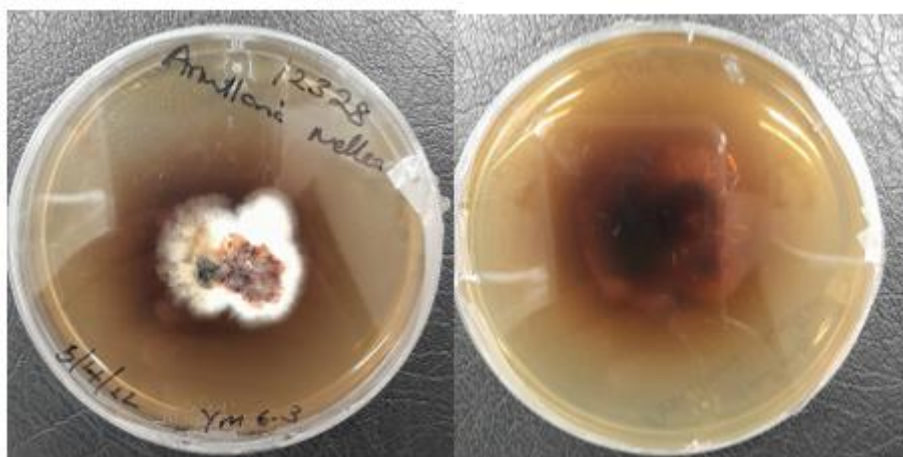


Figure 4.3: A photo of *A. mellea* on YM media

4.2 Antibacterial and nematocidal activity of crude extracts and pure compounds

The compounds 5'-O-methylmelledonal (**6**) and Melledonal (**7**) isolated from *A. mellea* did not show any activity against the test pathogens. Armillaridin (**1**) which was isolated from *D. ectypa* was active against *Bacillus subtilis* (DSM 10) at an MIC value of 8.3 µg/mL and *Mucor hiemalis* (DSM 2656) at an MIC value of 33.3 µg/mL on serial dilutions on a 96-well microtiter plate as shown in **table 4.1**. Compounds **1, 2, 4-10** (**Figure 4.4**) and the crude extracts showed a very weak activity against *E. coli* (ATCC 25922) and *S. aureus* (ATCC 25923) on disc agar diffusion assay. The compounds isolated did not show nematocidal activity.

Table 4.1: Minimum inhibitory concentrations (MIC in µg/mL) assays of compounds **1, 6** and **7**

Compound	Test organism	
	<i>Bacillus subtilis</i> (DSM10)	<i>Mucor hiemalis</i> (DSM 2656)
Armillaridin (1)	8.3	33.3
5'-O-methylmelledonal (6)	-	-
melledonal C (7)	-	-
	- No activity	

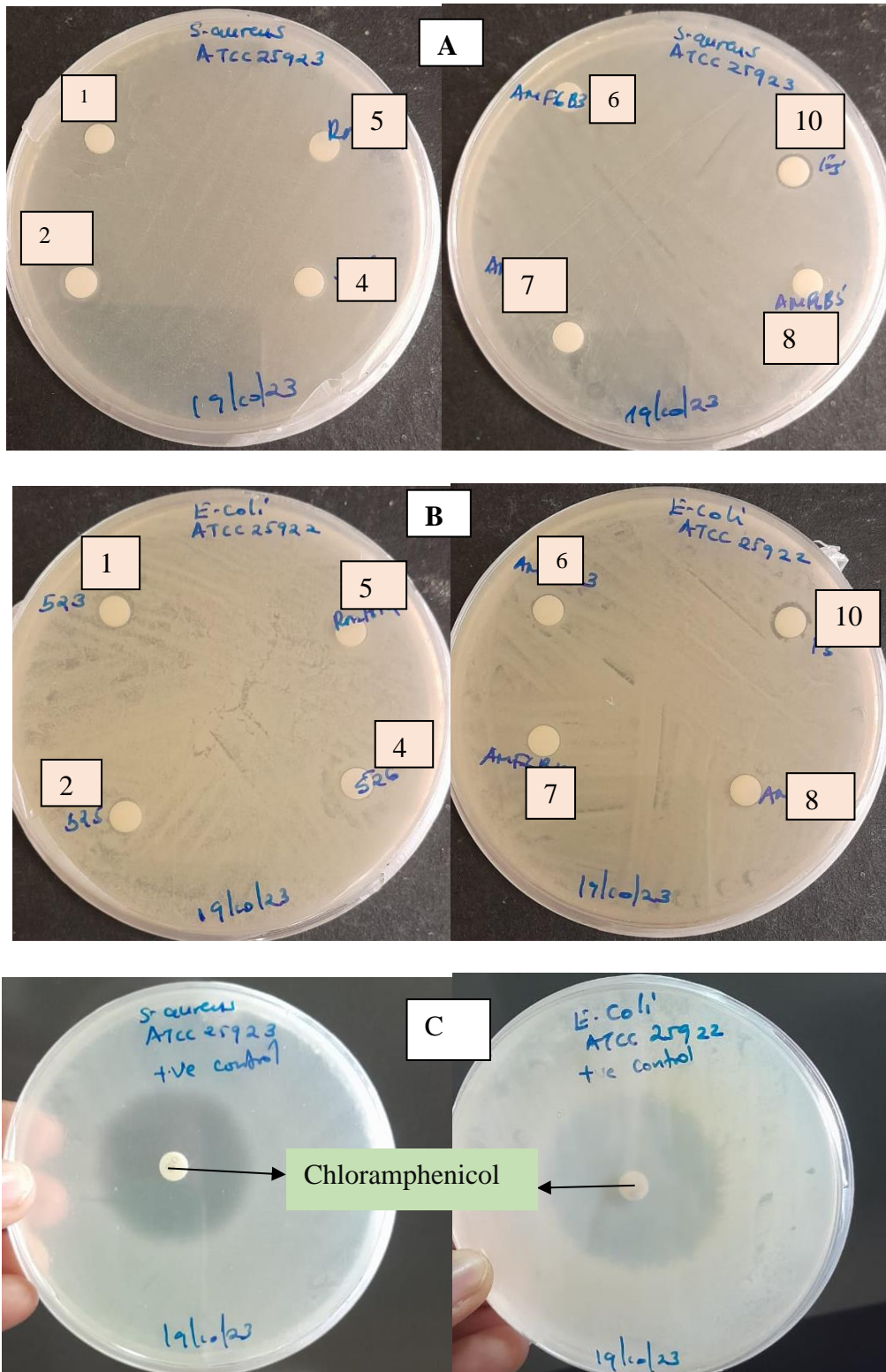


Figure 4.4: Disc diffusion agar assay of pure compounds (1, 2, 4-10) against *E. coli* (ATCC 25922) and *S. aureus* (ATCC 25923). **A** and **B** shows the bioactivity of the pure compounds against test microorganisms and **C** shows the positive control (Chloramphenicol) against the test microorganisms

4.3 Chemical structures of the isolated compounds from the study

The compounds shown in **figure 4.5** were isolated from *Desarmillaria ectypa*, *Armillaria mellea* and *Armillaria gallica*. Compounds **1**, **2**, **3**, **6**, **7**, **8**, and **9** were isolated as sesquiterpene aryl esters (melleolides) and compounds **4** and **10** were isolated as diketopiperazines. Compound **5** was isolated as an orsellinic acid residue.

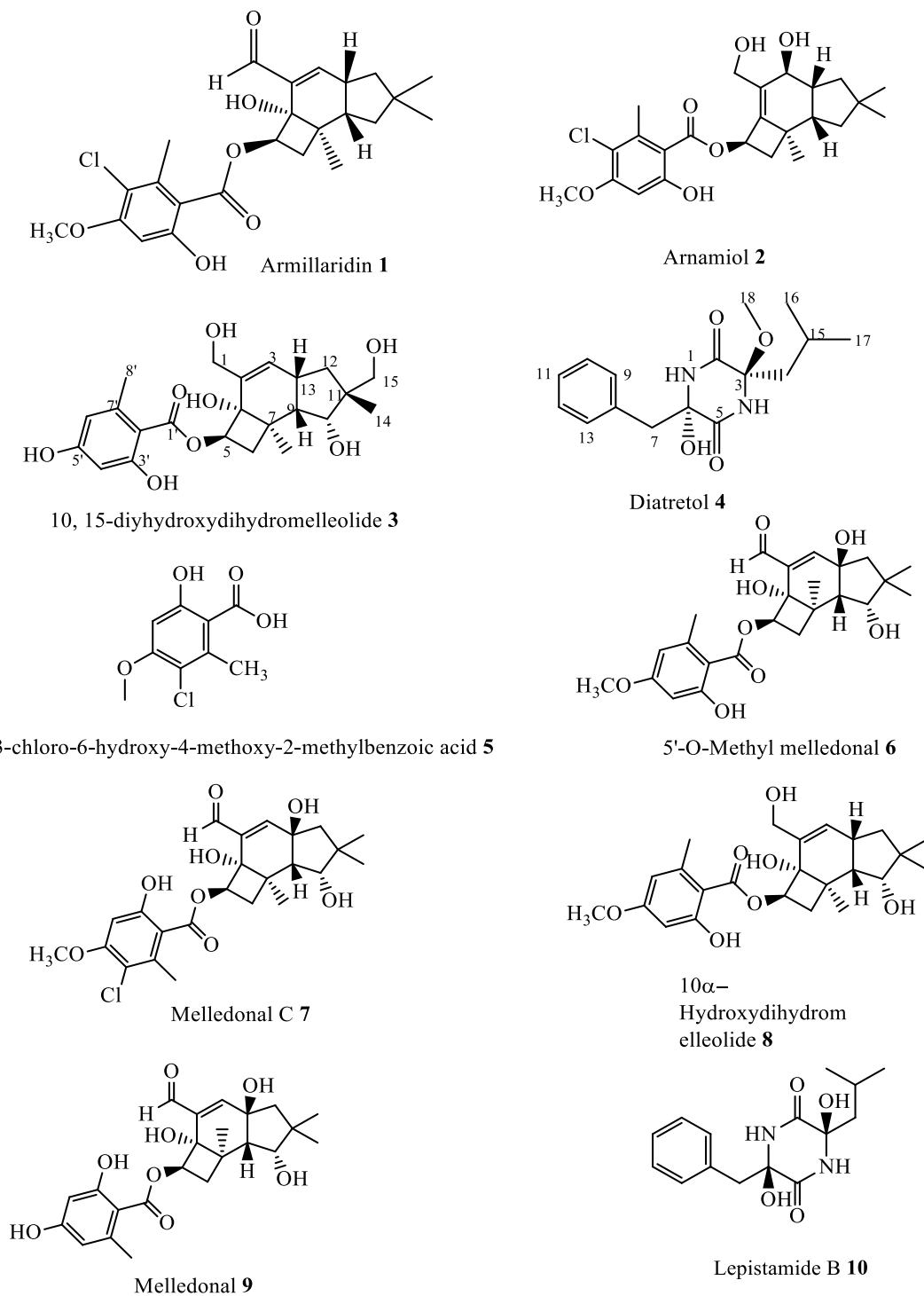


Figure 4.5: Chemical structures of the isolated compounds

4.3 Structure elucidation of isolated compounds from *Desarmillaria ectypa*

4.3.1 Structure elucidation of compound 1

Compound 1 (Figure 4.7) was isolated as a brown oil with a mass of 3.61 mg. The HRESIMS revealed molecular ion mass $[M + Na]^+$ to be m/z 471.15 and the retention at 14.25 mins. The UV spectrum values of the compound was observed to be 226 nm, 262 nm, and 310 nm (Figure 4.6). Interpretation of 1D and 2D NMR data (Table 4.2) led to structure elucidation of the compound.

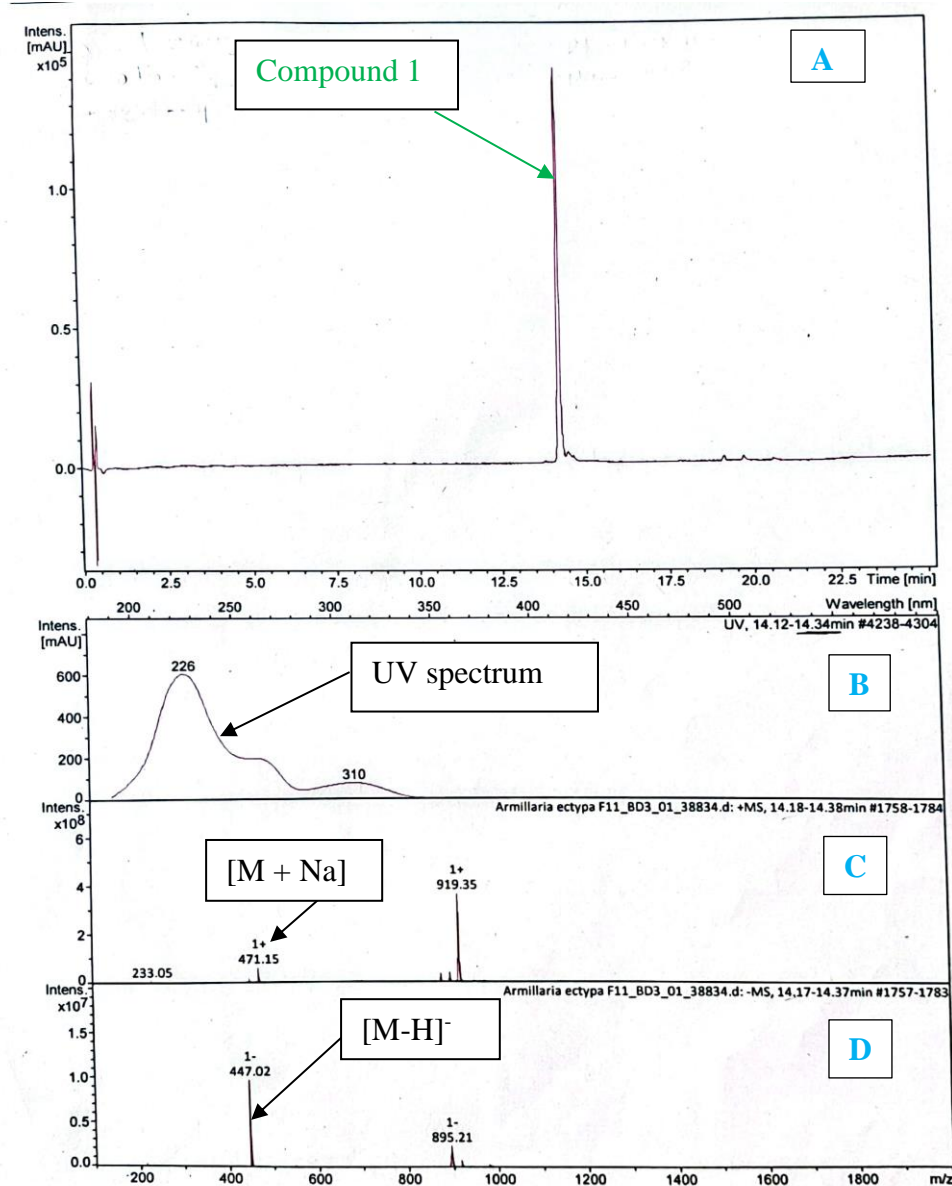


Figure 4.6: Mass spectrum of compound 1. A showing liquid (LC) chromatogram with the retention time. B showing the UV spectrum of the compound. C showing the molecular ion mass in positive mode and D showing the molecular on mass in the negative mode

Table 4.2: NMR data of compound **1**

No.	¹³ C NMR	TYPE	HSQC, mult.	COSY	HMBC
1	196.0	CHO	9.48, s	-	2, 3, 5, 7
2	137.1	C	-	-	-
3	158.5	CH	6.81, dd	13	1, 6, 9, 10, 12, 13
4	78.9	C	-	-	-
5	74.9	CH	4.94, m	9'	1', 4
6	33.1	CH ₂	2.10, d, 1.59, d	12, 13	5, 6, 9
7	37.6	C	-	-	-
8	21.2	CH ₃	1.34, s	12	4, 5, 6, 7, 9
9	44.1	CH	2.30, m	13	3, 5, 6, 7, 13
10	41.6	CH ₂	2.17, 1.51, d	-	6, 7, 9, 12, 13, 15
11	38.0	C	-	-	-
12	46.5	CH ₂	2.03, d	6, 8	3, 13, 15
13	40.3	CH	3.03, m	3, 6, 7	2, 3, 7, 10, 12
14	31.1	CH ₃	1.04, s	-	11, 12, 13, 15
15	31.6	CH ₃	1.01, s	-	11, 12, 13, 14
1'	170.1	C	-	-	-
2'	106.3	C	-	-	-
3'	163.0	C	-	-	-
4'	98.5	CH	6.42, s	8', 9'	2', 3', 5', 6'
5'	159.4	C	-	-	-
6'	115.1	C	-	-	-
7'	139.1	C	-	-	-
8'	19.8	CH ₃	2.45, s	4'	2', 6', 7'
9'	56.0	OCH ₃	3.89, s	4', 5	5'

The ^1H NMR of compound **1** revealed multiplicity of the protons in the compound. From the ^1H NMR spectral data (**Appendix 1**), the proton H-10 (δ_{H} 1.51), H-6 (δ_{H} 1.59 and δ_{H} 2.10), and H-12 (δ_{H} 2.03) showed a doublet (d) multiplicity. The protons δ_{H} 2.30, 3.03, 4.94 revealed a multiplet (m). A singlet (s) was observed in the protons δ_{H} 1.34, 9.48, 1.01, 1.04, 6.42, 2.45 and 3.89 indicating that there were no neighboring protons to these protons. The proton resonating at δ_{H} 9.48 revealed a characteristic of an aldehyde proton. The spectral data further revealed four methyl protons which were resonating at δ_{H} 1.01, 1.04, 1.34 and 2.45. Two aromatic protons were observed at δ_{H} 6.42 and δ_{H} 6.81 confirming the presence of a benzene in the compound. The proton resonating at δ_{H} 3.89 revealed a characteristic of a methoxy proton indicating that the compound contained a methoxy group.

The ^{13}C NMR spectral data (**Appendix 2**) showed that compound **1** had a total of 24 carbon atoms and ten quaternary carbon atoms which were obtained from the HMBC spectrum (**Appendix 3**). The quaternary carbon atoms were resonating at δ_{C} 37.6, 38.0, 78.9, 106.3, 115.1, 137.1, 139.1, 159.4, 163.0 and at 170.1. The spectral data further revealed a methoxy resonating at δ_{C} 56.3 (C-9'). C-3' and C-4 were observed to be resonating at δ_{C} 163.0 and 78.9 respectively therefore, these carbon atoms were oxygenated. C-6' showed a chemical shift of δ_{C} 115.1 this indicated that the carbon atom was chlorinated. A characteristic of an aldehyde carbon was observed resonating at δ_{C} 196.0. Four aromatic carbons were further observed at carbon atoms in position C-4' (δ_{C} 98.5), C-2' (δ_{C} 106.3), C-7' (δ_{C} 139.1) and C-2 (δ_{C} 137.1) and one carboxylic was observed at C-1' resonating at δ_{C} 170.1.

The HSQC spectral data (**Appendix 4**) was used to determine the correlation of protons and carbons in the compound. The protons were observed to be directly attached to the carbon atoms. In this compound, the protons H-3 (δ_{H} 6.81), H-5 (δ_{H} 4.94), H-6 (δ_{H} 2.10, 1.59), H-9 (δ_{H} 2.30), H-10 (δ_{H} 1.51, 1.27), H-12 (δ_{H} 2.03), H-13 (δ_{H} 3.03), H-14 (δ_{H} 1.04), H-15 (δ_{H} 1.01), H-4' (δ_{H} 6.42), H-8' (δ_{H} 2.45) were directly attached to C-3 (δ_{C} 158.5), C-5 (δ_{C} 74.9), C-6 (δ_{C} 33.1), C-9 (δ_{C} 44.1), C-10 (δ_{C} 41.6), C-12 (δ_{C} 46.5), C-13 (δ_{C} 40.3), C-14 (δ_{C} 31.1), C-15 (δ_{C} 31.6), C-4' (δ_{C} 98.5), C-8' (δ_{C} 19.8) respectively.

The HMBC spectrum was used to determine the correlations of protons with carbon atoms that are two to three bonds away. These correlations showed carbon atoms which are next to each other in the compound. In compound **1**, H-8' (δ_{H} 2.45) showed strong correlations with C-2' (δ_{C} 106.3) which is a quaternary carbon atom, C-6' (δ_{C} 115.1) which is a chlorinated carbon atom and C-7' (δ_{C} 139.1) which is a quaternary carbon atom. H-15 (δ_{H} 1.01) and H-14 (δ_{H} 1.04) showed similar correlations with each other. Therefore, the two protons showed correlations with C-11 (δ_{C} 38.0) which is a quaternary carbon, C-12 (δ_{C} 46.5) and C-10 (δ_{C}

41.6) which were both methylene carbons. Proton H-8 (δ_{H} 1.34, s) showed strong correlations with C-4 (δ_{C} 78.9) which is an oxygenated carbon atom, a weak correlation with C-5 (δ_{C} 74.9) which is an oxygenated methine carbon, C-6 (δ_{C} 33.1) which is a methylene carbon, C-7 (δ_{C} 37.6) which is a quaternary carbon atom, and with C-9 (δ_{C} 44.1) is a methine carbon. Proton H-5 (δ_{H} 4.94) showed a correlation with C-6 (δ_{C} 33.1), C-4 (δ_{C} 78.9), C-2 (δ_{C} 137.1) and with C-1' (δ_{C} 170.1). The correlation of H-5 and C-1' showed the connection of the Orsellinic ring structure to the protoilludane backbone structure through an oxygen bond.

Correlation spectroscopy (COSY) (**Appendix 5**) was used to show the correlations of the neighboring protons in the compound. H-9 (δ_{H} 2.30) showed a correlation with H-13 (3.03). H-6 (δ_{H} 2.10, 1.59) showed a correlation with H-13 (δ_{H} 3.03). H-12 (δ_{H} 2.03) showed a correlation with H-6 (δ_{H} 2.10, 1.59) and H-8 (δ_{H} 1.34). H-4' (δ_{H} 6.42) showed correlations with H-8' (δ_{H} 2.45) and H-9' (δ_{H} 3.89). H-9' (δ_{H} 3.89) showed a correlation with H-5 (δ_{H} 4.94).

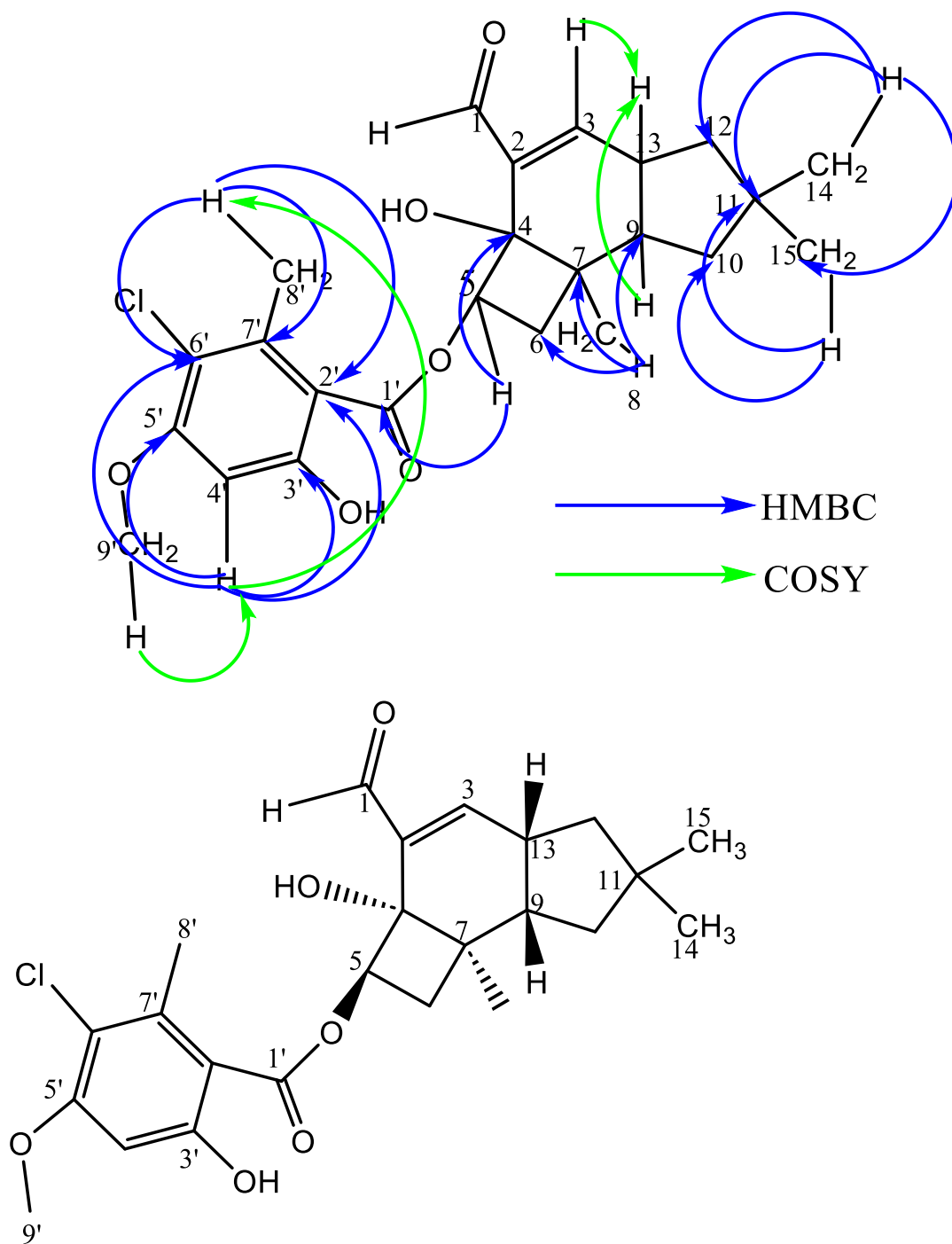


Figure 4.7: Structure of compound 1 with and without HMBC, COSY correlations

4.3.2 Structure elucidation of compound 2

Compound 2 (Figure 4.9) was obtained as a brown oil with a mass of 4.51 mg. The molecular ion mass $[M-H]^-$ was found to be m/z 449.01 (Figure 4.8). The retention time was found to be 13.1 min and the UV wavelengths was observed to be 221 nm, 263 nm, and 307 nm. Interpretation of 1D and 2D NMR data (Table 2) led to elucidation of the compound.

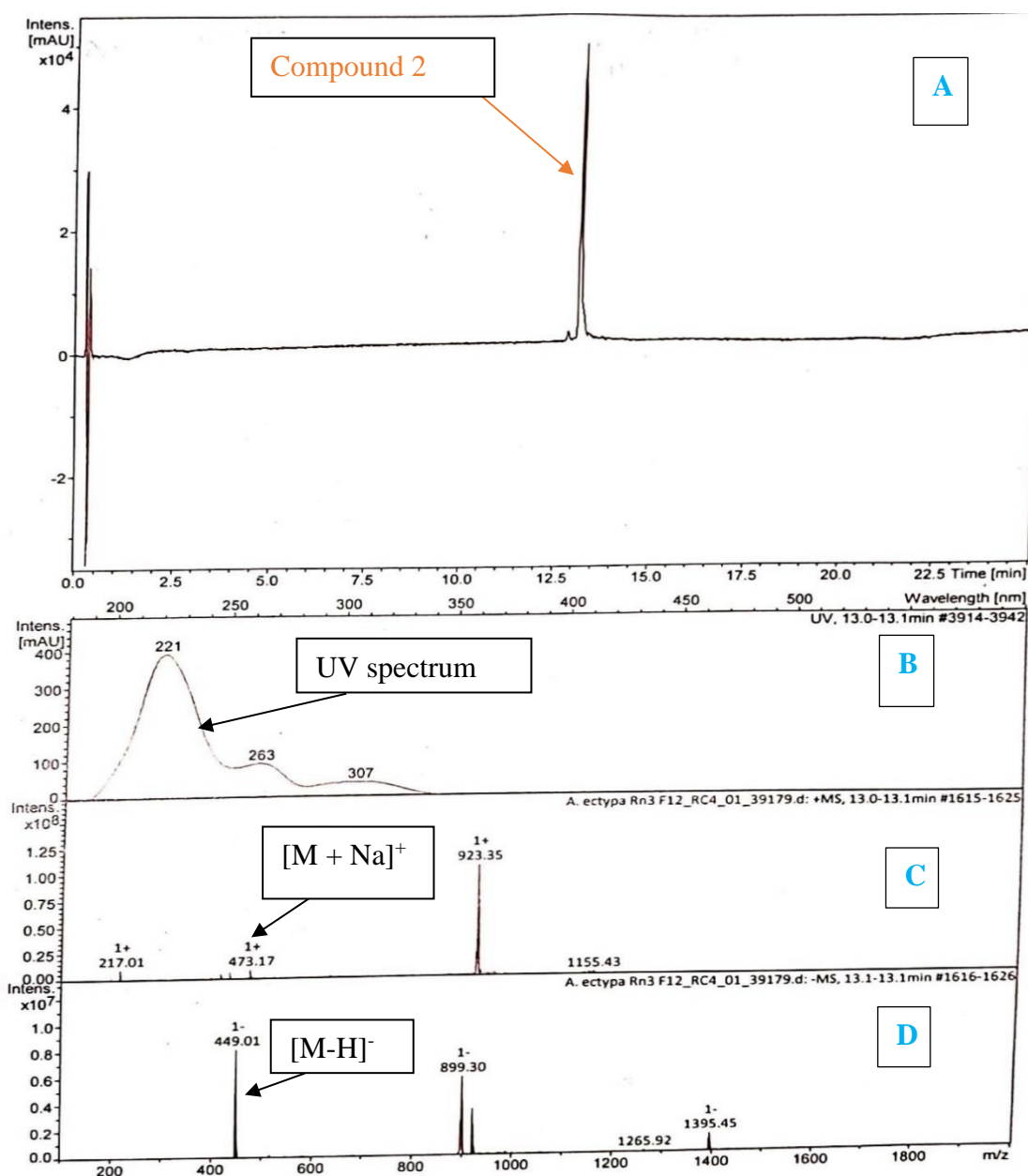


Figure 4.8: Mass spectrum of compound 2. A showing liquid (LC) chromatogram with the retention time. B showing the UV spectrum of the compound. C showing the molecular ion mass in positive mode and D showing the molecular on mass in the negative mode

Table 4.3: NMR data of compound **2**

NO	¹³ C NMR	TYPE	HSQC, mult.	COSY	HMBC
1	59.1	CH ₂	4.23, dd, 4.30, d	9	2, 3, 4
2	142.4	C	-		-
3	74.6	CH	4.21, d		1, 2, ,9, 12, 13
4	133.7	C	-		-
5	70.7	CH	6.00, m		2, 4, 6, 1'
6	46.6	CH ₂	2.55 d,1.84 d		2, 4, 5, 7, 8, 9
7	39.0	C	-		-
8	21.2	CH ₃	0.99, s		2, 6, 7, 9
9	47.4	CH	2.31,m	1	3, 6, 7, 8, 10, 13
10	40.9	CH ₂	1.36, 1.26 d	15	11, 12, 13, 15
11	40.2	C	-		-
12	46.2	CH ₂	1.08, m, 1.74, m		9, 10, 15
13	50.1	CH	2.37, m		3, 7, 9
14	29.5	CH ₃	1.02, s		10,11, 12, 15,
15	27.0	CH ₃	0.89, s	10	10, 11, 12, 14
1'	170.4	C	-		-
2'	106.3	C	-		-
3'	163.0	C	-		-
4'	98.5	CH	6.43, s		1', 2', 3', 5', 6',
5'	159.7	C	-		-
6'	115.7	C	-		-
7'	139.7	C	-		-
8'	19.8	CH ₃	2.58, s		1', 2', 3', 6', 5', 7'
9'	56.3	OCH ₃	3.82, s		5'

Compound **2** NMR data values were similar to those of compound **1**. The difference was the presence of alcohol in carbon atom at position C-1 and the absence of hydroxyl group at C-4. From the $^1\text{H-NMR}$ spectral data (**Appendix 6**), H-3 (δ_{H} 4.21), H-6 (δ_{H} 1.84 and δ_{H} 2.55) and H-10 (δ_{H} 1.36) showed a doublet multiplicity. This indicated that H-3, H-6, and H-10 protons had one neighboring proton. H-9 (δ_{H} 2.31) and H-13 (δ_{H} 2.37) showed a multiplet multiplicity. This indicated that there were multiple neighboring protons. H-8 (δ_{H} 0.99), H-15 (δ_{H} 0.89), H-14 (δ_{H} 1.02), H-4' (6.43) H-8' (δ_{H} 2.58) and H-9' (δ_{H} 3.82) showed a singlet indicating that there were no neighboring protons. The protons resonating at δ_{H} 0.89, 0.99, 1.02 and 2.58 showed that the presence of four methyl groups and the chemical shift at δ_{H} 3.82 indicated that the compound has a methyl group attached to an oxygen atom. The protons resonating at δ_{H} 4.23 and δ_{H} 4.30 showed that the compound has a methylene proton. The proton at δ_{H} 6.43 indicated that the compound contained an aromatic proton

The ^{13}C NMR spectral data (**Appendix 7**) showed that compound **2** had a total of 24 carbon atoms and the ten quaternary carbon atoms were obtained from the HMBC spectrum (**Appendix 8**). The quaternary carbon atoms were resonating at δ_{C} 39.0, 40.2, 106.3, 115.7, 133.7, 139.7, 142.4, 159.7, 163.0 and at 170.4. From the spectrum, C-9' had a resonance of δ_{C} 56.3, this indicated that the carbon atom was a methoxy. The carbon atoms at position C-3 and C-3' was observed to be resonating at δ_{C} 74.6 and 163.0 respectively. The two carbon atoms were hydroxylated. C-6' showed a chemical shift at δ_{C} 115.7 indicating that the carbon atom was chlorinated. The carbon at position C-1 showed a chemical shift of 59.1 revealing that the carbon atom was attached to a hydroxyl group. This was further confirmed by the HSQC spectrum because the carbon atom was shown to be a methylene. C-4' (δ_{C} 98.5), C-2' (δ_{C} 106.3), C-7' (δ_{C} 139.7) and C-7 (δ_{C} 142.4) showed the presence of the aromatic carbons. C-1' (δ_{C} 170.4) was a characteristic of carboxylic acid.

The HSQC spectrum (**Appendix 9**) was used to determine the correlation of protons and carbons in the compound. The protons were observed to be directly attached to the carbon atoms. In this compound, the protons H-3 (δ_{H} 4.13), H-5 (δ_{H} 5.91), H-6 (δ_{H} 2.55, 1.89), H-9 (δ_{H} 2.31), H-10 (δ_{H} 1.36, 1.26), H-12 (δ_{H} 1.08, 1.74), H-13 (δ_{H} 2.26), H-14 (δ_{H} 1.02), H-15 (δ_{H} 0.89), H-4' (δ_{H} 6.34), H-8' (δ_{H} 2.58) were directly attached to C-3 (δ_{C} 74.6), C-5 (δ_{C} 70.7), C-6 (δ_{C} 46.6), C-9 (δ_{C} 47.4), C-10 (δ_{C} 40.9), C-12 (δ_{C} 46.2), C-13 (δ_{C} 50.1), C-14 (δ_{C} 29.5), C-15 (δ_{C} 27.0), C-4' (δ_{C} 98.5), C-8' (δ_{C} 19.8).

The HMBC spectrum was used to determine the correlations of protons with carbon atoms that are two to three bonds away. These correlations showed carbon atoms which are next to each other in the compound. In compound **2**, the proton H-8' (δ_{H} 2.58) showed strong

correlations with C-2' (δ_C 106.3) which is a quaternary carbon atom, C-6' (δ_C 115.7) which is a chlorinated carbon atom and C-7' (δ_C 139.7) which is a quaternary carbon atom. H-14 (δ_H 1.02) and H-15 (δ_H 0.89) showed similar correlations with each other. Therefore, the two protons showed correlations with C-11 (δ_C 40.2) which is a quaternary carbon, C-12 (δ_C 46.2) and C-10 (δ_C 40.9) which were both methylene carbons. Proton H-8 (δ_H 0.99) showed strong correlations with C-4 (δ_C 133.7) which is a quaternary carbon atom, C-6 (δ_C 46.6) which is a methylene carbon, C-7 (δ_C 39.0) which is a quaternary carbon atom, C-9 (δ_C 47.4) which is a methine carbon and with a weak correlation with C-2 (142.4 ppm) which is a quaternary carbon. Proton H-5 (δ_H 5.91) showed a correlation with C-4 (δ_C 133.7) which is a quaternary carbon atom, C-6 (δ_C 46.6) which is a methylene carbon atom, C-7 (δ_C 142.4) which is a quaternary carbon and with C-1' (δ_C 170.4) which is a carbonyl carbon atom.

Correlation spectroscopy (COSY) (**Appendix 10**) was used to show the correlations of the neighboring protons in the compound. H-10 (δ_H 1.36) showed a correlation with H-15 (δ_H 0.89) and H-9 (δ_H 2.31) showed a correlation with H-1 (δ_H 4.32).

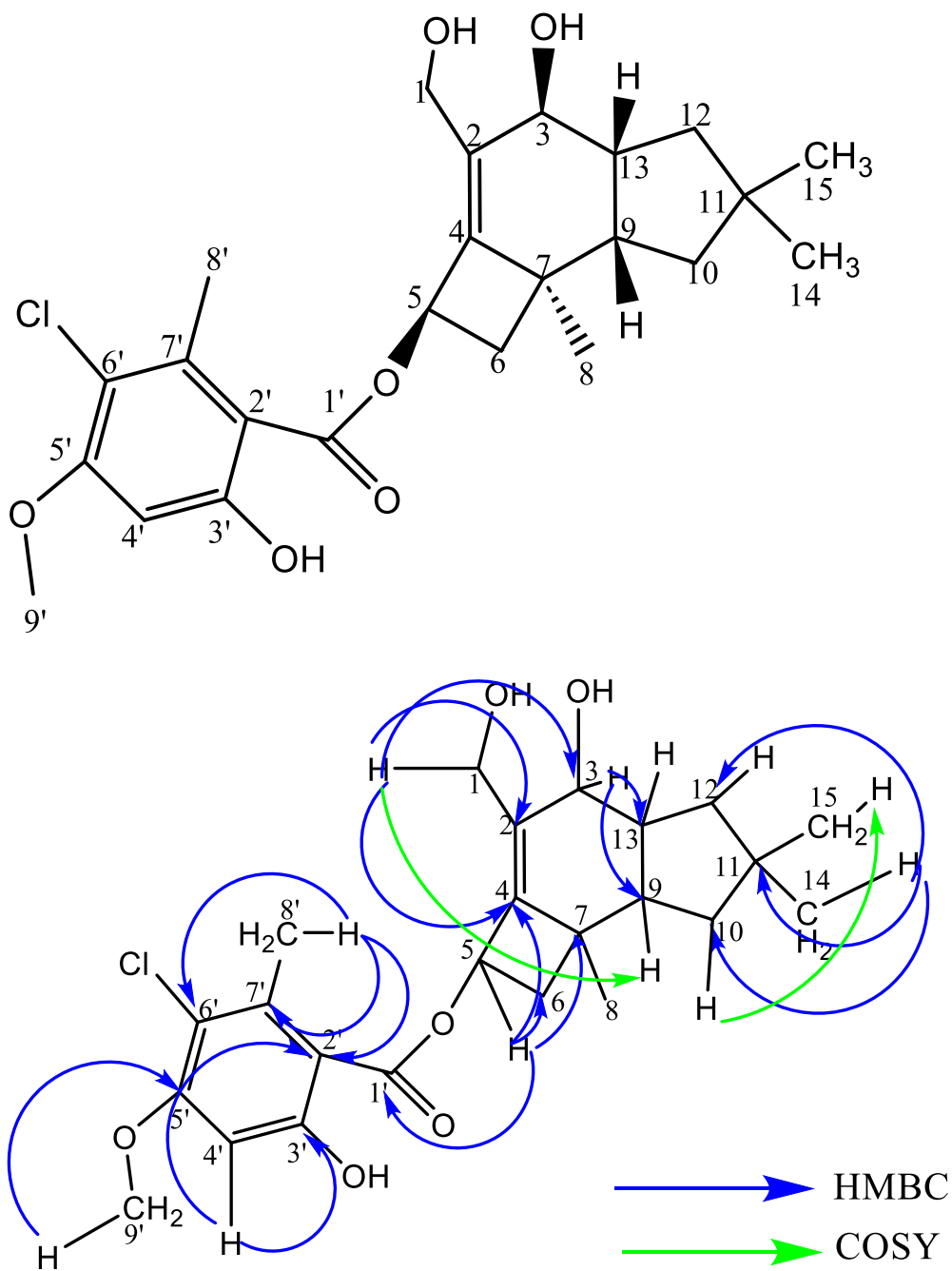


Figure 4.9: Structure of compound 2 without and with HMBC, COSY correlations

4.3.3 Structure elucidation of compound 3

Compound 3 (Figure 4.11) was obtained as a brown oil (1.0 mg) and HR-ESI-MS revealed its molecular formula as $C_{23}H_{31}O_8$ and a molecular ion mass m/z 435.2010 $[M+H]^+$. The UV spectrum revealed 229 and 266 nm values (Figure 4.10). Interpretation of 1D and 2D NMR data (Table 4.4) led to structure elucidation of the compound.

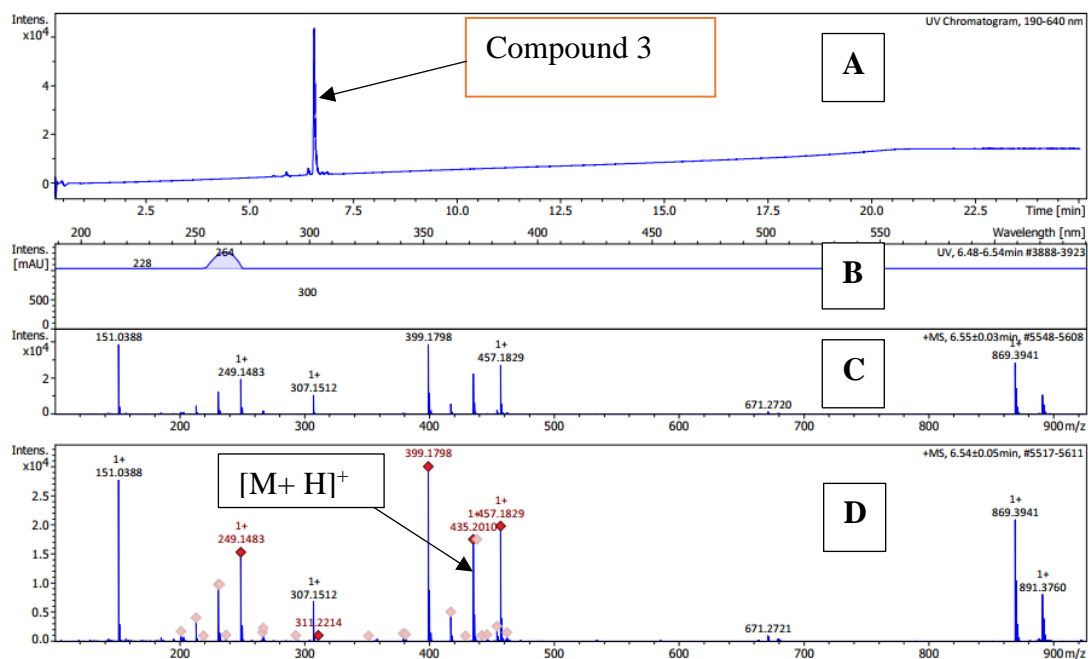


Figure 4.10: Mass spectrum of compound 3. A showing liquid (LC) chromatogram with the retention time. B showing the UV spectrum of the compound. C showing the molecular ion mass in positive mode and D also showing the molecular on mass in the positive mode

Table 4.4 : NMR data table of compound **3**

No.	¹³ CNMR	TYPE	HSQC, mult.	COSY	HMBC
1	64.1	CH ₂	3.98, d (13.31) 4.26, d (13.31)		3, 4
2	135.3	C	-	-	
3	132.4	CH	5.89, br s		1, 2, 5, 9, 13
4	77.0	C	-	-	
5	77.4	CH	5.70, m	-	1', 4, 6
6	33.6	CH ₂	1.78, 1.98, m	-	5, 7, 9
7	37.4	C	-	-	
8	21.6	CH ₃	1.36, s		5, 6, 9, 13
9	48.3	CH	2.29, d (4.15)	10, 13	3, 10, 13, 14
10	82.6	CH	3.83, d (4.15)	9	13, 12, 14
11	47.9	C	-	-	
12	41.1	CH ₂	1.77, m		3, 10, 11, 13, 14, 15
13	36.5	CH	2.93, m	9	3, 9, 12
14	25.2	CH ₃	0.98, s	-	10, 12, 11, 15,
15	68.3	CH ₂	3.53, dd (10.66)	-	10, 12, 11, 14
1'	171.9	C	-	-	-
2'	105.4	C	-	-	-
3'	166.5	C	-	-	-
4'	101.7	CH	6.23, d		2', 3', 6'
5'	163.4	C	-		
6'	112.5	CH	6.26, d		2', 4', 5', 8'
7'	145.6	C	-		
8'	24.2	CH ₃	2.40, s		2', 6', 7',

The ^1H -NMR of compound **3** was used to show the multiplicity and the type of protons in the compound. From the ^1H -NMR spectrum (**Appendix 11**), H-1 (δ_{H} 3.98 and δ_{H} 4.26), H-9 (δ_{H} 2.29), H-10 (δ_{H} 3.83), H-4' (δ_{H} 6.23) and H-6' (δ_{H} 6.26) showed a doublet multiplicity. This indicated that these protons had one neighboring proton. The protons H-5 (δ_{H} 5.70), H-6 (δ_{H} 1.78 and δ_{H} 1.99), H-12 (δ_{H} 1.77) and H-13 (δ_{H} 2.93) showed a multiplet. The protons H-3 (δ_{H} 5.89), H-8 (δ_{H} 1.36), H-14 (δ_{H} 0.98), H-8' (δ_{H} 2.40) showed a singlet indicating that there were no neighboring protons of H-3, H-8, H-14, H-8'. The protons resonating at δ_{H} 0.98, δ_{H} 1.36 and δ_{H} 2.40 showed that the compound has three methyl groups. The protons resonating at δ_{H} 1.78, δ_{H} 1.99, δ_{H} 1.76, δ_{H} 3.53 and δ_{H} 4.25 revealed a characteristic of methylene protons. The proton resonating at δ_{H} 6.23 and δ_{H} 6.26 indicated that the compound contained aromatic protons.

The ^{13}C NMR spectrum (**Appendix 12**) showed a total of 23 carbon atoms and the nine quaternary carbon atoms were obtained from the HMBC spectrum (**Appendix 13**). The quaternary carbon atoms were resonating at δ_{C} 37.0, 47.9, 77.0, 105.4, 135.3, 145.6, 163.4, 166.5 and 171.9. The ^{13}C -NMR spectral data further revealed the type of the carbon atoms in the compound. From the spectral data, C-3' and C-5' was observed to be resonating at δ_{C} 166.5 and δ_{C} 163.4 respectively. The two carbon atoms were hydroxylated. The carbons at position C-1 and C-15 were resonating at δ_{C} 64.1 and δ_{C} 68.3 respectively. This indicated that the two carbon atoms were hydroxylated. The carbons at position C-2' (δ_{C} 105.4), C-4' (δ_{C} 101.7), C-6' (δ_{C} 112.5), C-7' (δ_{C} 145.6) and at C-3 (δ_{C} 132.4) revealed the presence of the aromatic carbons. C-1' was a carboxylic acid because it was resonating at δ_{C} 171.9.

To further confirm the structure of the compound, the HSQC spectral data (**Appendix 14**) was used to determine the correlation of protons and carbons in the compound. The protons were observed to be directly attached to the carbon atoms. In this compound, the protons H-1 (δ_{H} 4.26 and δ_{H} 3.98), H-3 (δ_{H} 5.89), H-5 (δ_{H} 5.70), H-6 (δ_{H} 1.78, δ_{H} 1.98), H-8 (δ_{H} 1.36), H-9 (δ_{H} 2.29), H-10 (δ_{H} 3.85), H-12 (δ_{H} 1.77), H-13 (δ_{H} 2.93), H-14 (δ_{H} 0.98), H-15 (δ_{H} 3.53), H-4' (δ_{H} 6.23), H-6' (δ_{H} 6.26) and H-8' (δ_{H} 2.40) were directly attached to C-1 (δ_{C} 64.1), C-3 (δ_{C} 132.4), C-5 (δ_{C} 77.4), C-6 (δ_{C} 33.6), C-8 (δ_{C} 21.6), C-9 (δ_{C} 48.3), C-10 (δ_{C} 82.6), C-12 (δ_{C} 41.1), C-13 (δ_{C} 36.5), C-14 (δ_{C} 25.3), C-15 (δ_{C} 68.4), C-4' (δ_{C} 101.7), C-6' (δ_{C} 112.5) and to C-8' (δ_{C} 24.2) respectively.

The HMBC spectral data further determined the correlations of protons with carbon atoms that are two to three bonds away. These correlations showed carbon atoms which are next to each other in the compound. From the HMBC spectral data, the proton H-6' (δ_{H} 6.26) showed correlation with C-2' (δ_{C} 105.4) which is a quaternary carbon atom, C-4' (δ_{C} 101.7)

which is an aromatic carbon atom, C-5' (δ_C 163.4) which is an oxygenated quaternary carbon atom and C-8' (δ_C 24.2) which is a methyl. The proton H-8' (δ_H 2.40) showed strong correlations with C-2' (δ_C 105.4) which is a quaternary carbon atom, C-6' (δ_C 112.5) which is an aromatic carbon atom and C-7' (δ_C 145.6) which is a quaternary carbon atom. H-14 (δ_H 0.98) and H-15 (δ_H 3.53) showed similar correlations with each other. Therefore, the two protons showed strong correlations with C-11 (δ_C 47.9) which is a quaternary carbon, C-12 (δ_C 41.1) which is a methylene carbon atom and C-10 (δ_C 82.6) which is an oxygenated carbon atom. Proton H-8 (δ_H 1.36) showed strong correlations with C-6 (δ_C 33.6) which is a methylene carbon, C-7 (δ_C 37.0) which is a quaternary carbon atom and with C-9 (δ_C 48.3), which is a methine. Proton H-5 (δ_H 5.70) showed a correlation with C-6 (δ_C 33.6) which is a methylene carbon, C-4 (δ_C 77.0) C-1' (δ_C 171.9) which is a carbonyl carbon. The correlation of H-5 and C-1' confirmed the connection of the orsellinic ring structure to the protoilludane backbone structure through an oxygen bond.

Correlation spectroscopy (COSY) (**Appendix 15**) revealed the correlations of the neighboring protons in the compound. From the spectral data, the proton H-10 (δ_H 3.83) showed a correlation with H-9 (δ_H 2.29). Another correlation was observed between H-9 (δ_H 2.29) and H-13 (δ_H 2.93). The nuclear overhauser effect spectroscopy (NOESY) spectrum (**Appendix 16**) showed a correlation between δ_H 0.98 (C-14) and δ_H 2.29 (C-9) indicating that the methyl group (C-14) has a β -orientation.

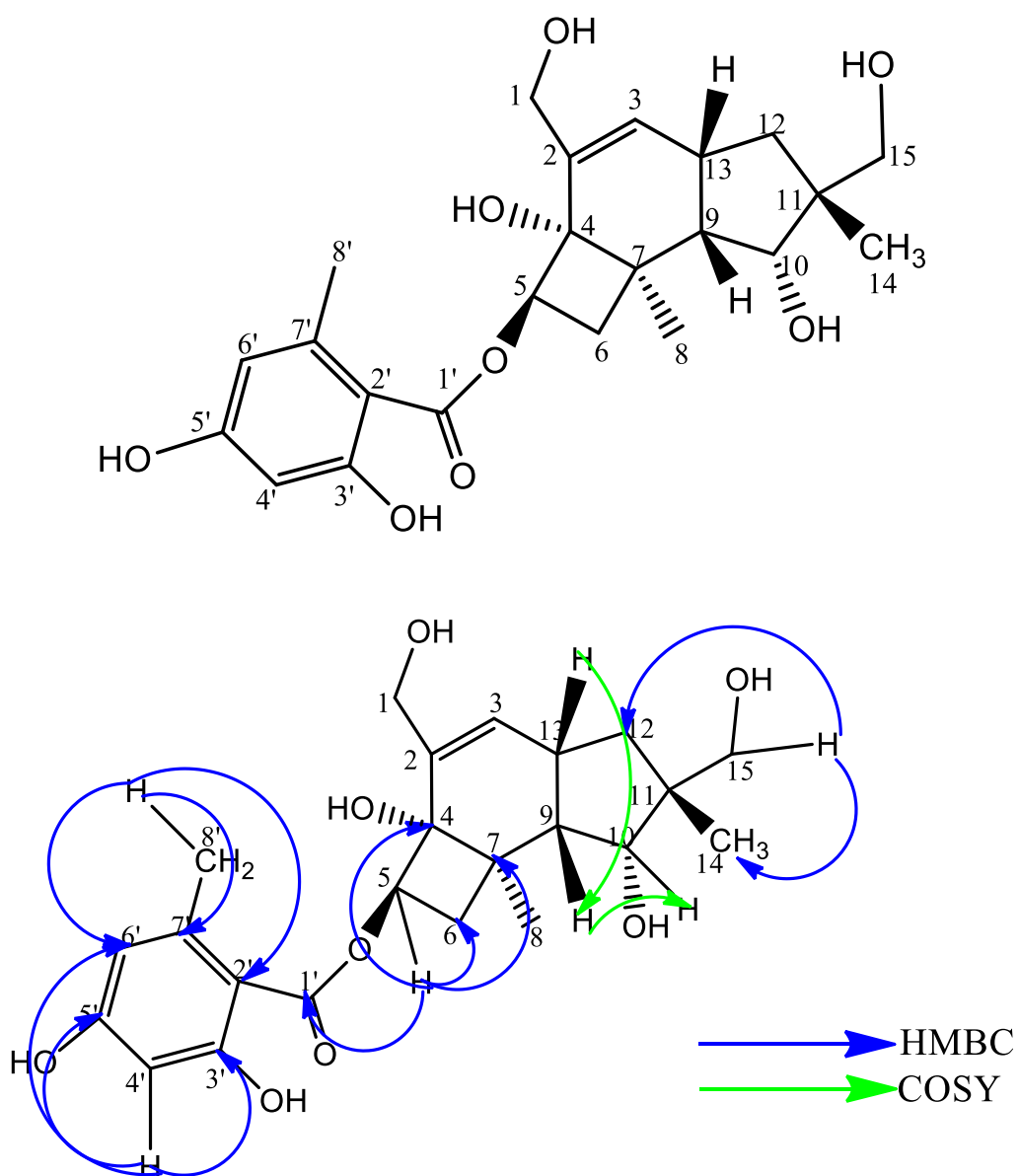


Figure 4.11: Structure of compound 3 with and without HMBC, COSY corrections

4.3.4 Structure elucidation of compound 4

Compound 4 (Figure 20) was obtained as a white solid with a mass of 23 mg. The compound had a molecular ion mass [2M-H] of m/z 611.10 (Figure 19). Interpretation of 1D and 2D NMR data (Table 4.5) led to structure elucidation of the compound.

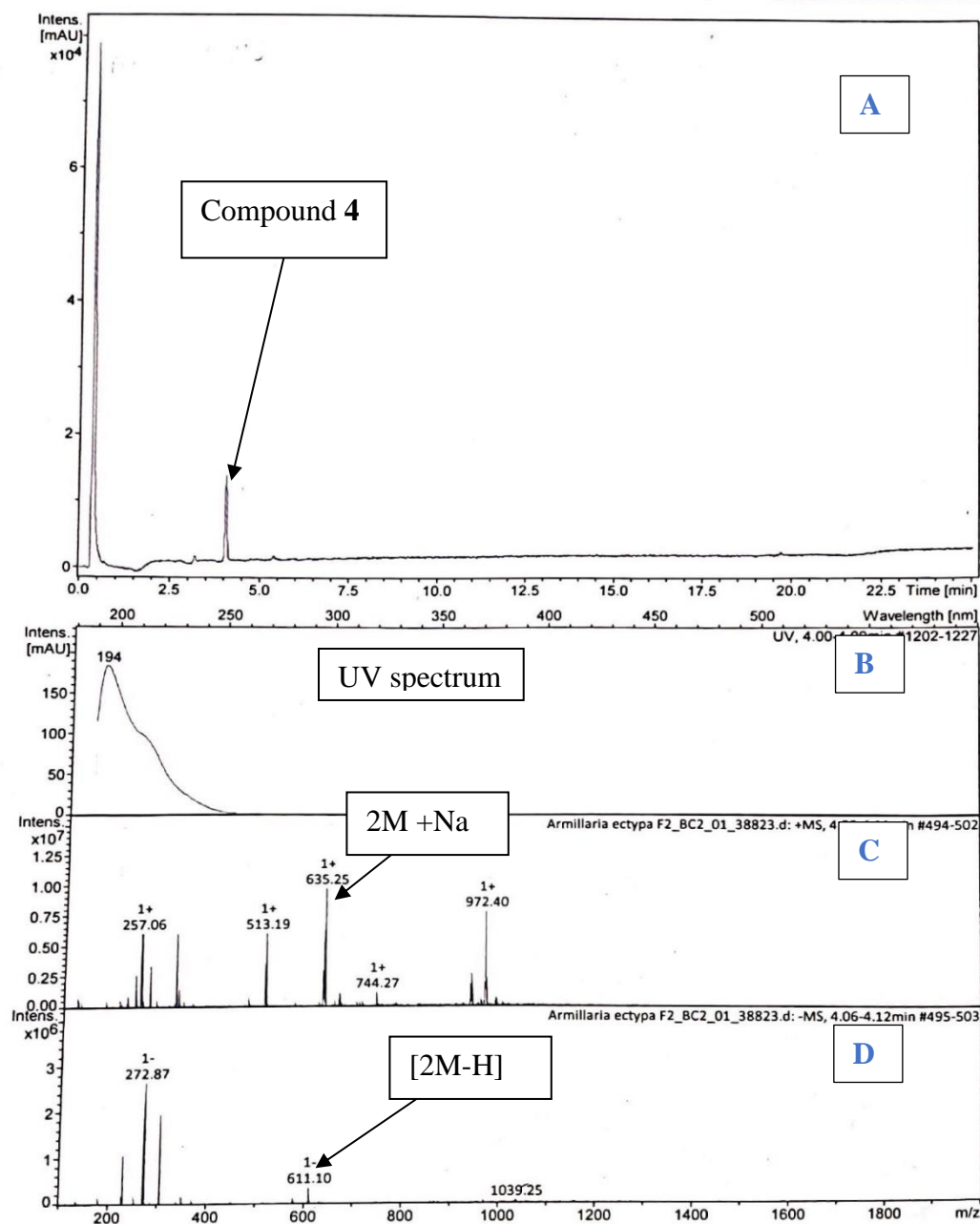


Figure 4.12: Mass spectrum of compound 4. A showing liquid (LC) chromatogram with the retention time. B showing the UV spectrum of the compound. C showing the molecular ion mass in positive mode and D showing the molecular on mass in the negative mode

Table 4.5: NMR data of compound **4**

NO	¹³ CNMR	TYPE	HSQC, mult.	COSY	HMBC
2	165.2	C	-	-	-
3	86.4	C	-	-	-
5	167.1	C	-	-	-
6	82.5	C	-	-	-
7	44.2	CH ₂	2.81, s ,3.42, s	2, 9, 12	2, 5, 6, 8, 10, 13,
8	135.3	C	-	-	-
9	127.8	CH	7.26, m	-	8, 7, 10, 11, 12, 13,
10	126.7	CH	7.14, m	-	3, 9, 13
11	129.3	CH	7.22, m	-	7, 8, 9, 13
12	127.9	CH	7.20, m	-	
13	130.8	CH	7.25, m	-	13
14	47.3	CH ₂	1.41, m, 1.68, m	16	2, 3, 5, 14, 15, 16, 17,
15	24.1	CH	0.83, dd	16	3, 14, 16, 17
16	22.6	CH ₃	1.42, d	14,15	3, 14, 17,
17	23.5	CH ₃	0.41, d	-	14, 15, 16
18	48.0	OCH ₃	1.95, s	-	3

The proton NMR of compound **4** was used to determine the multiplicity and the type of protons in the compound. From the ^1H -NMR spectrum (**Appendix 17**), H-7 (δ_{H} 2.81, 3.42) and H-18 (δ_{H} 1.95) showed a singlet indicating that there were no neighbouring protons to these two protons. H-9 (δ_{H} 7.26), H-10 (δ_{H} 7.14), H-11 (δ_{H} 7.22), H-12 (δ_{H} 7.20), H-13 (δ_{H} 7.25) and H-14 (δ_{H} 1.41, 1.68) showed a multiplet indicating that there were multiple neighbouring protons. H-16 (δ_{H} 1.42) and H-17 (δ_{H} 0.41) showed a doublet which indicated that one proton was neighbouring H-16 and H-17. The protons resonating at δ_{H} 7.14, 7.20, 7.22 and 7.26, were a characteristic of aromatic protons. The protons resonating at δ_{H} 1.42 and 0.41 were characteristic of methyl protons therefore this indicated that the compound contained two methyl groups. The proton resonating at δ_{H} 1.95 showed a characteristic of methyl protons attached to an oxygen atom. This indicated that the compound also contains a methoxy group.

The ^{13}C -NMR spectrum (**Appendix 18**) showed a total of sixteen carbon atoms. C-2 (δ_{C} 165.2), C-3 (δ_{C} 86.4), C-5 (δ_{C} 167.1), C-6 (δ_{C} 82.5), C-7 (δ_{C} 44.2), C-8 (δ_{C} 135.3), C-9 (δ_{C} 127.8), C-10 (δ_{C} 126.7), C-11 (δ_{C} 129.3), C-12 (δ_{C} 127.9), C-13 (δ_{C} 130.8), C-14 (δ_{C} 47.3), C-15 (δ_{C} 24.1), C-16 (δ_{C} 22.6), C-17 (δ_{C} 23.5) and C-18 (δ_{C} 48.0). The quaternary carbons were five; C-2 (δ_{C} 165.2), C-3 (δ_{C} 86.4), C-5 (δ_{C} 167.1), C-6 (δ_{C} 82.5), and C-8 (δ_{C} 135.3) were identified from the HMBC spectrum (**Appendix 19**). From the spectrum, C-9 (δ_{C} 127.8), C-10 (δ_{C} 126.7), C-11 (δ_{C} 129.3) C-12 (δ_{C} 127.9) and C-13 (δ_{C} 130.8) were identified as the aromatic carbons. C-2 (δ_{C} 165.2) and C-5 (δ_{C} 167.1) were identified as carbonyl carbon atoms. C-18 (δ_{C} 48.0) was a characteristic of methoxy carbon.

Heteronuclear single quantum coherence (HSQC) was used to show correlations of protons and carbons. From the HSQC spectrum (**Appendix 20**), protons were observed to be directly attached to the carbon atoms. H-7 (δ_{H} 2.81, 3.42), H-9 (δ_{H} 7.26), H-10 (δ_{H} 7.14), H-11 (δ_{H} 7.22), H-12 (δ_{H} 7.20), H-13 (δ_{H} 7.25), H-14 (δ_{H} 1.41, 1.68), H-15 (δ_{H} 0.83), H-16 (δ_{H} 1.42), H-17 (δ_{H} 0.41) and H-18 (δ_{H} 1.95) were observed to be directly attached to C-7 (δ_{C} 44.2), C-9 (δ_{C} 127.8), C-10 (δ_{C} 126.7), C-11 (δ_{C} 129.3) C-12 (δ_{C} 127.9), C-13 (δ_{C} 130.8), C-14 (δ_{C} 47.3), C-15 (δ_{C} 24.1), C-16 (δ_{C} 22.6), C-17 (δ_{C} 23.5) and C-18 (δ_{C} 48.0) respectively.

Heteronuclear multiple bond correlation (HMBC) spectroscopy was used to show correlation between protons and carbons that are two to three bonds away from each other. From HMBC spectrum, H-7 (δ_{H} 2.81, 3.42) showed strong correlations with C-5 (δ_{C} 167.1), C-6 (δ_{C} 82.5), C-8 (δ_{C} 135.3), C-9 (δ_{C} 127.8) and C-13 (δ_{C} 130.8). H-9 (δ_{H} 7.26) showed correlations with C-7 (δ_{C} 44.2), C-8 (δ_{C} 135.3), C-10 (δ_{C} 126.7), C-11 (δ_{C} 129.3) and C-13 (δ_{C} 130.8). H-10 (δ_{H} 7.14) showed correlations with C-3 (δ_{C} 86.4), C-9 (δ_{C} 127.8) and C-13 (δ_{C} 130.8). H-16 (δ_{H} 1.42) and H-17 (δ_{H} 0.41) showed similar correlations. The two protons

showed strong correlations with C-14 (δ_C 47.3) and C-15 (δ_C 24.1). H-18 (δ_H 1.95) showed only one correlation with C-3 (δ_C 86.4).

Correlation spectroscopy (COSY) was used to show the correlation between the neighbouring protons in the compound. From COSY spectrum (**Appendix 21**), H-7 (δ_H 2.81, 3.42) showed correlations with H-9 (δ_H 7.26) and H-12 (δ_H 7.20). H-14 (δ_H 1.41, 1.68,) showed a correlation with H-16 (δ_H 1.42). H-16 also had a correlation with H-14 (δ_H 1.41, 1.68) and H-15 (δ_H 0.83).

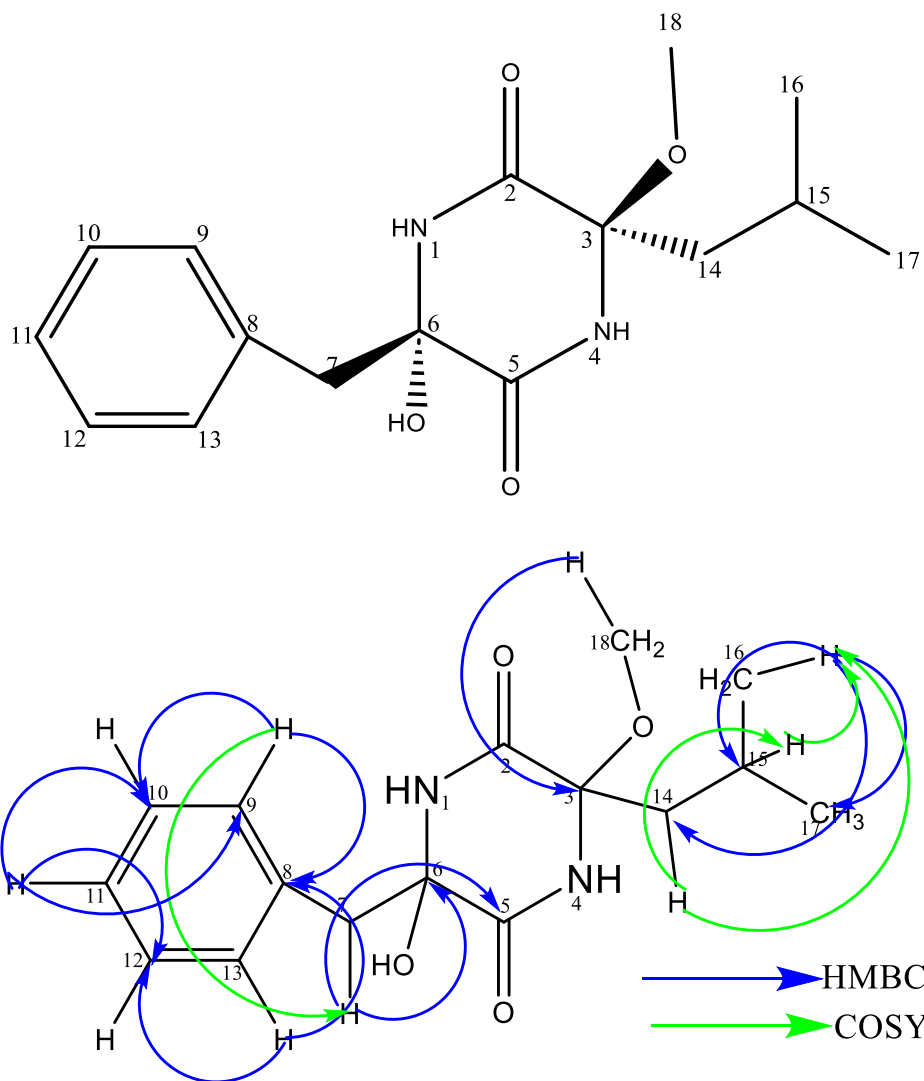


Figure 4.13: Structure of compound 4 with and without HMBC, COSY corrections

4.3.5 Structure elucidation of compound 5

Compound 5 (Figure 4.15) was isolated as a brown oil with a mass of 0.5 mg. From the mass spectrum (Figure 4.14), compound 5 had a molecular ion mass $[M-H]^-$ m/z 214.81 and the molecular formula $C_9H_9ClO_4$. The UV pattern was 222 nm, 259 nm, and 306 nm. The retention time of the compound was at 7.09 min. Interpretation of 1D and 2D NMR data (Table 4.6) led to structure elucidation of the compound.

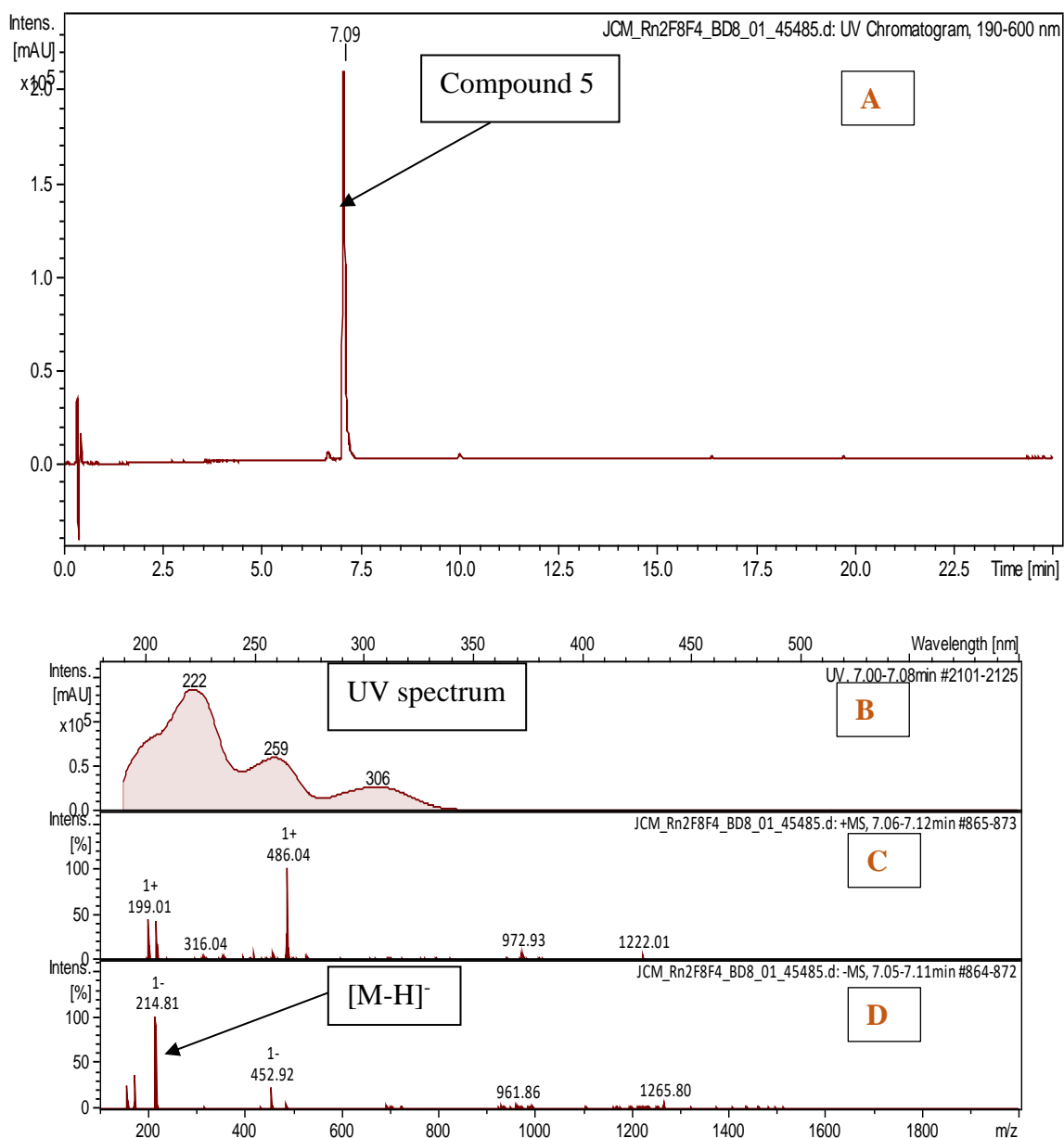


Figure 4.14: Mass spectrum of compound 5. A showing liquid (LC) chromatogram with the retention time. B showing the UV spectrum of the compound. C showing the molecular ion mass in positive mode and D showing the molecular on mass in the negative mode

Table 4.6: NMR data of compound **5**

NO	¹³ CNMR	TYPE	HSQC, mult.	COSY	HMBC
1'	168.2	C	-	-	-
2'	107.7	C	-	-	-
3'	163.7	C	-	-	-
4'	98.3	CH	6.49, s	8'	1', 3', 5', 6',
5'	159.5	C	-	-	-
6'	114.5	C	-	-	-
7'	139.9	C	-	-	-
8'	19.3	CH ₃	2.69, s	4'	2', 6', 7'
9'	55.8	OCH ₃	3.92, s		5'

From the ¹H-NMR spectrum (**Appendix 22**), H-4' (δ_{H} 6.49), H-8' (δ_{H} 2.69) and H-9' (δ_{H} 3.92) showed a singlet indicating that there were no neighboring protons of H-4', H-8', and H-9'. The proton resonating at δ_{H} 6.49 was a characteristic of an aromatic protons. This suggested that the compound contains a benzene ring. The proton resonating at δ_{H} 2.69 suggested that they are the methyl protons. This also indicated that the compound has a methyl group. The proton resonating at δ_{H} 3.92 was a characteristic of the methyl group attached to an oxygen atom. The high chemical shift of this methyl group is because of the attachment to an oxygen atom. Therefore, this indicated that the compound contains a methoxy group.

The carbon atoms of the compound were obtained from the HSQC (**Appendix 23**) and HMBC (**Appendix 24**) spectrum. From both spectrums, compound **5** had nine carbon atoms and six quaternary carbon atoms. The quaternary carbon atoms were C-1' (δ_{C} 168.2), C-2' (δ_{C} 107.7), C-3' (δ_{C} 163.7), C-5' (δ_{C} 159.5), C-6' (δ_{C} 114.5) and C-7' (δ_{C} 139.9). The carbon resonating at δ_{C} 168.2 (C-1') suggested that the compound contains a carboxylic acid functional group. The carbon resonating at δ_{C} 114.5 (C-6') was chlorinated. The carbon at δ_{C} 159.5 (C-5') indicated that this carbon is oxygenated and the carbon resonating at δ_{C} 163.7 (C-3') indicated that the carbon is hydroxylated. The carbon resonating at δ_{C} 55.8 (C-9') indicated that the carbon atom is methoxy.

The HSQC spectrum was used to show the correlations of protons and carbons. From the spectrum, H-4' (δ_{H} 6.49), H-8' (δ_{H} 2.69) and H-9' (δ_{H} 3.92) were directly attached to C-4' (δ_{C} 93.8), C-8' (δ_{C} 19.3) and C-9' (δ_{C} 55.8) respectively.

The HMBC was used to show the correlation of protons and carbons that are two to three bonds away from each other. From the spectrum, H-4' (δ_{H} 6.49) showed a correlation with C-1' (δ_{C} 168.2), C-2' (δ_{C} 139.9), C-3' (δ_{C} 163.7), C-5' (δ_{C} 159.5), and C-6' (δ_{C} 114.5). H-8' (δ_{H} 2.69) showed a correlation with, C-2' (δ_{C} 107.7), C-6' (δ_{C} 114.5) and C-7' (δ_{C} 139.9). H-9' (δ_{H} 3.92) showed a correlation with C-5' (δ_{C} 159.5).

Correlation spectroscopy (COSY) was used to show the correlation of protons in the compound. From the COSY spectrum (**Appendix 25**), there was a correlation between H-4' (δ_{H} 6.49) and H-8' (δ_{H} 2.69).

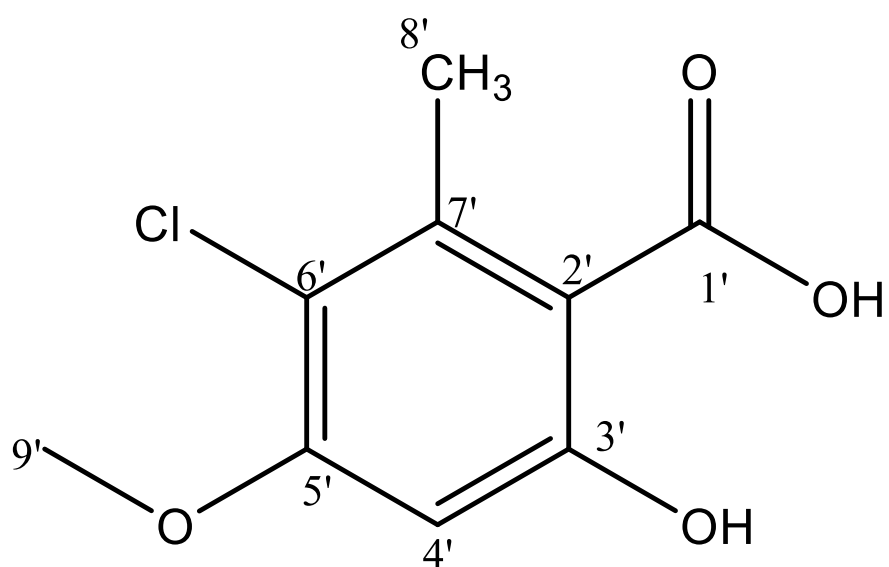
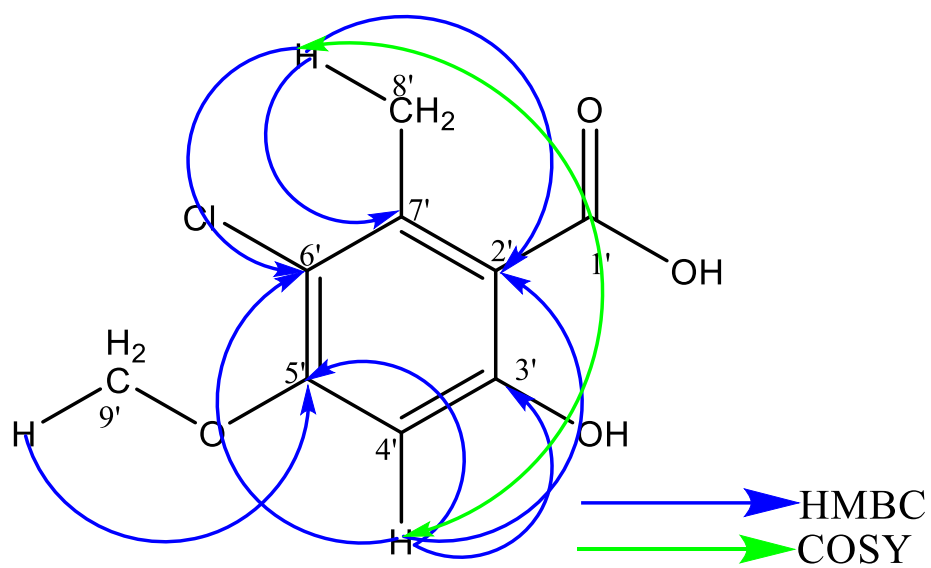


Figure 4.15 : Structure of compound 5 with and without HMBC and COSY correlations

4.4 Structure elucidation of isolated compounds from *Armillaria mellea*

4.4.1 Structure elucidation of compound 6

Compound **6** (Figure 4.17) was obtained as a brown oil with a mass of 2.40 mg and a retention time of 9.22 min. From the mass spectrum (Figure 4.16), the molecular formula of the compound was $C_{24}H_{30}O_8$ and the molecular ion mass $[M + Na]^+ m/z$ 469.18292. During the purification using prep- HPLC, the UV of compound **6** was observed to be 202 nm, 216 nm, 244 nm, 264 nm, 285 nm, 310 nm and 362 nm. Interpretation of 1D and 2D NMR data (Table 4.7) led to structure elucidation of the compound.

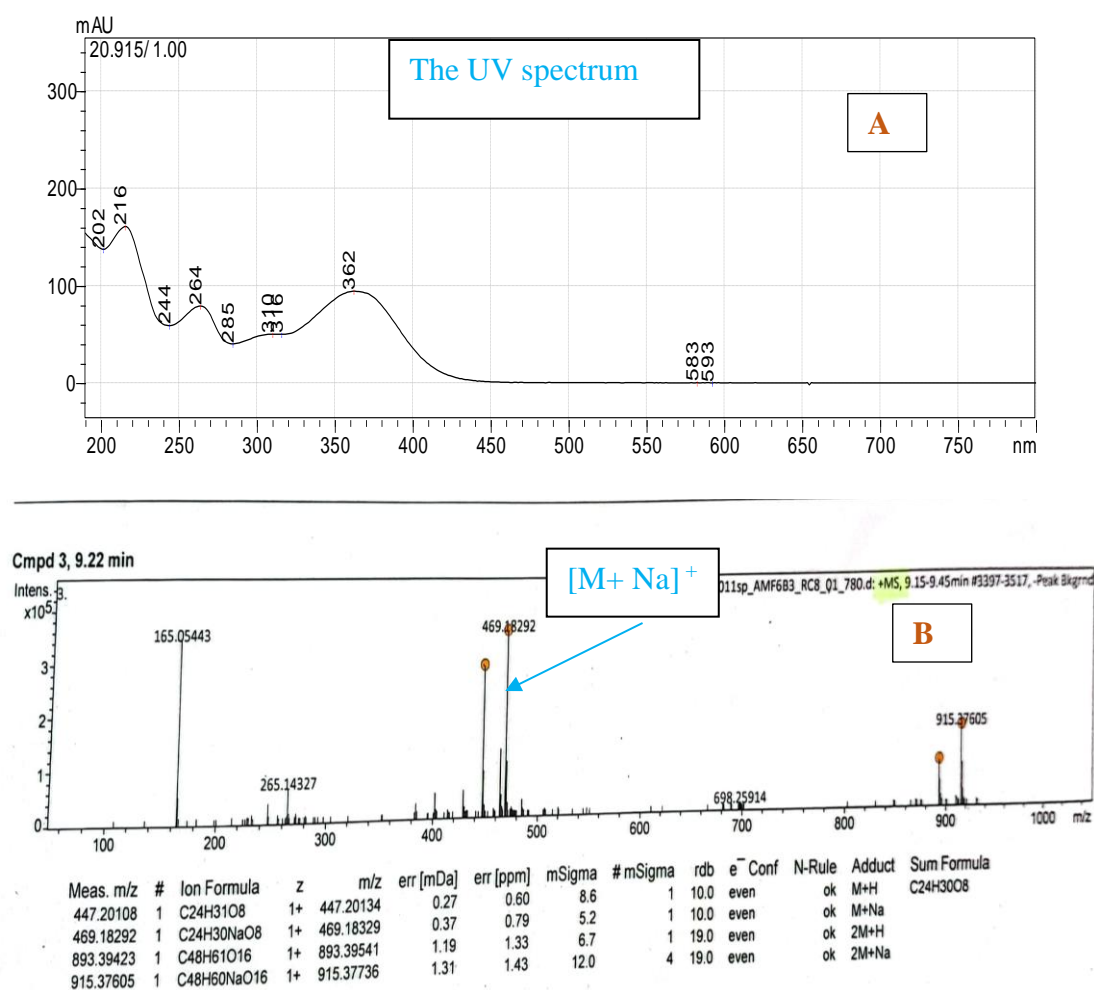


Figure 4.16: Spectrum of compound **6**. **A** showing the UV spectrum and **B** showing the molecular ion mass in positive mode

Table 4.7: NMR data of compound **6**

NO	¹³ CNMR	TYPE	HSQC	COSY	HMBC
1	196.6	CHO	9.52, s,		2, 3, 4
2	136.2	C	-	-	-
3	153.5	CH	6.92, s,		1, 4, 12
4	75.9	C	-	-	-
5	74.2	CH	5.78, d,	6	1', 2, 4, 6
6	32.9	CH ₂	1.98 m, 2.22, m,	5	4, 5, 7, 8, 9
7	37.5	C	-	-	-
8	21.8	CH ₃	1.41, s,		1, 4, 6, 7
9	55.4	CH	2.51, d,	10	3, 4, 6, 7, 10, 13
10	83.0	CH	3.70, d,	9	9, 13, 14
11	42.5	C	-	-	-
12	55.7	CH ₂	1.91, s,		10, 11, 13
13	77.5	C	-	-	-
14	28.7	CH ₃	1.18, s,		10, 11, 12, 15
15	24.3	CH ₃	0.99, s,		10, 11, 12, 14
1'	172.1	C	-	-	-
2'	106.9	C	-	-	-
3'	166.4	C	-	-	-
4'	100.0	CH	6.31, d,		3', 6'
5'	165.6	C	-	-	-
6'	111.8	CH	6.28, d,		2', 4', 5', 8'
7'	144.1	C	-	-	-
8'	24.6	CH ₃	2.33, s,		2', 6', 7'
9'	55.9	OCH ₃	3.80, s,		5'

The ^1H -NMR of compound **6** was used to show the multiplicity patterns and the type of protons in the compound. From the ^1H -NMR spectrum (**Appendix 26**), H5 (δ_{H} 5.78), H-9 (δ_{H} 2.51), H-10 (δ_{H} 3.70), H-4' (δ_{H} 6.31) and H-6' (δ_{H} 6.28) showed a doublet H-6 (δ_{H} 2.22, 1.98) showed a multiplet. H-1 (δ_{H} 9.52), H-3 (6.92), H-8 (δ_{H} 1.41), H-12 (δ_{H} 1.91), H-14 (δ_{H} 1.18), H-15 (δ_{H} 0.99) H-8' (δ_{H} 2.33) and H-9' (δ_{H} 3.80) showed a singlet indicating that there were no neighboring protons. The protons resonating at δ_{H} 0.99, 1.18, 1.41 and 2.33 indicated that that the compound has four methyl groups and the chemical shift at δ_{H} 3.80 indicated that the compound has a methyl group attached to an oxygen atom. The protons resonating at δ_{H} 6.28, 6.31 and 6.92, indicated a characteristic of aromatic protons therefore this suggested that the molecule contained a benzene ring. The proton resonating at δ_{H} 9.52 indicated a characteristic of an aldehyde proton.

The ^{13}C NMR spectrum (**Appendix 27**) showed that compound **6** had a total of 24 carbon atoms and the ten quaternary carbon atoms were obtained from the HMBC spectrum (**Appendix 28**). The quaternary carbon atoms were resonating at δ_{C} 37.5, 75.9, 136.2, 77.5, 42.5, 172.1, 106.9, 166.4, 165.6 and 144.1. From the spectrum, C-9' had a chemical shift of 55.9 ppm, this indicated that the carbon atom was oxygenated therefore it was a methoxy carbon. The carbon atoms resonating δ_{C} 83.0, 75.9, 77.5 and 166.4 was observed to be oxygenated with hydroxyl groups. C-1 (δ_{C} 196.6) indicated that the carbon atom was a carbonyl. The spectral data further revealed six aromatic carbons which were resonating at δ_{C} 136.2, 153.5, 106.9, 100.0, 111.8 and 144.1 showed a characteristic of the aromatic carbons. C-1' (δ_{C} 172.1) showed a characteristic of a carboxylic acid.

The HSQC spectrum (**Appendix 29**) was used to determine the correlation of protons and carbons in the compound. From the spectrum, the protons were observed to be directly attached to the carbon atoms. The protons H-1 (δ_{H} 9.52), H-3 (δ_{H} 6.92), H-5 (δ_{H} 5.78), H-6 (δ_{H} 1.98, 2.22), H-8 (δ_{H} 1.41), H-9 (δ_{H} 2.51), H-10 (δ_{H} 3.70), H-12 (δ_{H} 1.91), H-14 (δ_{H} 1.18), H-15 (δ_{H} 0.99), H-4' (δ_{H} 6.31), H-6' (δ_{H} 6.28), H-8' (δ_{H} 2.33) and H-9' (δ_{H} 3.80) were directly attached to C-1 (δ_{C} 196.6), C-3 (δ_{C} 153.5), C-5 (δ_{C} 74.2), C-6 (δ_{C} 32.9), C-8 (δ_{C} 21.8), C-9 (δ_{C} 55.4), C-10 (δ_{C} 83.0), C-12 (δ_{C} 55.7), C-14 (δ_{C} 28.7), C-15 (δ_{C} 24.3), C-4' (δ_{C} 100.0), C-6' (δ_{C} 111.8), C-8' (δ_{C} 24.6) and C-9' (δ_{C} 55.9) respectively.

The HMBC spectrum was used to determine the correlations of protons with carbon atoms that are two to three bonds away. These correlations showed carbon atoms which are next to each other in the compound. From the HMBC spectrum, the proton. H-8' (δ_{H} 2.33) showed strong correlations with C-2' (δ_{C} 106.9) which is a quaternary carbon atom, C-6' (δ_{C} 111.8) which is an aromatic carbon atom and C-7' (δ_{C} 144.1) which is a quaternary carbon

atom. H-14 (δ_{H} 1.18) and H-15 (δ_{H} 0.99) showed similar correlations with each other. Therefore, the two protons showed correlations with C-11 (δ_{C} 42.5) which is a quaternary carbon, C-12 (δ_{C} 55.7), which is methylene carbon and C-10 (δ_{C} 83.0) which is a hydroxylated carbon. Proton H-8 (δ_{H} 1.41) showed strong correlations with C-7 (δ_{C} 37.5) which is a quaternary carbon atom, C-6 (δ_{C} 32.9) which is a methylene carbon, and C-4 (δ_{C} 75.9) which is an oxygenated carbon atom. Proton H-5 (δ_{H} 5.78) showed a correlation with C-2 (δ_{C} 136.2) which is a quaternary carbon, C-4 (δ_{C} 75.9) which is an oxygenated carbon atom, C-6 (δ_{C} 32.9) which is a methylene carbon atom and with C-1' (170.4) which is a carbonyl carbon atom. The correlation of H-5 and C-1' showed the connection of the two rings through an oxygen bond. H-1 (δ_{H} 9.52) showed strong correlation with C-2 (δ_{C} 136.2) which is a quaternary carbon C-3 (δ_{C} 153.5) which is an aromatic carbon and C-4 (δ_{C} 75.9) which is an oxygenated carbon. H-9' (δ_{H} 3.80) showed a correlation with C-5' (δ_{C} 165.6) which is an oxygenated carbon.

Correlation spectroscopy (COSY) (**Appendix 30**) was used to show the correlations of the neighboring protons in the compound. From the spectrum, H-10 (δ_{H} 3.70) showed a correlation with H-9 (δ_{H} 2.51). H-6 (δ_{H} 1.98, 2.22) showed a correlation with H-5 (δ_{H} 5.78).

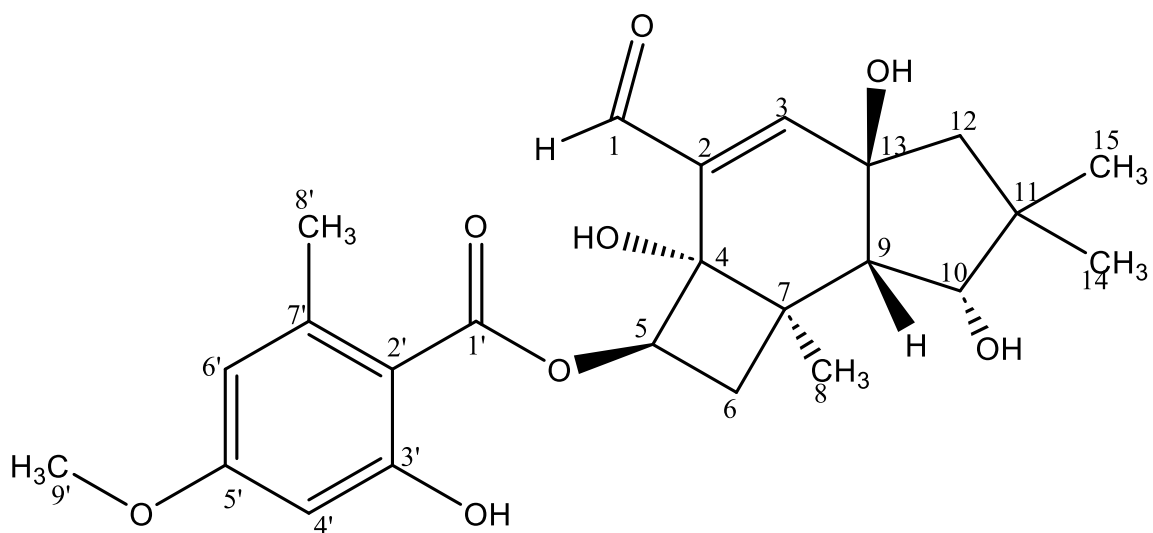
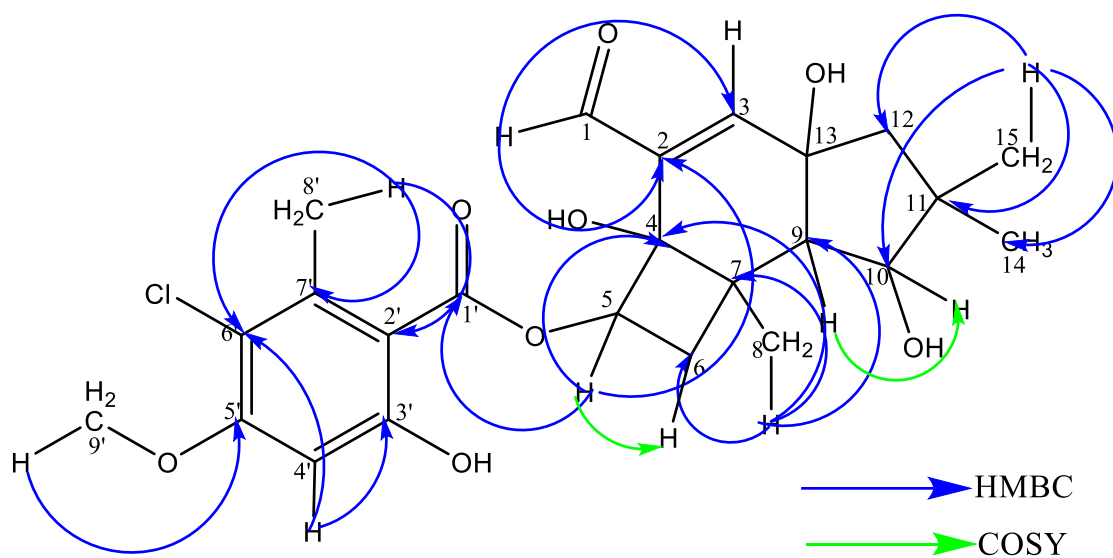
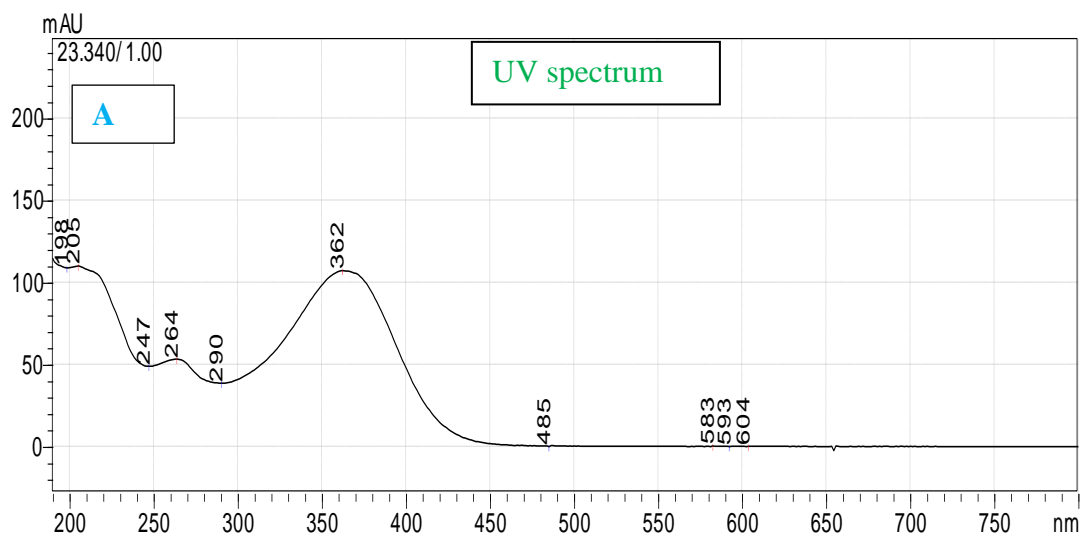


Figure 0.17: Structure of compound **6** with and without HMBC, COSY corrections

4.4.2 Structure elucidation of compound 7

Compound 7 (Figure 4.19) was obtained as a brown oil with a mass of 2.5 mg. During the purification using prep- HPLC, the UV of compound 7 was observed to be 205 nm, 247 nm, 264 nm, 290 nm and 362nm. From the mass spectrum, the molecular formula was $C_{24}H_{29}ClO_8$ and the molecular ion mass $[M + Na]^+$ was m/z 503.1442 (Figure 4.18). Interpretation of 1D and 2D NMR data (Table 4.8) led to structure elucidation of the compound.



Compound Spectrum SmartFormula Report

Analysis Info		Acquisition Date	
Analysis Name	D:\Data\sp\4013sp_AMF6B4_RE8_01_782.d	8/7/2023 7:53:28 PM	
Method	UHPLC ESI pos autoMSMS.m	Operator	MS-Labor, Uni Bremen
Sample Name	i4013sp_AMF6B4	Instrument	impact II 1825265.10199
Comment			

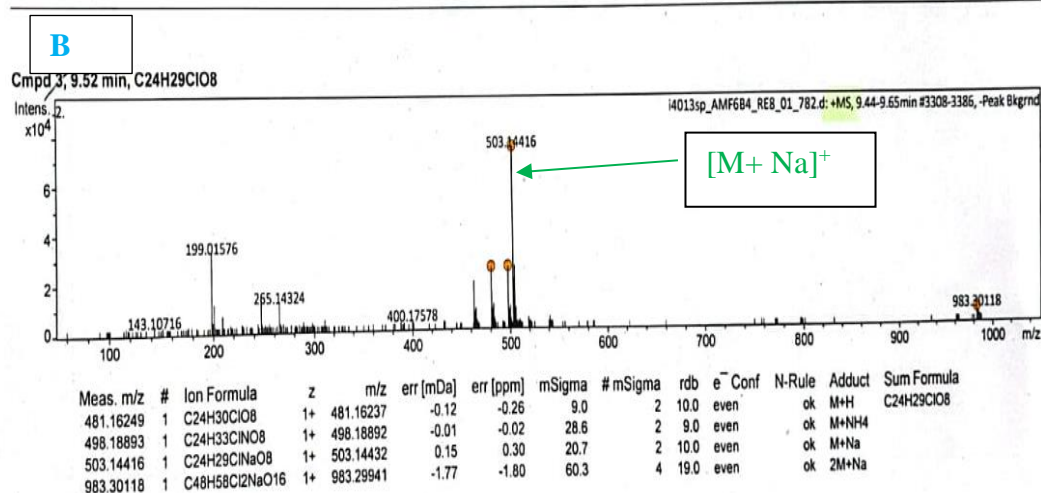


Figure 4.18 : Spectrum of compound 7. A showing the UV spectrum and B showing the molecular ion mass in positive mode

Table 4.8 :NMR data of compound **7**

NO	¹³ CNMR	TYPE	HSQC	COSY	HMBC
1	193.1	CHO	9.52, s		2, 3, 4
2	134.3	C	-	-	-
3	150.7	CH	6.90, s		1, 2, 4, 9,
4	74.6	C	-	-	-
5	73.4	CH	5.68, t		1', 2, 6
6	31.8	CH ₂	2.18, 2.03, d		5, 7, 9, 10
7	36.2	C	-	-	-
8	20.2	CH ₃	1.41, s,		4, 6, 7, 9
9	53.9	CH	2.50, m	10	5, 6, 7, 10,13
10	81.4	CH	3.70, d,	9	9, 13, 14
11	40.9	C	-	-	-
12	53.7	CH ₂	1.98, 1.90, s,		9, 10, 11, 13, 14, 15
13	75.8	C	-	-	-
14	27.1	CH ₃	1.18, s		10, 11, 12, 15
15	22.7	CH ₃	0.99, s		10, 11, 12, 14
1'	169.2	C	-	-	-
2'	108.8	C	-	-	-
3'	160.1	C	-	-	-
4'	97.8	CH	6.48, s		3', 5', 6', 7'
5'	158.8	C	-	-	-
6'	114.3	C	-	-	-
7'	137.6	C	-	-	-
8'	17.8	CH ₃	2.39, s		2', 6', 7'
9'	55.3	OCH ₃	3.88, s		5'

The ^1H -NMR of compound **7** was used to show the multiplicity and the type of protons in the compound. From the ^1H -NMR spectrum (**Appendix 31**), H-5 (δ_{H} 5.78), H-9 (δ_{H} 2.50), H-10 (δ_{H} 3.70) and H-4' (δ_{H} 6.31) showed a doublet. H-4 (δ_{H} 2.03, 2.18) showed a multiplet. Singlet protons were observed in H-8 (δ_{H} 6.90), H-10 (δ_{H} 1.90, 1.98), H-12 (δ_{H} 1.41), H-13 (δ_{H} 9.52), H-14 (δ_{H} 0.99) H-15 (δ_{H} 1.18), H-8' (δ_{H} 2.33) and H-9' (δ_{H} 3.80). The protons resonating at δ_{H} 0.99, 1.18, 1.41 and 2.33 showed a characteristic of methyl protons therefore this indicated that that the compound contained four methyl groups and the proton resonating at δ_{H} 3.80 indicated that the compound has a methyl group attached to an oxygen atom (methoxy). The higher chemical shift of these methyl protons is due to the presence of the oxygen atom. The protons resonating at δ_{H} 6.48 and 6.90, indicated a characteristic of aromatic. The proton resonating at δ_{H} 9.52 indicated a characteristic of an aldehyde proton.

The ^{13}C NMR spectrum (**Appendix 32**) showed that compound **7** had a total of 24 carbon atoms and the eleven quaternary carbon atoms were obtained from the HMBC spectrum (**Appendix 33**). The quaternary carbon atoms were resonating at δ_{C} 36.2, 40.9, 74.6, 75.8, 108.8, 114.3, 134.3, 137.6, 158.8, 160.1, and 169.2. The spectral data further revealed a methoxy group resonating at δ_{C} 55.3 and four hydroxylated carbons resonating at δ_{C} 74.6, 77.8, 81.4 and 160.1. The carbon resonating at δ_{C} 193.1 revealed a characteristic of an aldehyde functional group and six aromatic carbons were observed to be resonating at δ_{C} 97.8, 108.8, 114.3, 134.3, 137.6, 150.7. A characteristic of a carboxylic acid was observed in a carbon resonating at δ_{C} 169.2. To further determine the structure of the compound, HSQC (**Appendix 34**) spectral data was used to reveal the correlation of protons and carbons in the compound. From the spectrum, the protons were observed to be directly attached to the carbon atoms. The protons H-1 (δ_{H} 9.52), H-3 (δ_{H} 6.90), H-5 (δ_{H} 5.68), H-6 (δ_{H} 2.03, 2.18), H-8 (δ_{H} 1.41), H-9 (δ_{H} 2.50), H-10 (δ_{H} 3.70), H-12 (δ_{H} 1.90, 1.98), H-14 (δ_{H} 1.18), H-15 (δ_{H} 0.99), H-4' (δ_{H} 6.48), H-8' (δ_{H} 2.39) and H-9' (δ_{H} 3.88) were directly attached to C-1 (δ_{C} 193.1), C-3 (δ_{C} 150.7), C-5 (δ_{C} 73.4), C-6 (δ_{C} 31.8), C-8 (δ_{C} 20.2), C-9 (δ_{C} 53.9), C-10 (δ_{C} 81.4), C-12 (δ_{C} 53.7), C-14 (δ_{C} 27.1), C-15 (δ_{C} 22.7), C-4' (δ_{C} 97.8), C-8' (δ_{C} 17.8) and C-9' (δ_{C} 55.3) respectively.

The HMBC spectral data was further used to determine the correlations of protons with carbon atoms that are two to three bonds away. These correlations showed carbon atoms which are next to each other in the compound. From the HMBC spectrum, the proton H-8' (δ_{H} 2.39) showed strong correlations with C-2' (δ_{C} 108.8) which is a quaternary carbon atom, C-6' (δ_{C} 114.3) which is a chlorinated carbon atom and C-7' (δ_{C} 137.6) which is a quaternary carbon atom. H-14 (δ_{H} 1.18) and H-15 (δ_{H} 0.99) showed similar correlations with each other. Therefore, the two protons showed correlations with C-10 (δ_{C} 81.4) which is a hydroxylated

carbon, C-11 (δ_C 40.9) which is a quaternary carbon and with C-12 (δ_C 57.3) which is a methylene carbon. Proton H-18 (δ_H 1.41) showed strong correlations with C-4 (δ_C 74.6) which is an oxygenated carbon atom, C-6 (δ_C 31.8) which is a methylene carbon and C-7 (δ_C 36.2) which is a quaternary carbon atom. Proton H-5 (δ_H 5.68) showed a correlation with C-2 (δ_C 134.3) C-6 (δ_C 31.8) and C-1' (δ_C 169.2). H-1 (δ_H 9.52) showed strong correlation with C-2 (δ_C 134.3) which is a quaternary carbon, C-3 (δ_C 150.7) which is an aromatic carbon and C-4 (δ_C 74.6) which is an oxygenated carbon. H-9' (δ_H 3.80 ppm) showed a correlation with C-5' (δ_C 165.6) which is a quaternary carbon.

Correlation spectroscopy (COSY) (**Appendix 35**) was used to show the correlations of the neighboring protons in the compound. From the spectrum, H-10 (δ_H 3.70) showed a correlation with H-9 (δ_H 2.50).

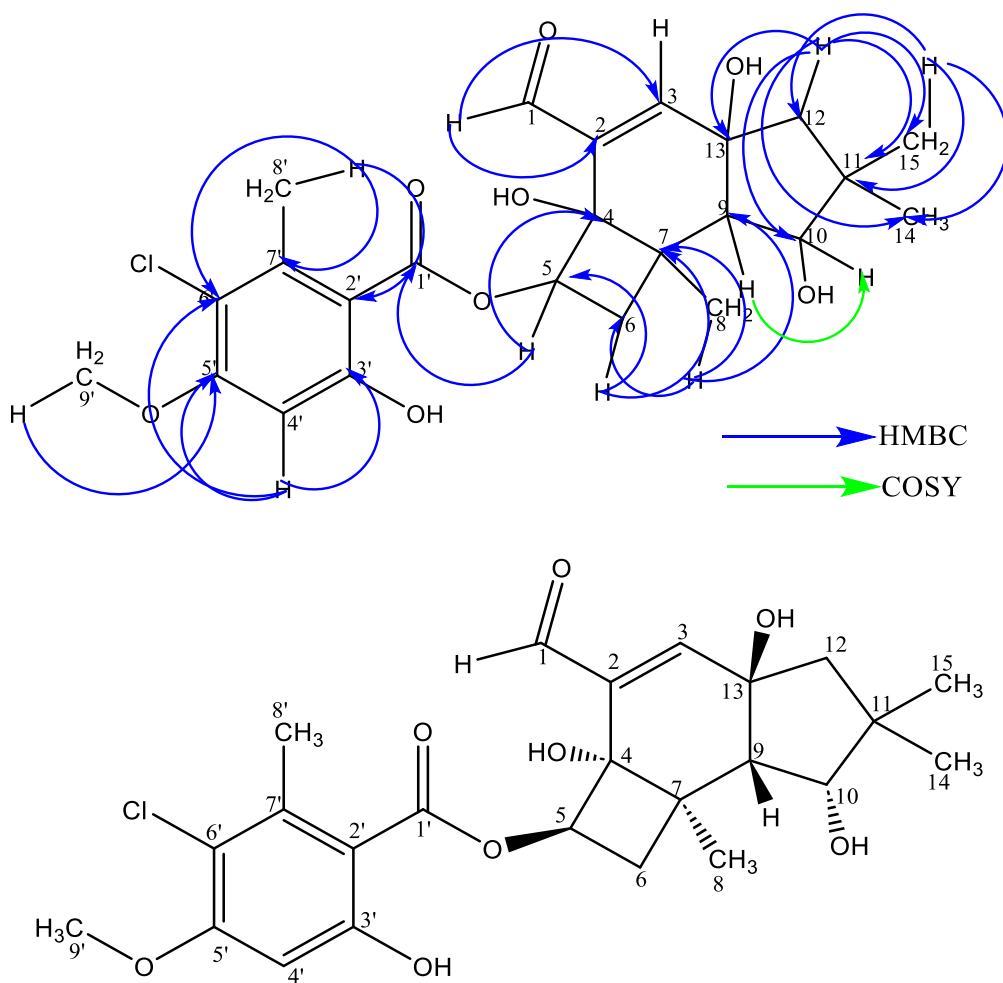
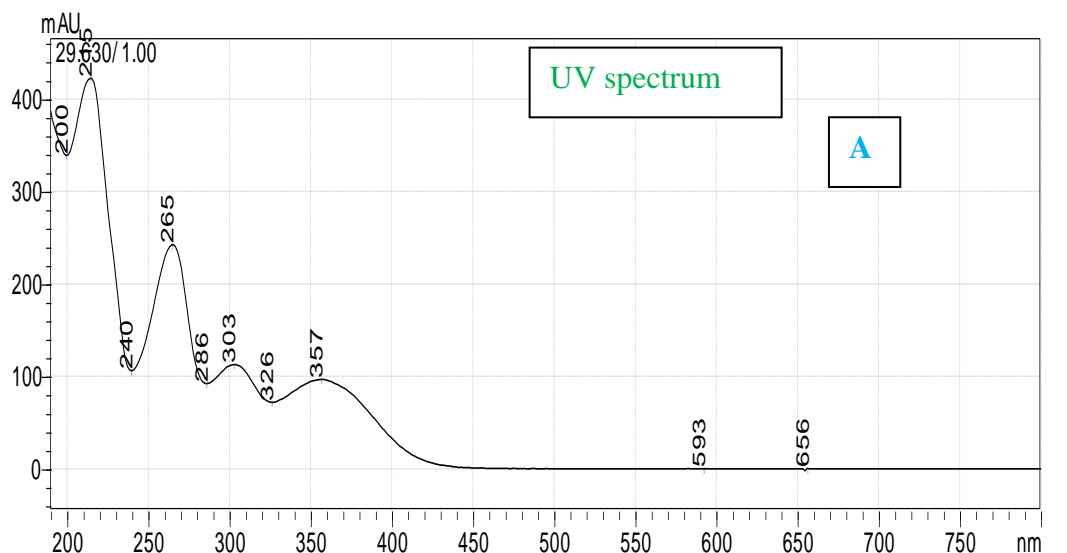


Figure 4.19: Structure of compound 7 with and without HMBC, COSY correlations

4.4.3 Structure elucidation of compound 8

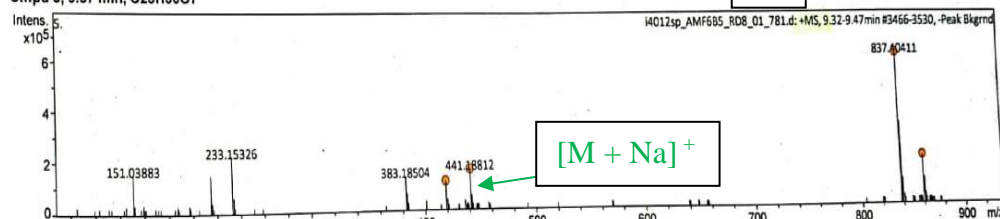
Compound **8** (Figure 4.21) was obtained as a brown oil with a mass of 2.0 mg. During the purification using prep- HPLC, the UV of compound **8** was observed to be 215 nm, 265 nm, 303 nm, and 357 nm. The mass spectrum revealed a molecular formula to be $C_{23}H_{30}O_7$ and the molecular ion mass $[M + Na]^+$ m/z 441.1881 (Figure 4.20). Interpretation of 1D and 2D NMR data (Table 4.9) led to structure elucidation of the compound.



Compound Spectrum SmartFormula Report

Analysis Info		Acquisition Date	8/7/2023 7:23:47 PM
Analysis Name	D:\Data\sp\i4012sp_AMF6B5_RD8_01_781.d	Operator	MS-Labor, Uni Bremen
Method	UHPLC ESI pos autoMSMS.m	Instrument	impact II 1825265.10199
Sample Name	i4012sp_AMF6B5		
Comment			

Cmpd 5, 9.37 min, C23H30O7



Meas. m/z	#	Ion Formula	z	m/z	err [mDa]	err [ppm]	mSigma	#mSigma	rdb	e ⁻ Conf	N-Rule	Adduct	Sum Formula
419.20612	1	C23H31O7	1+	419.20643	0.31	0.73	3.0	1	9.0	even	ok	M+H	C23H30O7
441.18812	1	C23H30NaO7	1+	441.18837	0.25	0.57	11.7	2	9.0	even	ok	M+Na	
837.40411	1	C46H61O14	1+	837.40558	1.47	1.76	12.4	3	17.0	even	ok	2M+H	
859.38600	1	C46H60NaO14	1+	859.38753	1.53	1.78	6.9	2	17.0	even	ok	2M+Na	

Figure 4.20: Spectrum of compound **8**. A showing the UV spectrum and B showing the molecular ion mass in positive mode

Table 4.9: NMR data of compound **8**

NO	¹³ C NMR	TYPE	HSQC	COSY	HMBC
1	62.2	CH ₂	3.94, d, 4.22, d		2, 3, 4
2	46.7	C	-		-
3	132.7	CH	5.90, s		1, 2, 12, 13
4	76.0	C	-		-
5	75.7	CH	5.65, t		1', 4, 6
6	32.3	CH ₂	1.76, m, 1.98, t		5, 7, 8
7	36.3	C	-		-
8	20.4	CH ₃	1.38, s		4, 6, 7, 9
9	80.9	CH	3.61, s		7
10	81.5	CH	3.57, s		12, 13, 14
11	42.3	C	-		-
12	44.5	CH ₂	1.50, dd, 1.98, t		3, 10, 11, 13
13	34.8	CH	2.89, s		2, 3, 10, 12
14	28.0	CH ₃	1.01, s		10, 11, 12
15	22.7	CH ₃	1.05, s		10, 11, 12, 14
1'	170.8	C	-		-
2'	143.6	C	-		-
3'	164.7	C	-		-
4'	100.4	CH	6.18, s		1', 3', 5'
5'	162.5	C	-		-
6'	111.1	CH	6.20, s		4', 7'
7'	104.4	C			
8'	23.0	CH ₃	2.29, s		2', 6', 7'

The ^1H - NMR (**Appendix 36**) of compound **8** revealed three doublets which were resonating at δ_{H} 3.57, 3.61 and 5.90, six singlets resonating at δ_{H} 1.01, 1.05, 1.38, 2.29, 6.18, 6.20. The spectral data further revealed three aromatic protons were resonating at δ_{H} 5.90, 6.18, 6.20, four methyl protons resonating at δ_{H} 1.01, 1.05, 1.38 and 2.29 and two methylene protons resonating at δ_{H} 3.94 and 4.22

The ^{13}C NMR spectrum (**Appendix 37**) showed that compound **7** had a total of 23 carbon atoms and the nine quaternary carbon atoms were obtained from the HMBC spectrum (**Appendix 38**). The quaternary carbon atoms were resonating at δ_{C} 36.3, 46.7, 42.3, 76.0, 104.4, 143.6, 162.5, 164.7, and 170.8. The spectral data further revealed four methyl groups resonating at δ_{H} 20.4 (H-8), 22.7 (H-15), 28.0 (H-14) and 23.0 (H-8'). The carbon atom resonating at δ_{C} 62.2 (H-1) suggested that the compound contained an alcohol group. The carbon resonating at δ_{C} 81.5 (H-10), 75.7 (H-5), 164.7 (H-3') and 162.5 (H-5') were a characteristic of oxygenated carbon atoms. The carbons resonating at δ_{C} 132.7 (H-3), 143.6 (H-2'), 100.4 (H-4'), 111.1 (H-6') and 104.4 (H-7') indicated that the compound contained the aromatic protons. The carbons resonating at δ_{C} 32.3 and 44.5 suggested they are the methylene protons. The chemical shift at δ_{C} 170.8 (H-1') suggested that the compound also contains a carboxylic acid.

The HSQC spectrum (**Appendix 39**) was used to determine the correlation of protons and carbons in the compound. The protons were observed to be directly attached to the carbon atoms. From the spectrum, the protons H-1 (δ_{H} 3.94, 4.22), H-3 (δ_{H} 5.90), H-5 (δ_{H} 5.65), H-6 (δ_{H} 1.76, 1.98), H-8 (δ_{H} 1.38), H-9 (δ_{H} 3.61), H-10 (δ_{H} 3.57), H-12 (δ_{H} 1.50, 1.98), H-13 (δ_{H} 2.89), H-14 (δ_{H} 1.01), H-15 (δ_{H} 1.05), H-4' (δ_{H} 6.18), H-6' (δ_{H} 6.20), H-8' (δ_{H} 2.29) were directly attached to C-1 (δ_{C} 62.2), C-3 (δ_{C} 132.7), C-5 (δ_{C} 75.7), C-6 (δ_{C} 32.3), C-8 (δ_{C} 20.4), C-9 (δ_{C} 80.9), C-10 (δ_{C} 81.5), C-13 (δ_{C} 34.8), C-12 (δ_{C} 44.5), C-14 (δ_{C} 28.0), C-15 (δ_{C} 22.7), C-4' (δ_{C} 100.4), C-6' (δ_{C} 111.1) and C-8' (δ_{C} 23.0) respectively.

The HMBC spectrum was used to determine the correlations of protons with carbon atoms that are two to three bonds away. These correlations showed carbon atoms which are next to each other in the compound. From the spectrum, the proton H-8' (δ_{H} 2.29) showed strong correlations with C-2' (δ_{C} 143.6) which is a quaternary carbon atom, C-6' (δ_{C} 111.1) which is an aromatic carbon atom and C-7' (δ_{C} 104.4) which is a quaternary carbon atom.

The proton H-14 (δ_{H} 1.01) and H-15 (δ_{H} 1.05) showed similar correlations which each other. Therefore, the two protons showed correlations with C-10 (δ_{C} 81.5) which is the hydroxylated carbon, C-11 (δ_{C} 42.3) which is a quaternary carbon and C-12 (δ_{C} 44.5 ppm) which is a methylene carbon atom. Proton H-8 (δ_{H} 1.38) showed strong correlations with C-7

(δ_C 36.3) which is a quaternary carbon atom, C-6 (δ_C 32.3) which is a methylene carbon, and C-4 (δ_C 76.0) which is a quaternary carbon atom and with C-2 (δ_C 46.7) which is a quaternary carbon. Proton H-5 (δ_H 5.65) showed a correlation with C-6 (δ_C 32.3) which is a methylene carbon atom, C-4 (δ_C 76.0) which is an oxygenated quaternary carbon atom and C-1' (δ_C 170.8) which is a carbonyl carbon atom.

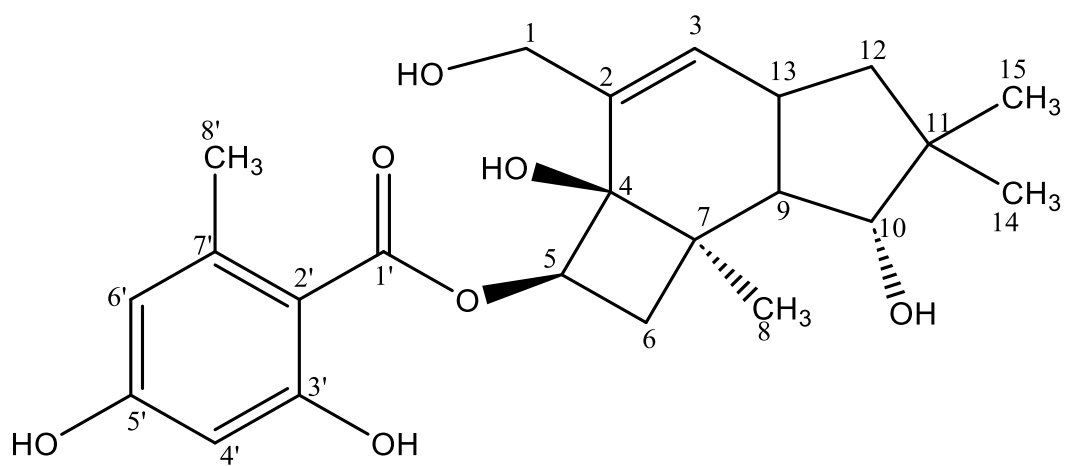
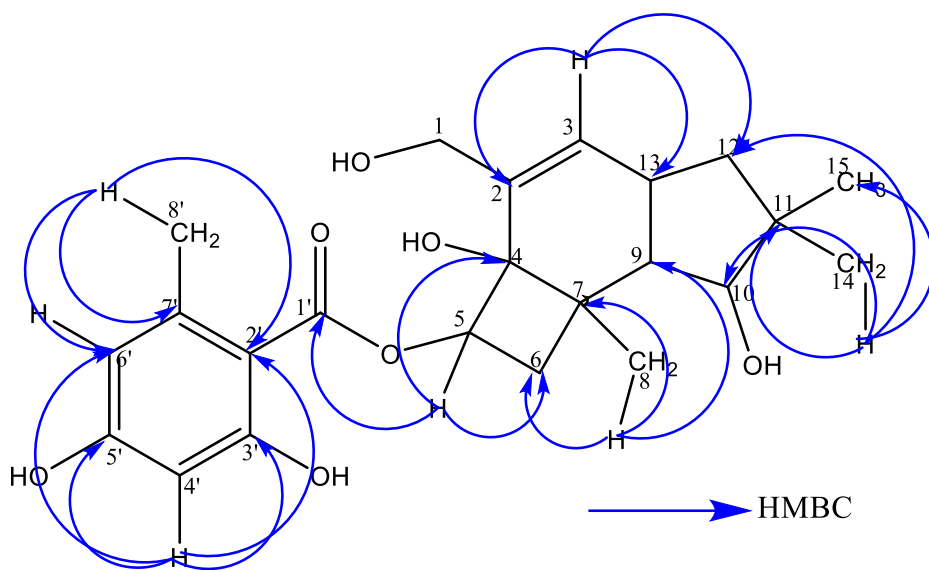
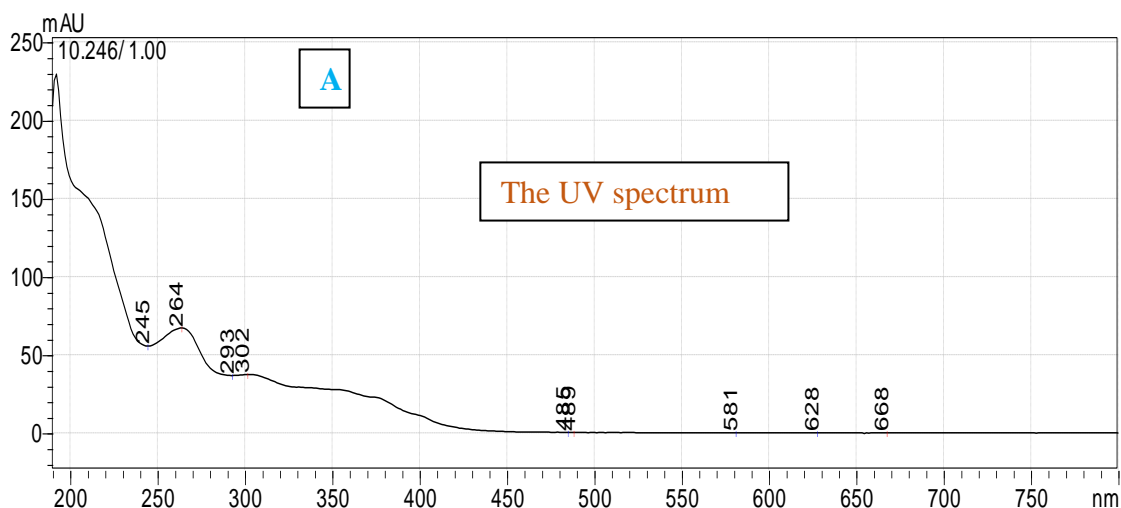


Figure 4.21: Structure of compound **8** with and without HMBC correlations

4.4.4 Structure elucidation of compound 9

Compound 9 (Figure 4.23) was obtained as a brown oil with a mass of 2.5mg. The spectrum of prep- HPLC revealed the UV of compound 9 to be 215 nm, 264 nm, 302 nm, and 357 nm and the mass spectrum showed a molecular ion mass $[M+H]^+$ m/z 433.1853 with the molecular formula of $C_{23}H_{28}O_8$ (Figure 4.22). Interpretation of 1D and 2D NMR data (Table 4.10) led to structure elucidation of the compound.



Compound Spectrum SmartFormula Report

Analysis Info		Acquisition Date	
Analysis Name	D:\Data\Josphat\i4029sp_AMF5A_RB6_01_834.d	8/14/2023 11:02:12 PM	
Method	UHPLC ESI pos autoMSMS.m	Operator	MS-Labor, Uni Bremen
Sample Name	i4029sp_AMF5A	Instrument	impact II 1825265.10199
Comment			

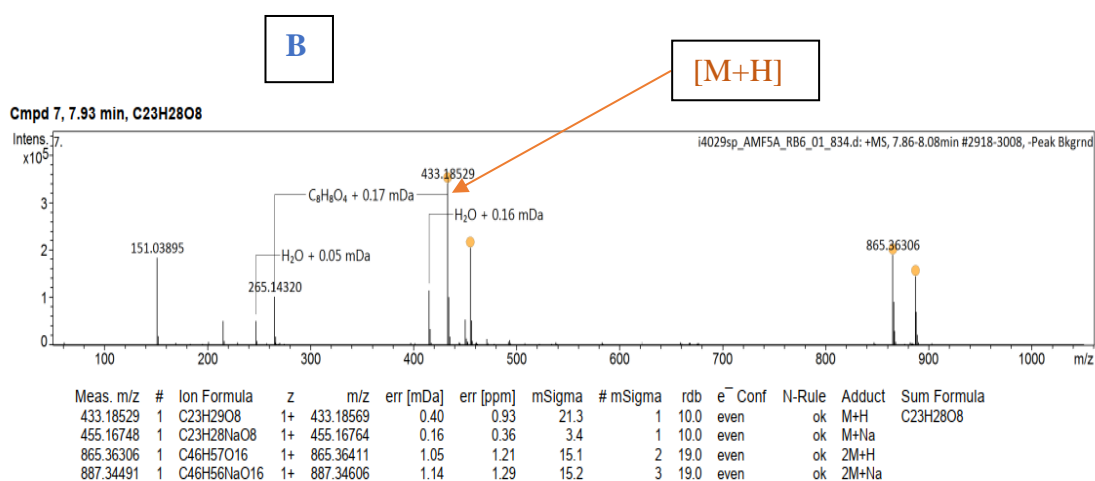


Figure 4.22: Spectrum of compound 9. A showing the UV spectrum and B showing the molecular ion mass in positive mode

Table 4.10: NMR data of compound **9**

NO	¹³ CNMR	TYPE	HSQC, mult.	COSY	HMBC
1	195.2	CHO	9.52, s		2, 4, 12
2	134.9	C	-	-	-
3	152.1	CH	7.01 s		
4	74.1	C	-	-	-
5	72.8	CH	5.76, t		1', 2, 4, 6,
6	31.7	CH ₂	1.34, m,		11, 7, 13
7	35.9	C	-	-	-
8	20.8	CH ₃	1.40, s,		6, 7, 9
9	54.1	CH	2.51, d,	10	
10	81.3	CH	3.71, d	9	11, 12, 13, 14
11	53.8	C	-	-	-
12	40.9	CH ₂	3.61, s,		
13	76.0	C	-	-	-
14	27.2	CH ₃	1.18, s,		10, 11, 12, 15
15	22.7	CH ₃	0.97, s,		10, 11, 12, 14
1'	174.4	C	-	-	-
2'	143.5	C	-	-	-
3'	166.8	C	-	-	-
4'	128.1	CH	7.32, m		
5'	164.2	C			
6'	111.6	CH	6.17, s		5', 6', 7', 8'
7'	104.2	C	-	-	-
8'	23.1	CH ₃	2.29, s		1', 2', 6', 7'

The ^1H -NMR of compound **9** was used to show the multiplicity patterns and the type of protons in the compound. From the ^1H -NMR spectrum (**Appendix 40**), H-10 (δ_{H} 3.70) and H-9 (δ_{H} 2.51) showed a doublet. This indicated that H-10 and H-9, protons had one neighboring proton. H-6 (δ_{H} 1.34) and H-4' (δ_{H} 7.32) showed a multiplet multiplicity. This indicated that there were multiple protons neighboring these two protons. H-12 (δ_{H} 3.61), H-8 (δ_{H} 1.40), H-1 (δ_{H} 9.52), H-15 (δ_{H} 0.97) H-14 (δ_{H} 1.18), and H-8' (δ_{H} 2.29) showed a singlet indicating that there were no neighboring protons to these protons. The protons resonating at δ_{H} 0.97, 1.18, 1.40 and 2.29 showed a characteristic of methyl protons therefore this indicated that that the compound has four methyl groups. The protons resonating at δ_{H} 6.17 and 7.32 indicated a characteristic of aromatic protons therefore this suggested that the molecule contained a benzene ring. The proton resonating at δ_{H} 9.52 indicated a characteristic of an aldehyde proton therefore this suggested that the compound contained an aldehyde functional group.

The ^{13}C NMR spectrum (**Appendix 41**) showed that compound **9** had a total of 23 carbon atoms and the nine quaternary carbon atoms were obtained from the HMBC spectrum (**Appendix 42**). The quaternary carbon atoms were C-2 (δ_{C} 134.9), C-4 (δ_{C} 74.1), C-7 (δ_{C} 35.9), C-11 (δ_{C} 53.8), C-13 (δ_{C} 76.0), C-1' (δ_{C} 174.4), C-2' (δ_{C} 143.5), C-3' (δ_{C} 166.8), C-5' (δ_{C} 164.2) and C-7' (δ_{C} 104.2). The spectral data was also used to show the type of the carbon in the compound. From the spectrum, C-4 (δ_{C} 74.1), C-10 (δ_{C} 81.3), C-13 (δ_{C} 76.0) C-3' (δ_{C} 166.8) and C-5' (δ_{C} 164.2) was observed to be oxygenated with hydroxyl groups. C-1 (δ_{C} 195.2) indicated that the carbon atom was a carbonyl. C-2 (δ_{C} 134.9), C-3 (δ_{C} 152.1), C-2' (δ_{C} 143.5), C-4' (δ_{C} 128.1), C-6' (δ_{C} 111.6) and C-7' (δ_{C} 104.2) showed a characteristic of the aromatic carbons. C-1' (δ_{C} 174.4) showed a characteristic of a carboxylic acid. This suggested that the compound contained a carboxylic acid.

The HSQC spectrum (**Appendix 43**) was used to determine the correlation of protons and carbons in the compound. From the spectrum, the protons were observed to be directly attached to the carbon atoms. The protons H-1 (δ_{H} 9.52), H-3 (δ_{H} 7.01), H-5 (δ_{H} 5.76), H-6 (δ_{H} 1.34), H-8 (δ_{H} 1.40), H-9 (δ_{H} 2.51), H-10 (δ_{H} 3.71), H-12 (δ_{H} 3.61), H-14 (δ_{H} 1.18), H-15 (δ_{H} 0.97), H-4' (δ_{H} 7.32), H-6' (δ_{H} 6.17) and H-8' (δ_{H} 2.29). Were directly attached to C-1 (δ_{C} 195.2), C-3 (δ_{C} 152.1), C-5 (δ_{C} 72.8), C-6 (δ_{C} 31.7), C-9 (δ_{C} 54.1), C-10 (δ_{C} 81.3), C-12 (δ_{C} 40.9), C-8 (δ_{C} 20.8), C-15 (δ_{C} 22.7), C-14 (δ_{C} 27.2), C-4' (δ_{C} 128.1), C-6' (δ_{C} 111.6) and C-8' (δ_{C} 23.1) respectively.

The HMBC spectrum was used to determine the correlations of protons with carbon atoms that are two to three bonds away. These correlations showed carbon atoms which are next to each other in the compound. From the HMBC spectrum, the proton H-8' (2.29) showed

strong correlations with C-2' (δ_C 143.5) which is a quaternary carbon atom, C-6' (δ_C 111.6) which is an aromatic carbon atom and C-7' (δ_C 104.2) which is a quaternary carbon atom. H-15 (δ_H 0.97) and H-14 (δ_H 1.18) showed similar correlations with each other. Therefore, the two protons showed correlations with C-10 (δ_C 81.3) which is a hydroxylated carbon, C-11 (δ_C 53.8) which is a quaternary carbon and C-12 (δ_C 40.2), which is methylene carbon. Proton H-8 (δ_H 1.40) showed strong correlations with C-6 (δ_C 31.7) which is a methylene carbon, C-7 (δ_C 35.9) which is a quaternary carbon atom and C-9 (δ_C 54.1). Proton H-5 (δ_H 5.76) showed a correlation with C-6 (δ_C 31.7) which is a methylene carbon atom, C-4 (δ_C 74.1) which is an oxygenated carbon atom, C-2 (δ_C 134.9) which is a quaternary carbon and with C-1' (δ_C 174.4) which is a carbonyl carbon atom. H-1 (δ_H 9.52) showed strong correlation with C-4 (δ_C 74.1) which is an oxygenated carbon, C-2 (δ_C 134.9) which is a quaternary carbon and C-3 (δ_C 152.1) which is an aromatic carbon. The COSY spectrum (**Appendix 44**) showed a correlation between H-10 (δ_H 3.71) and H-9 (δ_H 2.51)

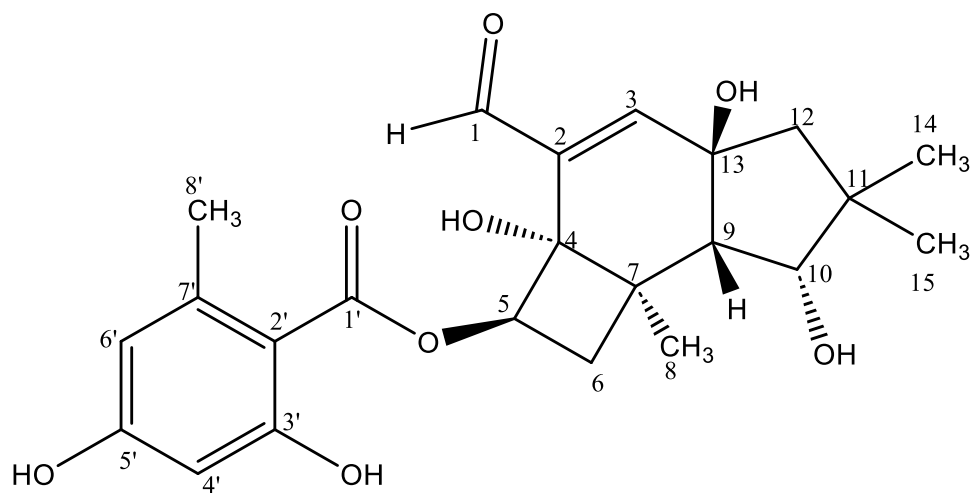
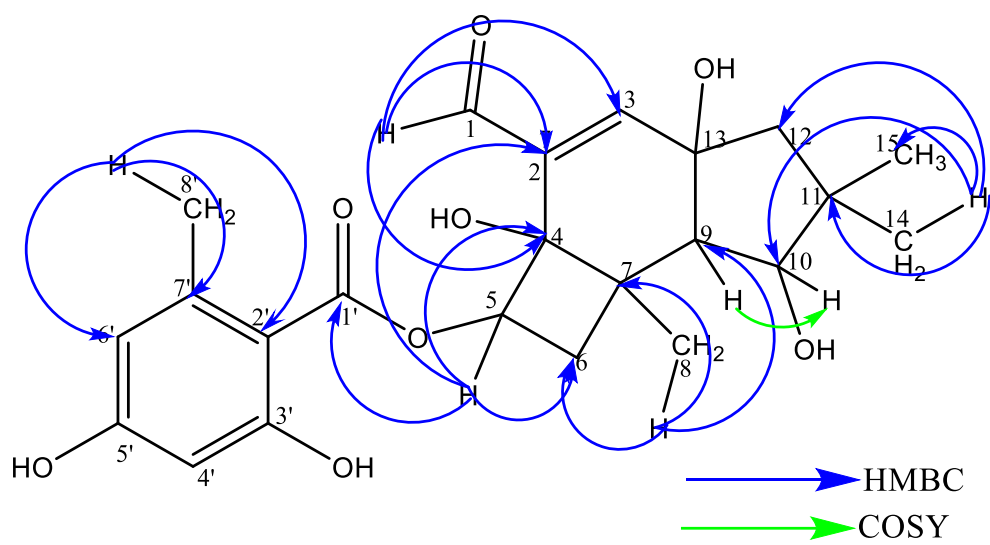


Figure 4.23: Structure of compound **9** with and without HMBC correlations

4.5 Structure elucidation of isolated compound(s) from *Armillaria gallica*

4.5.1 Structure elucidation of compound 10

Compound 10 (Figure 4.25) was isolated a white solid with a mass of 0.8 mg. The retention time of the compound was 4.12 mins and its UV at 194 nm (Figure 4.24). Mass spectrometry revealed a molecular ion mass m/z 292.18 Interpretation of 1D and 2D NMR data (Table 4.11) led to structure elucidation of the compound.

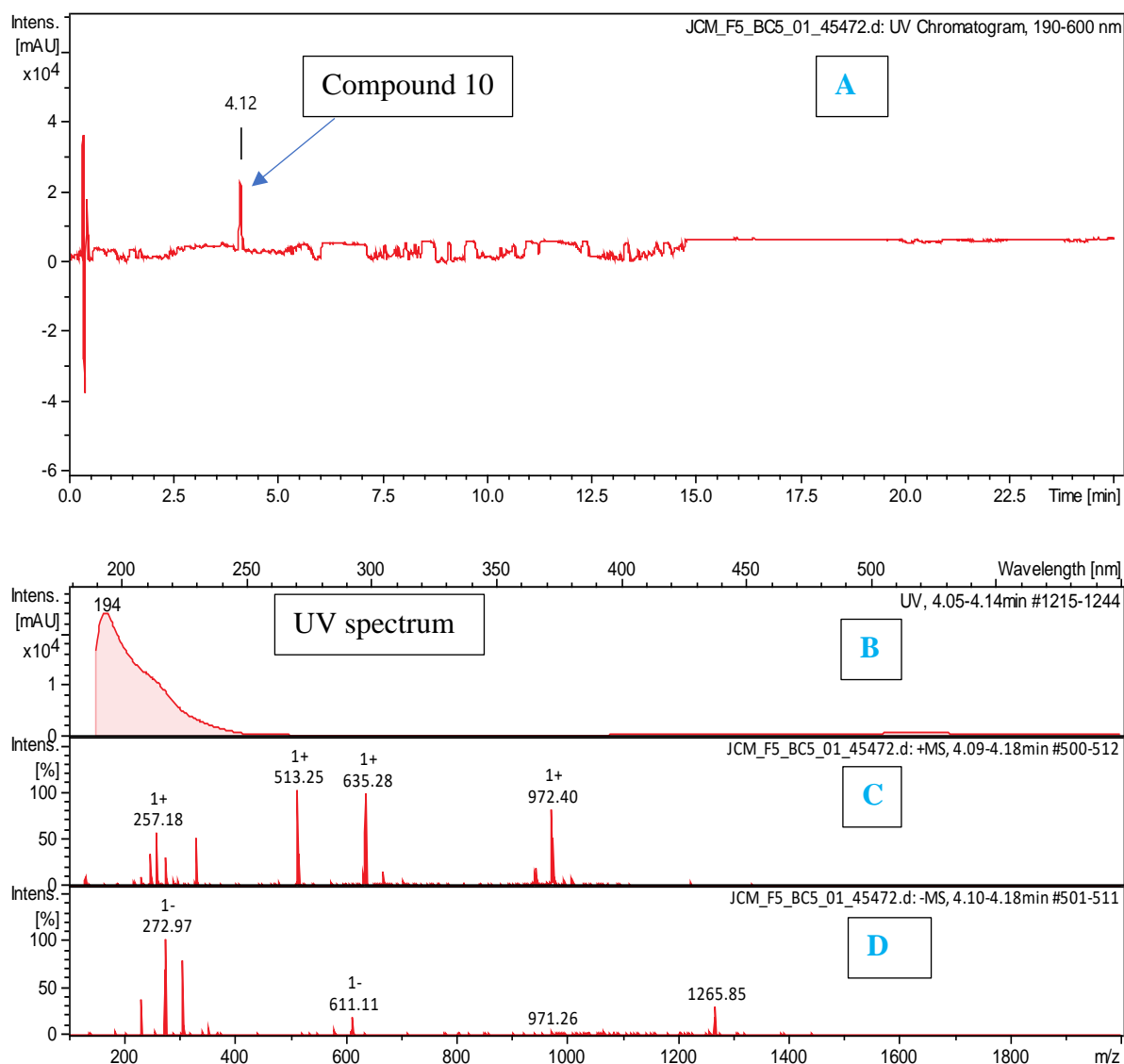


Figure 4.24: Mass spectrum of compound 10. A showing liquid (LC) chromatogram with the retention time. B showing the UV spectrum of the compound. C showing the molecular ion mass in positive mode and D showing the molecular on mass in the negative mode

Table 4.11: NMR data of compound **10**

NO	¹³ CNMR	TYPE	HSQC, mult.	COSY	HMBC
2	168.6	C	-	-	-
3	87.2	C	-	-	-
5	169.9	C	-	-	-
6	84.0	C	-	-	-
7	44.7	CH ₂	2.92, d, 3.57, d		5, 6, 8, 9
8	126.9	C	-	-	-
9	132.1	CH	7.30, m	10	8, 12
10	129.3	CH	7.23, m	11,9	11
11	127.9	CH	7.18, m	10	10
12	130.9	CH	7.23, m	11,9	11
13	132.1	CH	7.30, m	10	12
14	48.5	CH ₂	1.55, dd, 1.83, dd	17	2, 3, 15
15	23.2	CH	0.93, m	17	14, 16, 17
16	22.7	CH ₃	0.90, d		15, 14, 17
17	22.8	CH ₃	1.72, d	15	15, 14, 16

The ^1H -NMR of compound **10** was used to determine the multiplicity and the type of protons in the compound. From the ^1H -NMR spectrum (**Appendix 45**), H-7 (δ_{H} 2.92, 3.57), H-16 (δ_{H} 0.90) and H-17 (δ_{H} 1.72) showed a doublet indicating that there was a single proton neighbouring these two protons. H-9 (δ_{H} 7.30), H-10 (δ_{H} 7.23), H-11 (δ_{H} 7.18), H-12 (δ_{H} 7.23), H-13 (δ_{H} 7.30) and H-15 (δ_{H} 0.93) showed a multiplet indicating that there were multiple neighbouring protons to these protons. The protons resonating at δ_{H} 7.18, 7.23 and 7.30, were a characteristic of aromatic protons. The protons resonating at δ_{H} 0.90 and 0.93 were a characteristic of methyl protons therefore this indicated that the compound has two methyl groups. The protons resonating at δ_{H} 2.92 and 3.57 indicated the methylene protons.

The ^{13}C -NMR spectrum (**Appendix 46**) showed a total of fifteen carbon atoms. C-2 (δ_{C} 168.6), C-3 (δ_{C} 87.2), C-5 (δ_{C} 169.9), C-6 (δ_{C} 84.0), C-7 (δ_{C} 44.7), C-8 (δ_{C} 126.9), C-9 (δ_{C} 132.1), C-10 (δ_{C} 129.3), C-11 (δ_{C} 127.9), C-12 (δ_{C} 130.9), C-13 (δ_{C} 132.1), C-14 (δ_{C} 48.5), C-15 (δ_{C} 23.2), C-16 (δ_{C} 22.7), and C-17 (δ_{C} 22.8). The quaternary carbons were five; C-2 (δ_{C} 168.6), C-3 (δ_{C} 87.2), C-5 (δ_{C} 169.9), C-6 (δ_{C} 84.0) and C-8 (δ_{C} 126.9) were identified using the HMBC spectrum (**Appendix 47**). The ^{13}C -NMR spectrum was also used to show the type of carbon atoms present in the compound. From the spectrum, C-9 (δ_{C} 132.1), C-10 (δ_{C} 129.3), C-11 (δ_{C} 127.9) C-12 (δ_{C} 130.9) and C-13 (δ_{C} 132.1) were identified as the aromatic carbons. C-2 (δ_{C} 168.6) and C-5 (169.9) were identified as carbonyl carbon atoms. C-3 (δ_{C} 87.2) and C-6 (δ_{C} 84.0) were a characteristic of hydroxylated carbons.

Heteronuclear single quantum coherence (HSQC) spectroscopy was used to show correlations of protons and carbons. From the HSQC spectrum (**Appendix 48**), protons were observed to be directly attached to the carbon atoms. H-7 (δ_{H} 2.92, 3.57), H-9 (δ_{H} 7.30), H-10 (δ_{H} 7.23), H-11 (δ_{H} 7.18), H-12 (δ_{H} 7.23), H-13 (δ_{H} 7.30), H-14 (δ_{H} 1.55, 1.83), H-15 (δ_{H} 0.93), H-16 (δ_{H} 0.90), and H-17 (δ_{H} 1.72) were observed to be directly attached to C-7 (δ_{C} 44.7), C-9 (δ_{C} 132.1), C-10 (δ_{C} 129.3), C-11 (δ_{C} 127.9) C-12 (δ_{C} 130.9), C-13 (δ_{C} 132.1), C-14 (δ_{C} 48.5), C-15 (δ_{C} 23.2), C-16 (δ_{C} 22.7), and C-17 (δ_{C} 22.8) respectively.

Heteronuclear multiple bond correlation (HMBC) spectroscopy was used to show correlation between protons and carbons that are two to three bonds away from each other. From HMBC spectrum, H-7 (δ_{H} 2.92, 3.57) showed strong correlations with C-5 (δ_{C} 168.6), C-6 (δ_{C} 84.0), C-8 (δ_{C} 126.9), and C-9 (δ_{C} 132.1). H-9 (δ_{H} 7.26) showed correlations with C-8 (δ_{C} 129.9), and C-12 (δ_{C} 130.9). H-10 (δ_{H} 7.14) showed correlations with C-11 (δ_{C} 127.9). H-16 (δ_{H} 0.90) and H-17 (δ_{H} 1.72) showed similar correlations. The two protons showed strong correlations with C-14 (δ_{C} 48.5) and C-15 (δ_{C} 23.2).

Correlation spectroscopy (COSY) was used to show the correlation between the neighbouring protons in the compound. From COSY spectrum (**Appendix 49**), H-9 (δ_{H} 7.30) showed a correlation with H-10 (δ_{H} 7.23). H-14 (δ_{H} 1.55, 1.83) showed a correlation with H-17 (δ_{H} 1.72). H-15 (δ_{H} 0.93) also had a correlation with H-17

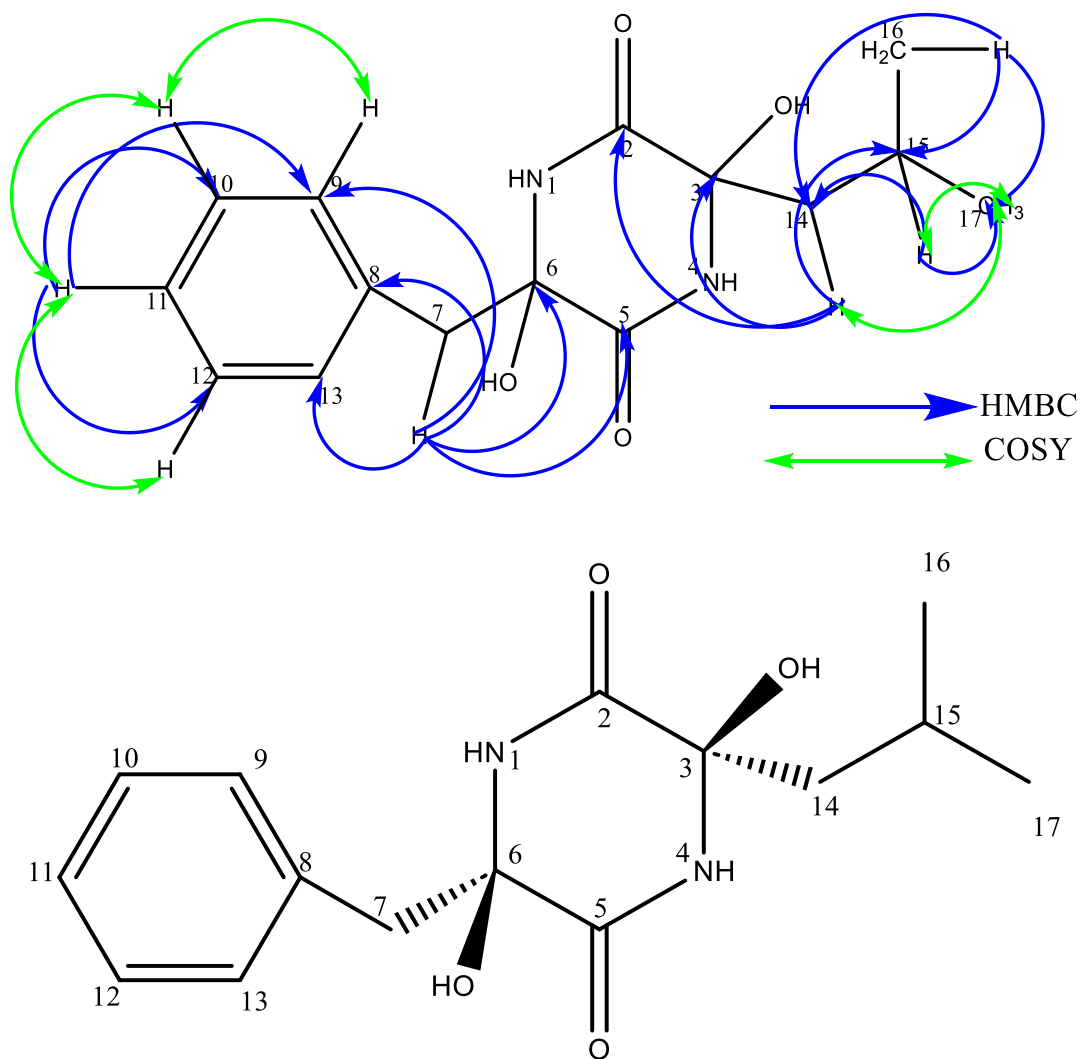


Figure 4.25: Structure of compound 10 with and without HMBC, COSY correlations

4.6 Discussion

4.6.1 Characterization and bioactivity of the secondary metabolites

Compound **1** and compound **2** were isolated from *Desarmillaria ectypa* fermented on rice media the two compounds were observed to be chlorinated at C-6' (δ_C 115.1 and 115.7 respectively). The difference between the two compounds was observed in C-1 and C-3. In compound **1**, C-1 was observed to be resonating at δ_C 196.0, which is an aldehyde. The $^1\text{H-NMR}$ spectrum showed a peak resonating at δ_H 9.48 which was a singlet. This indicated that it was an aldehyde proton therefore attached to C-1. While in compound **2**, the chemical shift of C-1 was observed to be resonating at δ_C 59.2 in which the HSQC spectrum indicated a methylene carbon, and the $^1\text{H-NMR}$ spectrum showed a chemical shift at δ_H 4.23 and 4.30. From the analysis of both 1D and 2D NMR data, C-1 of compound two was an alcohol group. C-3 of compound **1** showed a chemical shift of δ_C 158.5 and its proton was δ_H 6.81 indicating that C-3 in this compound is an aromatic carbon while in compound **2**, C-3 was observed to be resonating at δ_C 74.6 and its proton had a chemical shift of δ_H 4.21. The analysis of the experimental data indicated that C-3 was hydroxylated. Compound **1**, is a known compound and have been isolated from cultured mycelium of *Armillaria mellea* (Yang *et al.*, 1984). Comparison of the reported data of Yang *et al.* (1984) and the experimental results shows that compound **1**, is highly similar as Armillaridin isolated from *A. mellea*. Compound **1** was active against *B. subtilis* (DSM 10) and *M. hiemalis* (DSM 2656) showing that the compound is a potential candidate for antimicrobials. Armillaridin have been reported to possess anticancer activity (Chi *et al.*, 2013). Therefore, this compound have recently gained attention for its antimicrobial activity and also for possessing activity against several cancer cell lines (Hovey *et al.*, 2017). Compound **2**, is also a known compound and have been isolated from the mycelia of *Armillaria mellea* (Donnelly *et al.*, 1986). The comparison of the experimental data and the reported data by Donnelly *et al.* (1986) were similar indicating that compound **2** is Arnamiol isolated from *A. mellea*.

Compound **3** was isolated from the supernatant of *D. ectypa* which was cultured on Q6 media (5 g of D-glucose, 20 g of glycerine and 10 g of cotton seed flour). In comparison to compound **1** and **2**, there was a difference at C-5' (δ_C 163.4), C-6' (δ_C 112.5), and at C-14 (δ_C 68.4). Compound **3** lacked chlorination at C-6' (δ_C 112.5). The carbon at position C-5' in compound **3** was observed to be hydroxylated whereas in compound **1** and **2** C-5' was observed to contain a methoxy group. C-6' in compound **3** was an aromatic carbon with its proton resonating at δ_H 6.26 which was a doublet. C-15 (δ_C 68.4) in compound **3** was an alcohol group with its proton resonating at δ_H 3.53 whereas in compound **1** and **2**, C-15 (δ_C 31.6 and 27.0

respectively) was a methyl group. This is the first report on isolation and structure elucidation of compound **3**. Therefore it is isolated as a new melleolide to be 10, 15-dihydroxydihydromelleolide.

Compound **4** is similar to compound **10** the difference between the two compounds was observed to be in C-3. Compound **4** was isolated from *D. ectypa* which was fermented in rice media. In compound **4**, C-3 was observed to be resonating at δ_C 86.4 in which the methoxy group was attached to this carbon. The correlation between C-18 (δ_C 48.0, which is a methoxy carbon) and C-3 which is a quaternary carbon atom from the HMBC spectrum confirmed that C-3 was attached to a methoxy carbon. While in compound **10**, C-3 was observed to be resonating at δ_C 87.2 in which the hydroxy group was attached to this carbon atom. The absence of C-18 in compound **10** indicated the difference between the two compounds. Compound **4** is a known compound and have been isolated as Diatretol from *D. ectypa* and also from *Clitocybe diatreta* a basidiomycete fungus (Arnone *et al.*, 1996). The similarity of chemical shifts of carbons and protons in the experimental results to the studies of Arnone *et al.* (1996) confirms that the two compounds are the same. From the study, Diatretol was tested for the activity against *Bacillus cereus* and *B. subtilis* and was found to be active at 50 μg discs⁻¹. Diatretol have also been reported to be antiparasitic against *Plasmodium falciparum* (Ishiyama *et al.*, 2021). This indicates that the compound have antiparasitic and antimicrobial properties. Compound **10** was isolated from *A. gallica* also fermented on rice media. The compound was obtained from isocratic method (35 % Methanol + 65 % Water) in prep-HPLC from which it had a retention time of 12.0 mins. Compound **10** showed a very weak activity against *S. aureus* (ATCC 25923) and *E.coli* (ATCC 25922). This no activity observed was contributed by low amounts of the compounds. This compound has also been reported from *Lapista sordida* (Phylum Basidiomycota, Family Tricholomataceae) as a yellowish amorphous powder. Therefore it is a known compound, Lepistamide B (3,6-dioxygenated diketopiperazine) (Chen *et al.*, 2011). The comparison of reported data by Chen *et al.* (2011) with the experimental data shows that the two compounds are similar the report shows that the compound was reported to possess antibacterial activity. This indicates that compound **10** is a good candidate of antimicrobials.

Compound **5**, 3-chloro-6-hydroxy-4-methoxy-2-methylbenzoic acid, was isolated from *D. ectypa* which was cultured in rice media. The UV (222 nm, 259 nm, 306 nm) pattern observed in this compound resembled the UV of the isolated melleolides (compounds **1**, **2**, **3**, **6**, **7**, **8** and **9**). Compound **5** had nine carbon atoms from the NMR data obtained. The elucidated

structure suggested that compound **5** was isolated only as the Orsellinic ring residue without the protoilludane (5/6/4 ring system) backbone.

The structure of compound **6** and compound **9** were similar the difference was observed in C-5'. In compound **6**, C-5' (δ_C 165.6) was attached to a methoxy group while in compound **9**, C-5' (δ_C 164.2) was attached to hydroxyl group. The correlation of H-9' (δ_H 3.80) with C-5' in HMBC spectrum in compound **6** confirmed that it was a methoxy carbon attached to C-5'. Compound **6** is a known compound and have been isolated as 5'-O-methylmelledonal (Donnelly *et al.*, 1987). The comparison of experimental data and the reported data of Donnelly (1987) shows that compound **6** is the isolated compound, 5'-O-methylmelledonal. Compound **9**, Melledonal, is also a known compound and was isolated from *Armillaria mellea* (Donnelly *et al.*, 1985). Compound **8**, 10 α -hydroxydihydromelleolide is a known compound and was isolated from *A. mellea* (Donnelly *et al.*, 1990). In comparison of compound **8** with compound **6** and **9**, the difference was observed mainly in C-13 and C-1. C-1 (δ_C 62.2) in compound **8** was observed to be an alcohol and C-13 (δ_C 34.8) was observed to be a methine carbon. For compound **6** and **9**, C-1 was an aldehyde while C-13 was hydroxylated. Compound **7** was isolated from *A. mellea* which was fermented on rice media. This compound was purified using isocratic method in Prep- HPLC using 75 % Methanol and 25 % water. Compound **7** was also similar to compound **6**. The difference between the two compounds was observed in carbon at position 6'. In compound **7**, C-6' was chlorinated while in compound **6** the C-6' carbon was an aromatic carbon. Compound **7** was previously isolated from *A. mellea* cultured on liquid media (Arnone *et al.*, 1988) therefore it is a known compound, melledonal C. The studies of Arnone *et al.* (1988), shows that this compound was tested for antibacterial activity against *Bacillus cereus* (ATCC 10702) and *B. subtilis* (ATCC 6633) and was reported to be active against these test microorganisms. This indicates that the compounds from *A. mellea* are a potential candidate for antimicrobial drugs.

CHAPTER FIVE

CONCLUSIONS AND RECOMMENDATIONS

6.1 Conclusions

In relation to the study, the following conclusions were made;

- i. The crude extracts from *Armillaria* species were successfully characterized where, the ethyl acetate crude extracts of *D. ectypa* (MUCL 31078), *A. mellea* (STMA 12328) and *A. gallica* (STMA 12242) yielded compounds **1-10**. Only compound **3** was isolated as a previously undescribed compound while the other compounds were known compounds. The melleolides were identified as compound **1, 2, 3, 6, 7, 8** and compound **9** because they contain 6/5/4 ring system. Compound **5** was isolated as orsellinic acid residue without the protoilludane backbone structure. Compounds **4** and **10** were isolated as diketopiperazines. Most of the compounds that were isolated from *D. ectypa* have been reported from *A. mellea* but not from *D. ectypa*.
- ii. The compounds and the crude extracts showed a very weak activity against *S. aureus* and *E. coli*. Compound **1** showed an activity against *M. hiemalis* (33.3 µg/mL) and *B. subtilis* (8.3 µg/mL). This shows that compound **1** is a potential candidate for antimicrobial.
- iii. The chemical structures of compounds **1-10** were successfully elucidated using liquid-chromatography mass spectroscopy and 1D, 2D NMR spectroscopy.

6.2 Recommendations

In relation to this study, the following recommendations were made.

- i. The crude extracts and the pure compounds should be tested for their bioactivity against wide range microorganisms. The pure compounds and crude extracts may show activity against other microorganisms.
- ii. The fungi in this study were fermented on rice media and Q6^{1/2} (2.5 g/L of D-glucose, 10 g/L of glycerine and 5 g/L of cotton seed flour) media. Different types of media should also be used to ferment these fungi since different secondary metabolites could be isolated other than the ones that have been isolated.
- iii. Only one previously undescribed compound was isolated from the supernatant of liquid cultures of *D. ectypa* therefore more exploration of secondary metabolites on liquid cultures should be conducted since more new compounds could be isolated. From the study, the metabolites from the mycelium were not explored therefore further studies should be conducted on the mycelium since novel secondary metabolites could be isolated.

REFERENCES

- Alara, J. A., & Alara, O. R. (2024). An overview of the global alarming increase of multiple drug resistant: A major challenge in clinical diagnosis. *Infectious Disorders-Drug Targets (Formerly Current Drug Targets-Infectious Disorders)*, 24(3), 26–42. <https://doi.org/10.2174/1871526523666230725103902>
- Antonín, V., Tomšovský, M., Sedlák, P., Májek, T., & Jankovský, L. (2009). Morphological and molecular characterization of the *Armillaria cepistipes*–*A. gallica* complex in the Czech Republic and Slovakia. *Mycological Progress*, 8(3), 259–271. <https://doi.org/10.1007/s11557-009-0597-1>
- Arnone, A., Capelli, S., Nasini, G., Meille, S. V., & Vajna de Pava, O. (1996). Secondary mould metabolites. 52. Structure elucidation of diatretole-A new diketopiperazine metabolite from the fungus *Clitocybe diatretole*. *Liebigs Annalen*, 1996(11) 1875–1877. <https://doi.org/10.1002/jlac.199619961123>
- Arnone, A., Cardillo, R., Nasini, G., & Meille, S. V. (1988). Secondary mould metabolites. Part 19. Structure elucidation and absolute configuration of melledonals B and C, novel antibacterial sesquiterpenoids from *Armillaria mellea*. X-ray molecular structure of melledonal C. *Journal of the Chemical Society, Perkin Transactions 1*(3), 503–510. <https://doi.org/10.1002/chin.198825315>
- Baumgartner, K., Coetzee, M. P. A., & Hoffmeister, D. (2011). Secrets of the subterranean pathosystem of *Armillaria*. *Molecular Plant Pathology*, 12(6), 515–534. <https://doi.org/10.1111/j.1364-3703.2010.00693.x>
- Bohnert, M., Nützmann, H.-W., Schroeckh, V., Horn, F., Dahse, H.-M., Brakhage, A. A., & Hoffmeister, D. (2014). Cytotoxic and antifungal activities of melleolide antibiotics follow dissimilar structure–activity relationships. *Phytochemistry*, 105(3), 101–108. <https://doi.org/10.1016/j.phytochem.2014.05.009>
- Breijyeh, Z., Jubeh, B., & Karaman, R. (2020). Resistance of gram-negative bacteria to current antibacterial agents and approaches to resolve it. *Molecules*, 25(6), 1340–1348. <https://doi.org/10.3390/molecules25061340>
- Cadelis, M. M., Copp, B. R., & Wiles, S. (2020). A review of fungal protoilludane sesquiterpenoid natural products. *Antibiotics*, 9(12), 928–929. <https://doi.org/10.3390/antibiotics9120928>
- Carneiro, R., Lima, F. S. O., & Correia, V. R. (2017). Methods and tools currently used for the identification of plant parasitic nematodes. *Nematology-Concepts, Diagnosis and*

- Control*, 19(1), 21–25. <https://doi.org/10.5772/intechopen.69403>
- Castañeda-Ramírez, G. S., Torres-Acosta, J. F. de J., Sánchez, J. E., Mendoza-de-Gives, P., González-Cortázar, M., Zamilpa, A., Al-Ani, L. K. T., Sandoval-Castro, C., de Freitas Soares, F. E., & Aguilar-Marcelino, L. (2020). The possible biotechnological use of edible mushroom bioproducts for controlling plant and animal parasitic nematodes. *BioMed Research International*, 2020(1), 6-17. <https://doi.org/10.1155/2020/6078917>
- Chen, X., Wu, M., Ti, H., Wei, X., & Li, T. (2011). Three New 3, 6-Dioxygenated Diketopiperazines from the Basidiomycete *Lepista sordida*. *Helvetica Chimica Acta*, 94(8), 1426–1430. <https://doi.org/10.1002/hlca.201000455>
- Chi, C.-W., Chen, C.-C., & Chen, Y.-J. (2013). Therapeutic and radiosensitizing effects of armillaridin on human esophageal cancer cells. *Evidence-Based Complementary and Alternative Medicine*, 2013(1), 459271-459272. <https://doi.org/10.1155/2013/459271>
- Ciurea, C. N., Kosovski, I.-B., Mare, A. D., Toma, F., Pinteá-Simon, I. A., & Man, A. (2020). *Candida* and *candidiasis*—opportunism versus pathogenicity: A review of the virulence traits. *Microorganisms*, 8(6), 857-860. <https://doi.org/10.3390/microorganisms8060857>
- Coetzee, M. P. A., Wingfield, B. D., & Wingfield, M. J. (2018). *Armillaria* root-rot pathogens: species boundaries and global distribution. *Pathogens*, 7(4), 83-85. <https://doi.org/10.3390/pathogens7040083>
- Devkota, P., & Hammerschmidt, R. (2020). The infection process of *Armillaria mellea* and *Armillaria solidipes*. *Physiological and Molecular Plant Pathology*, 112(3), 101543-101545. <https://doi.org/10.1016/j.pmpp.2020.101543>
- Donnelly, D. M. X., Coveney, D. J., Fukuda, N., & Polonsky, J. (1986). New sesquiterpene aryl esters from *Armillaria mellea*. *Journal of Natural Products*, 49(1), 111–116. <https://doi.org/10.1021/np50043a013>
- Donnelly, D. M. X., Coveney, D. J., & Polonsky, J. (1985). Melledonal and melledonol, sesquiterpene esters from *Armillaria mellea*. *Tetrahedron Letters*, 26(43), 5343–5344. [https://doi.org/10.1016/s0040-4039\(00\)95035-4](https://doi.org/10.1016/s0040-4039(00)95035-4)
- Donnelly, D. M. X., Hutchinson, R. M., Coveney, D., & Yonemitsu, M. (1990). Sesquiterpene aryl esters from *Armillaria mellea*. *Phytochemistry*, 29(8), 2569–2572. [https://doi.org/10.1016/0031-9422\(90\)85190-q](https://doi.org/10.1016/0031-9422(90)85190-q)
- Donnelly, D. M. X., Quigley, P. F., Coveney, D. J., & Polonsky, J. (1987). Two new sesquiterpene esters from *Armillaria mellea*. *Phytochemistry*, 26(11), 3075–3077. [https://doi.org/10.1016/s0031-9422\(00\)84599-9](https://doi.org/10.1016/s0031-9422(00)84599-9)

- Dyshko, V., Hilszczańska, D., Davydenko, K., Matic, S., Moser, W. K., Borowik, P., & Oszako, T. (2024). An overview of mycorrhiza in pines: Research, species, and applications. *Plants*, *13*(4), 506-508. <https://doi.org/10.3390/plants13040506>
- Gressler, M., Löhr, N. A., Schäfer, T., Lawrinowitz, S., Seibold, P. S., & Hoffmeister, D. (2021). Mind the mushroom: natural product biosynthetic genes and enzymes of Basidiomycota. *Natural Product Reports*, *38*(4), 702–722. <https://doi.org/10.1039/d0np00077a>
- Harms, K., Surup, F., Stadler, M., Stchigel, A. M., & Marin-Felix, Y. (2021). Morinagadepsin, a Depsipeptide from the Fungus *Morinagamyces vermicularis* gen. et comb. nov. *Microorganisms*, *9*(6), 1191-1192. <https://doi.org/10.3390/microorganisms9061191>
- He, M.-Q., Zhao, R.-L., Liu, D.-M., Denchev, T. T., Begerow, D., Yurkov, A., Kemler, M., Millanes, A. M., Wedin, M., & McTaggart, A. R. (2022). Species diversity of Basidiomycota. *Fungal Diversity*, *114*(1), 281–325. <https://doi.org/10.1007/s13225-021-00497-3>
- Heinzelmann, R., Dutech, C., Tsykun, T., Labbé, F., Soularue, J.-P., & Prospero, S. (2019). Latest advances and future perspectives in *Armillaria* research. *Canadian Journal of Plant Pathology*, *41*(1), 1–23. <https://doi.org/10.1080/07060661.2018.1558284>
- Hovey, M. T., Cohen, D. T., Walden, D. M., Cheong, P. H., & Scheidt, K. A. (2017). A carbene catalysis strategy for the synthesis of protoilludane natural products. *Angewandte Chemie*, *129*(33), 9996–9999. <https://doi.org/10.1002/ange.201705308>
- Ishiyama, A., Hokari, R., Nonaka, K., Chiba, T., Miura, H., Otoguro, K., & Iwatsuki, M. (2021). Diatretol, an α , α' -dioxo-diketopiperazine, is a potent in vitro and in vivo antimalarial. *The Journal of Antibiotics*, *74*(4), 266–268. <https://doi.org/10.1038/s41429-020-00390-2>
- Kajaria, D. K., Gangwar, M., Kumar, D., Sharma, A. K., Tilak, R., Nath, G., Tripathi, Y. B., Tripathi, J. S., & Tiwari, S. K. (2012). Evaluation of antimicrobial activity and bronchodialator effect of a polyherbal drug–Shrishadi. *Asian Pacific Journal of Tropical Biomedicine*, *2*(11), 905–909. [https://doi.org/10.1016/s2221-1691\(12\)60251-2](https://doi.org/10.1016/s2221-1691(12)60251-2)
- Khan, H. A., Ahmad, A., & Mehboob, R. (2015). Nosocomial infections and their control strategies. *Asian Pacific Journal of Tropical Biomedicine*, *5*(7), 509–514. <https://doi.org/10.1016/j.apjtb.2015.05.001>
- Koch, R. A., Wilson, A. W., Séné, O., Henkel, T. W., & Aime, M. C. (2017). Resolved phylogeny and biogeography of the root pathogen *Armillaria* and its gasteroid relative,

- Guyanagaster*. *BMC Evolutionary Biology*, 17(4), 1–16. <https://doi.org/10.1186/s12862-017-0877-3>
- Kostić, M., Smiljković, M., Petrović, J., Glamočlija, J., Barros, L., Ferreira, I. C. F. R., Ćirić, A., & Soković, M. (2017). Chemical, nutritive composition and a wide range of bioactive properties of honey mushroom *Armillaria mellea* (Vahl: Fr.) Kummer. *Food & Function*, 8(9), 3239–3249. <https://doi.org/10.1039/c7fo00887b>
- Kumar, Y., & Yadav, B. C. (2020). Plant-parasitic nematodes: Nature's most successful plant parasite. *International Journal of Research and Review*, 7(3), 379–386.
- Kyndt, T., Vieira, P., Gheysen, G., & de Almeida-Engler, J. (2013). Nematode feeding sites: unique organs in plant roots. *Planta*, 238(1), 807–818. <https://doi.org/10.1007/s00425-013-1923-z>
- Li, G., Zhang, K., Xu, J., Dong, J., & Liu, Y. (2007). Nematicidal substances from fungi. *Recent Patents on Biotechnology*, 1(3), 212–233. <https://doi.org/10.2174/187220807782330165>
- Liu, Z., Wu, Y., Zhao, H., Lian, Y., Wang, Y., Wang, C., Mao, W., & Yuan, Y. (2022). Outline, divergence times, and phylogenetic analyses of *Trechisporales* (Agaricomycetes, Basidiomycota). *Frontiers in Microbiology*, 13(1), 81–83. <https://doi.org/10.3389/fmicb.2022.818358>
- Lima, F. S., Correa, V. R., Nogueira, S. R., & Santos, P. R. (2017). Nematodes affecting soybean and sustainable practices for their management. *Soybean–Basis of Yield, Biomass and Productivity*, 2017(1) 95–110. <https://doi.org/10.5772/67030>
- Lou, S.-Z., Feng, J., Yang, R., Li, Y.-P., Gao, L., Du, G., Yang, H.-Y., Hu, Q.-F., Zhou, W.-B., & Wang, L.-S. (2022). Two new sesquiterpene aryl esters from *Armillaria gallica* 012m. *Journal of Asian Natural Products Research*, 24(1), 59–65. <https://doi.org/10.1080/10286020.2021.1878156>
- Lu, W., Wang, X., Wang, F., & Liu, J. (2020). Fine root capture and phenotypic analysis for tomato infected with *Meloidogyne incognita*. *Computers and Electronics in Agriculture*, 173(2), 105455. <https://doi.org/10.1016/j.compag.2020.105455>
- Midland, S. L., Izac, R. R., Wing, R. M., Zaki, A. I., Munnecke, D. E., & Sims, J. J. (1982). Melleolide, a new antibiotic from *Armillaria mellea*. *Tetrahedron Letters*, 23(25), 2515–2518. [https://doi.org/10.1016/s0040-4039\(00\)87383-9](https://doi.org/10.1016/s0040-4039(00)87383-9)
- Mihail, J. D., & Bruhn, J. N. (2007). Dynamics of bioluminescence by *Armillaria gallica*, *A. mellea* and *A. tabescens*. *Mycologia*, 99(3), 341–350. <https://doi.org/10.3852/mycologia.99.3.341>

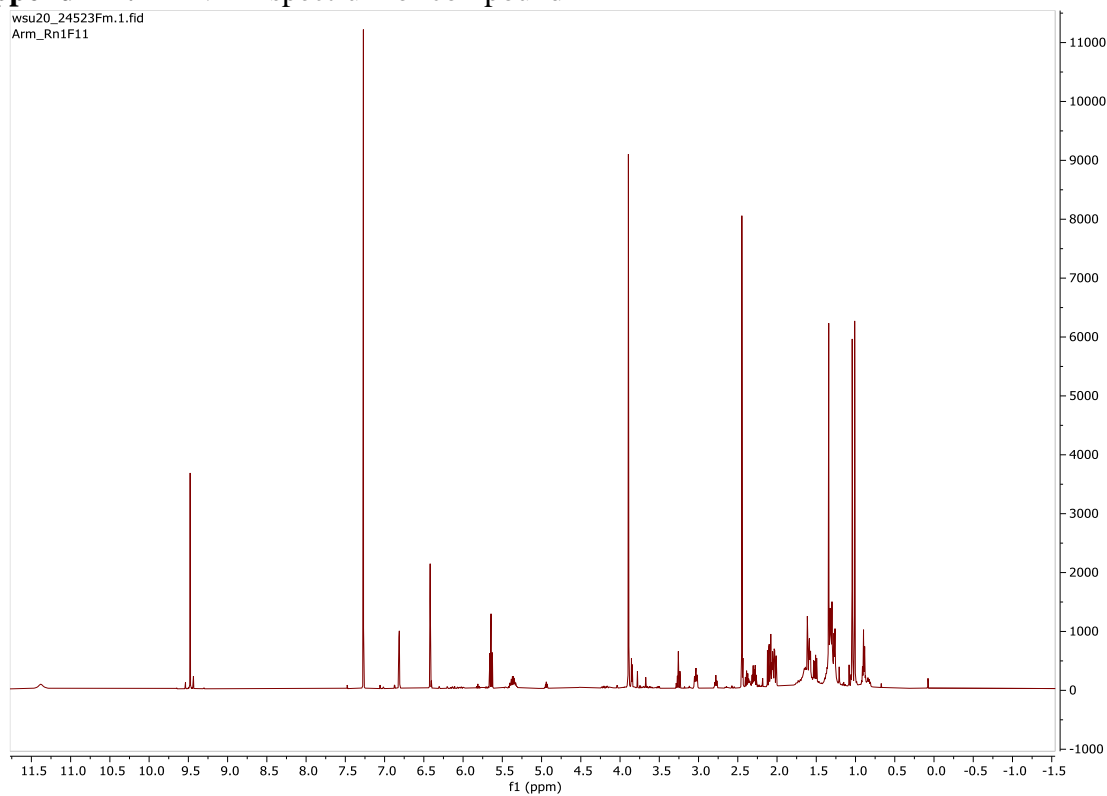
- Muszynska, B., Sulkowska-Ziaja, K., Wolkowska, M., & Ekiert, H. (2011). Chemical, pharmacological, and biological characterization of the culinary-medicinal honey mushroom, *Armillaria mellea* (Vahl) P. Kumm.(Agaricomycetidae): A review. *International Journal of Medicinal Mushrooms*, 13(2), 167-175. <https://doi.org/10.1615/intjmedmushr.v13.i2.90>
- Naranjo-Ortiz, M. A., & Gabaldón, T. (2019). Fungal evolution: diversity, taxonomy and phylogeny of the Fungi. *Biological Reviews*, 94(6), 2101–2137. <https://doi.org/10.1111/brv.12550>
- Ntalli, N. G., Ozalexandridou, E. X., Kasiotis, K. M., Samara, M., & Golfinopoulos, S. K. (2020). Nematicidal activity and phytochemistry of Greek *Lamiaceae* species. *Agronomy*, 10(8), 11-19. <https://doi.org/10.3390/agronomy10081119>
- Pfütze, S., Nedder, D. L., Surup, F., & Stadler, M. (2023). 5'-O-methyl-14-hydroxyarmillane, a new armillane-type sesquiterpene from cultures of *Guyanagaster necrorhiza*. *Mycological Progress*, 22(10), 70-72. <https://doi.org/10.1007/s11557-023-01920-6>
- Sahu, N., Indic, B., Wong-Bajracharya, J., Merényi, Z., Ke, H.-M., Ahrendt, S., Monk, T.-L., Kocsubé, S., Drula, E., & Lipzen, A. (2023). Vertical and horizontal gene transfer shaped plant colonization and biomass degradation in the fungal genus *Armillaria*. *Nature Microbiology*, 8(9), 1668–1681. <https://doi.org/10.1038/s41564-023-01448-1>
- Sandargo, B., Chepkirui, C., Cheng, T., Chaverra-Muñoz, L., Thongbai, B., Stadler, M., & Hüttel, S. (2019). Biological and chemical diversity go hand in hand: Basidiomycota as source of new pharmaceuticals and agrochemicals. *Biotechnology Advances*, 37(6), 107344. <https://doi.org/10.1016/j.biotechadv.2019.01.011>
- Shah, M. M., & Mahamood, M. (2017). Introductory chapter: nematodes-a lesser known group of organisms. *Nematology-Concepts, Diagnosis and Control*, 1(4), 68589-685590. <https://doi.org/10.5772/intechopen.68589>
- Sośnicka, A., Górska, S., & Turło, J. (2018). Biological, chemical and ecological properties of *Armillaria mellea* (Vahl) P. Kumm. *Biology Education*, 2(2018), 10-18.
- Stasinska, M. (2015). *Armillaria ectypa*, a rare fungus of mire in Poland. *Acta Mycologica*, 50(1), 10-15. <https://doi.org/10.5586/am.1064>
- Subedi, S., Thapa, B. & Shrestha, J. (2020). Root-knot nematode (*Meloidogyne incognita*) and its management: A Review. *Journal of Agriculture and Natural Resources*, 3(2), 21-31. <https://doi.org/10.3126/janr.v3i2.32298>
- Sum, W. C., Indieka, S. A., & Matasyoh, J. C. (2019). Antimicrobial activity of Basidiomycetes fungi isolated from a Kenyan tropical forest. *African Journal of Biotechnology*, 18(5),

112–123. <https://doi.org/10.5897/ajb2018.16660>

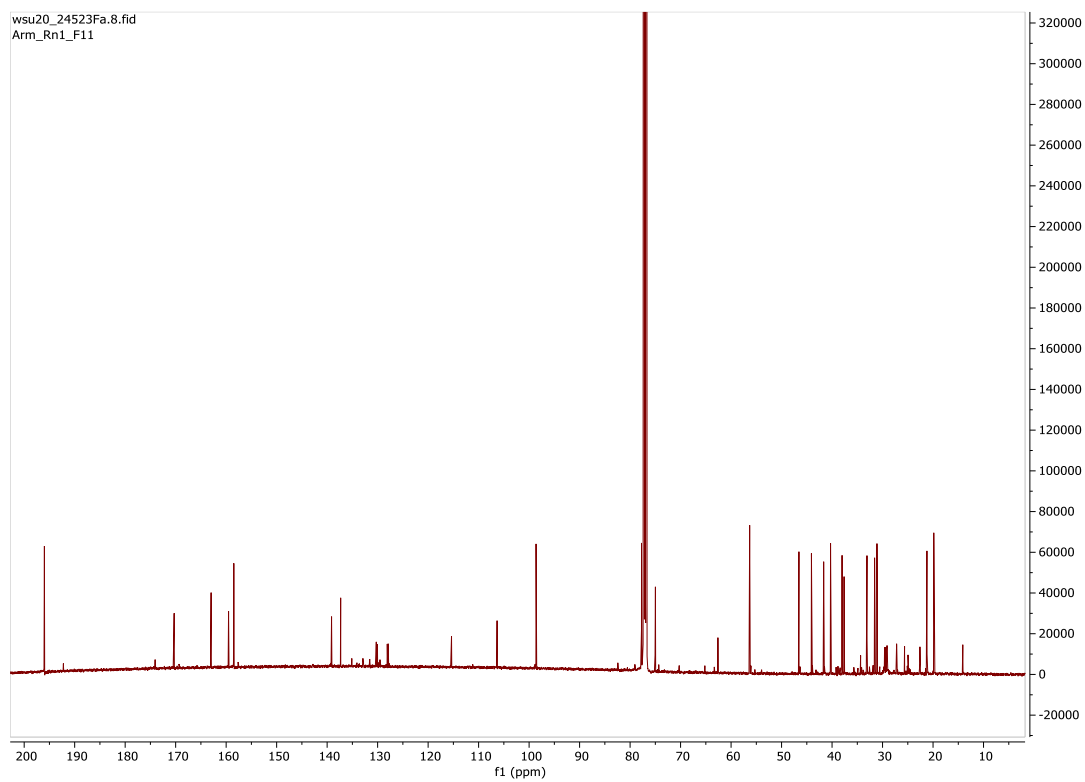
- Vallavan, V., Krishnasamy, G., Zin, N. M., & Abdul Latif, M. (2020). A review on antistaphylococcal secondary metabolites from basidiomycetes. *Molecules*, 25(24), 5848.- 5848. <https://doi.org/10.3390/molecules25245848>
- Wasser, S. P. (2011). Current findings, future trends, and unsolved problems in studies of medicinal mushrooms. *Applied Microbiology and Biotechnology*, 89(1), 1323–1332.
- Xie, J. L., O’Meara, T. R., Polvi, E. J., Robbins, N., & Cowen, L. E. (2017). Staurosporine induces filamentation in the human fungal pathogen *Candida albicans* via signaling through Cyr1 and protein kinase A. *Mosphere*, 2(2), 10–1128. <https://doi.org/10.1128/msphere.00056-17>
- Xie, J. L., Polvi, E. J., Shekhar-Guturja, T., & Cowen, L. E. (2014). Elucidating drug resistance in human fungal pathogens. *Future Microbiology*, 9(4), 523–542. <https://doi.org/10.2217/fmb.14.18>
- Yamaç, M., & Bilgili, F. (2006). Antimicrobial activities of fruit bodies and/or mycelial cultures of some mushroom isolates. *Pharmaceutical Biology*, 44(9), 660–667. <https://doi.org/10.1080/13880200601006897>
- Yang, J., Yuwu, C., Xiaozhang, F., Dequan, Y., & Xiaotian, L. (1984). Chemical constituents of *Armillaria mellea* mycelium I. Isolation and characterization of armillarin and armillaridin. *Planta Medica*, 50(4), 288–290. <https://doi.org/10.1055/s-2007-969711>

APPENDICES

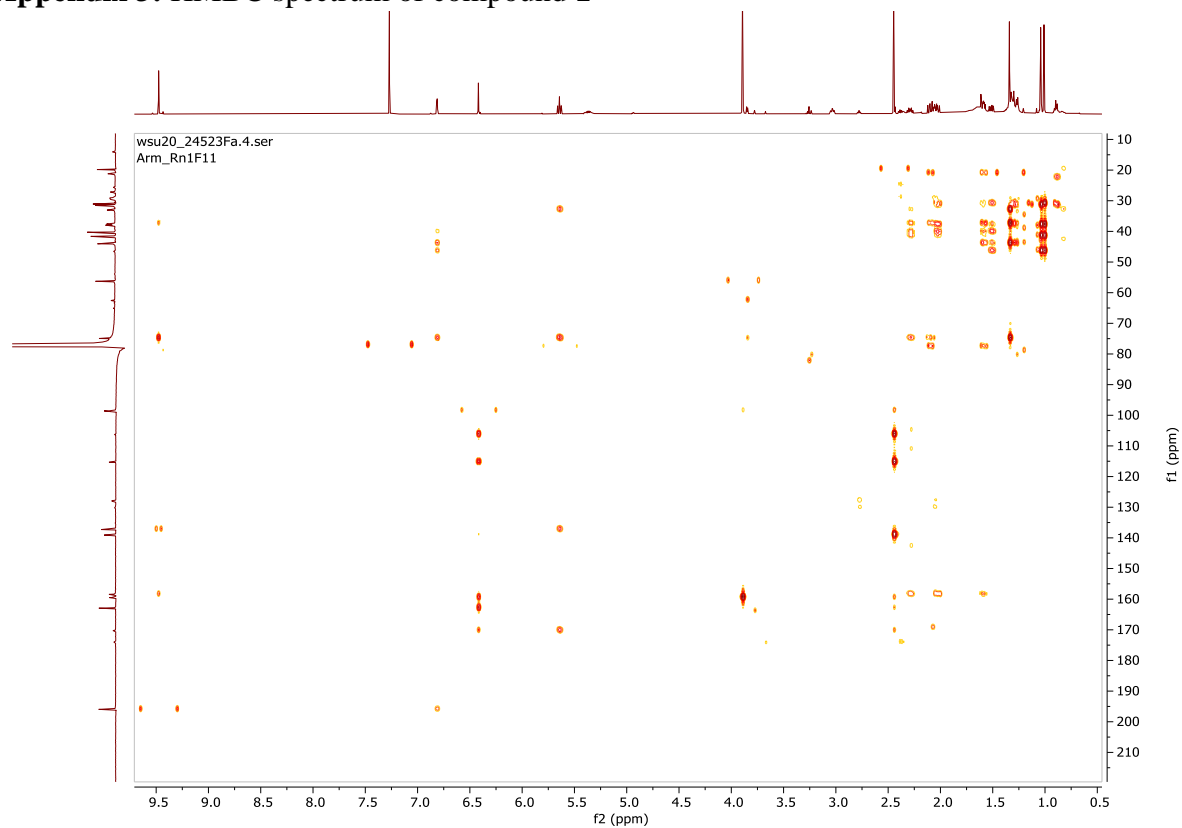
Appendix 1: ^1H -NMR spectrum of compound 1



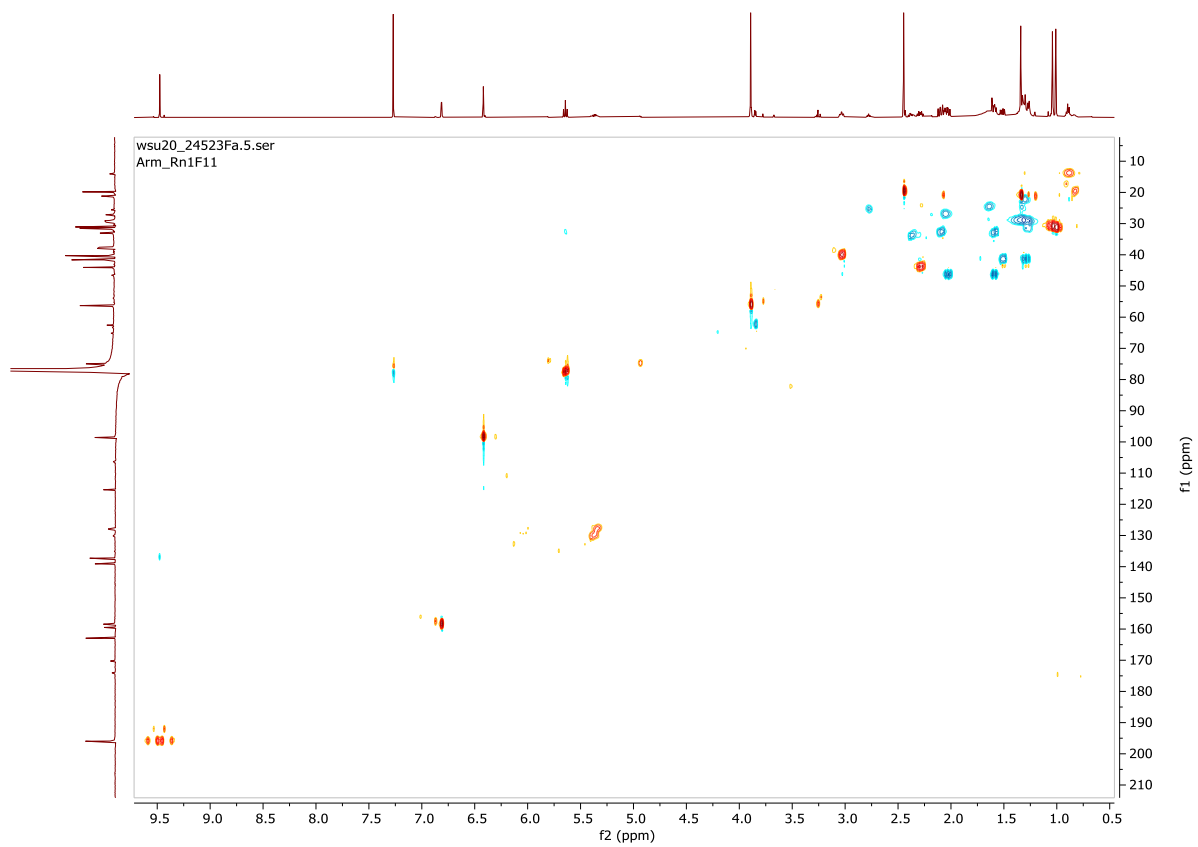
Appendix 2: ^{13}C -NMR spectrum of compound 1



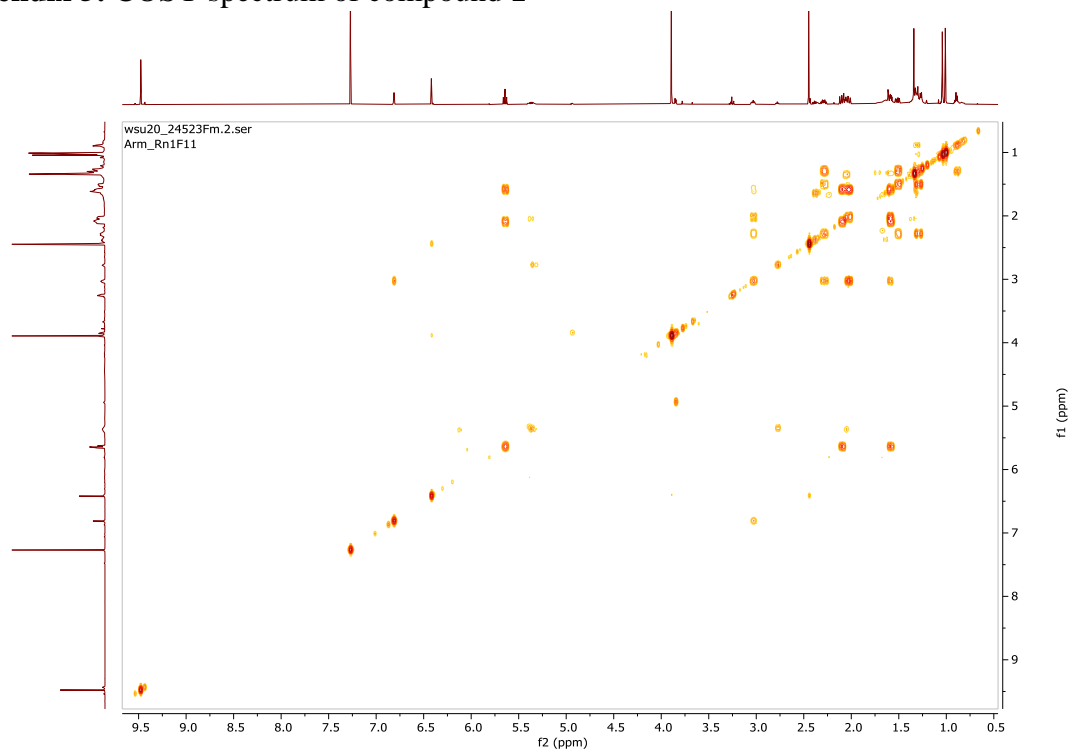
Appendix 3: HMBC spectrum of compound 1



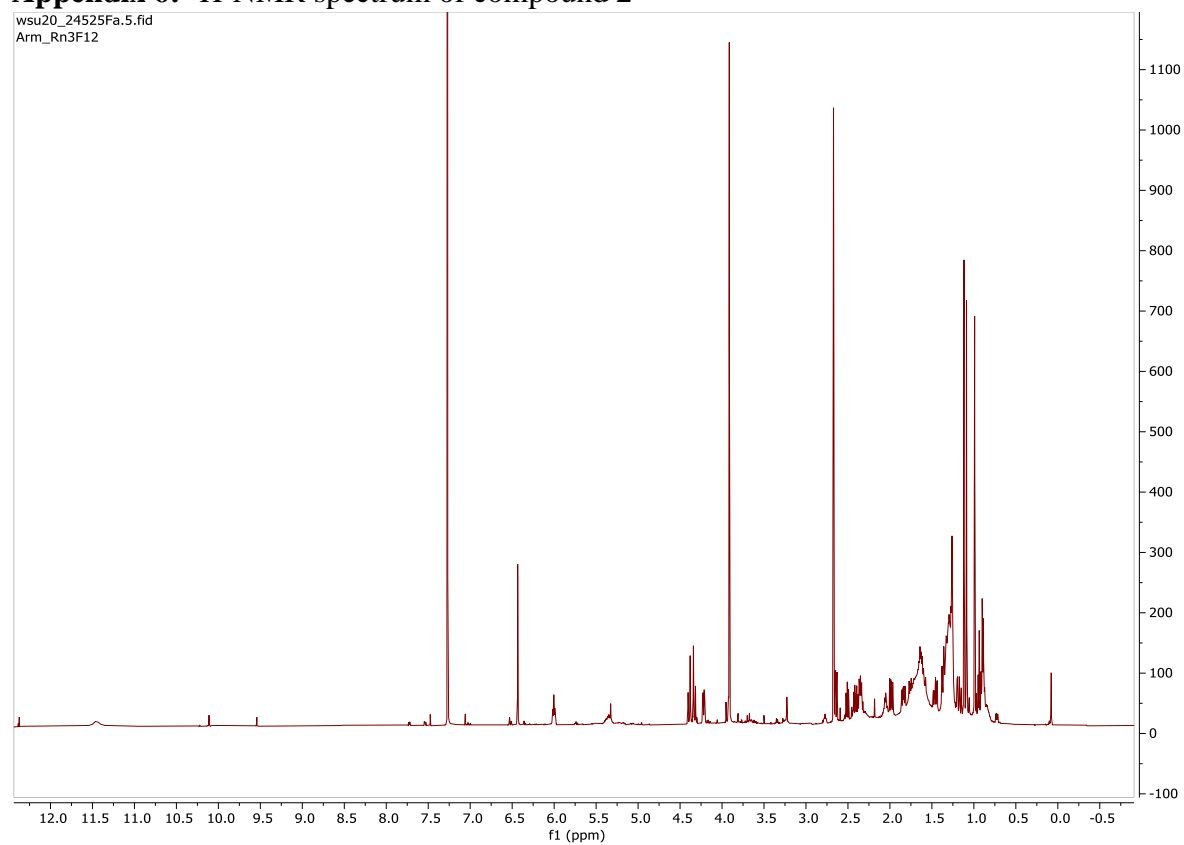
Appendix 4: HSQC spectrum of compound 1



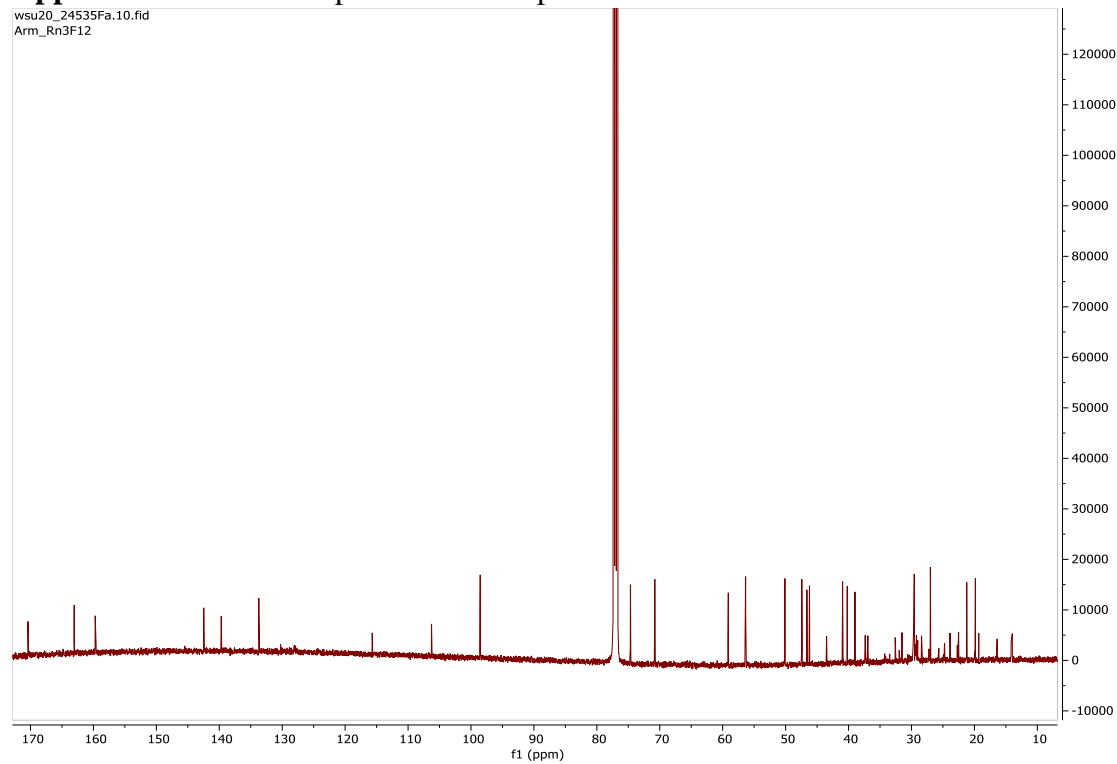
Appendix 5: COSY spectrum of compound 1



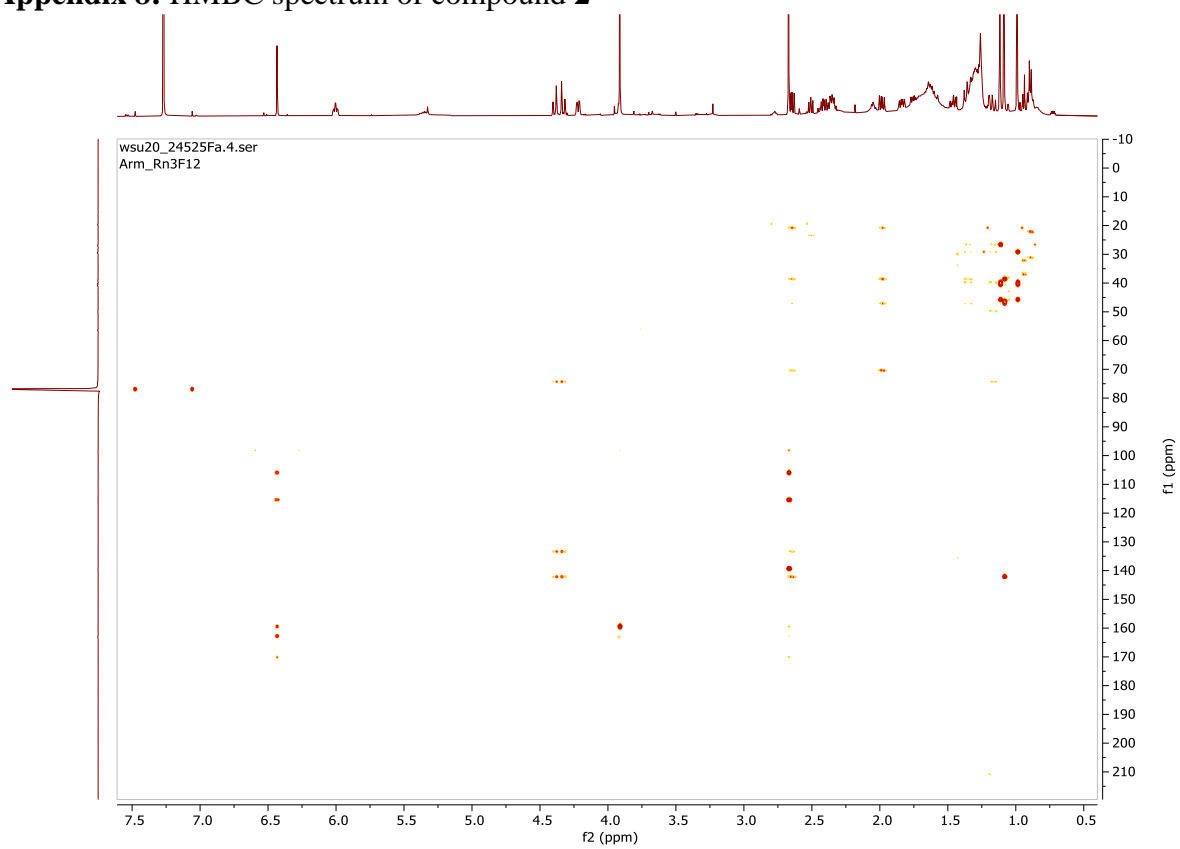
Appendix 6: ¹H-NMR spectrum of compound 2



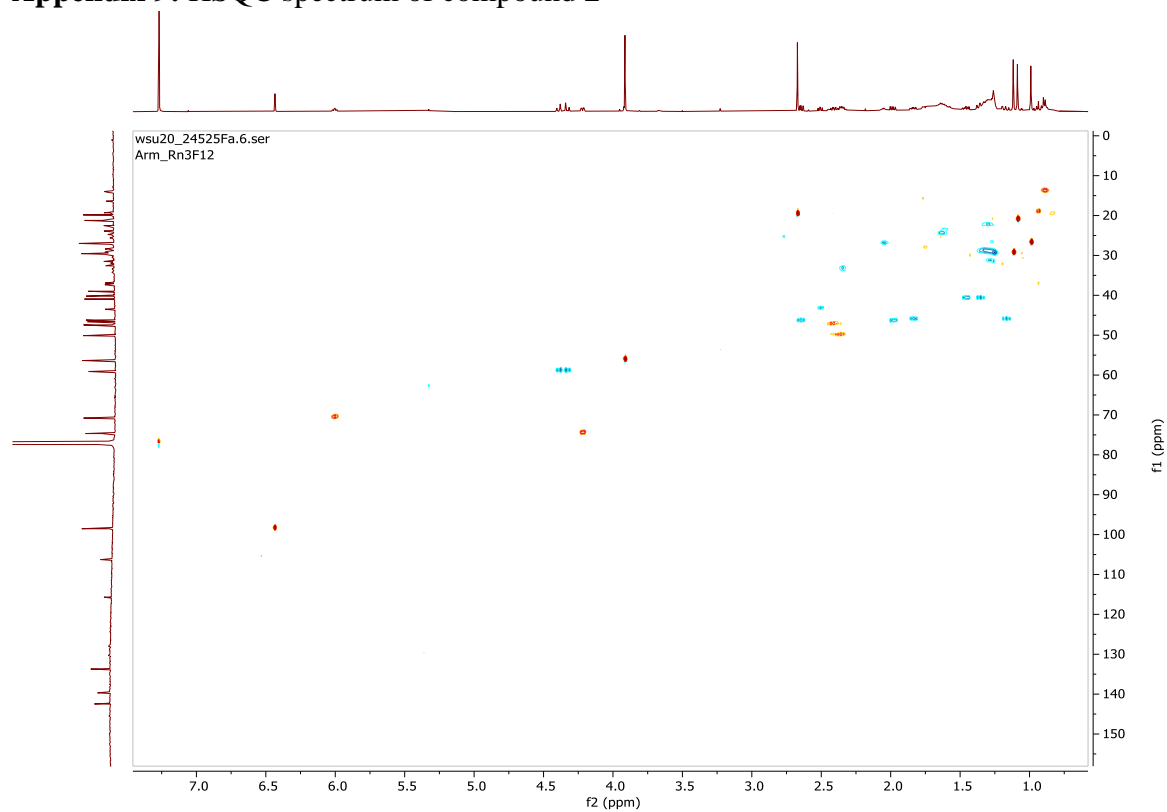
Appendix 7: ^{13}C -NMR spectrum of compound 2



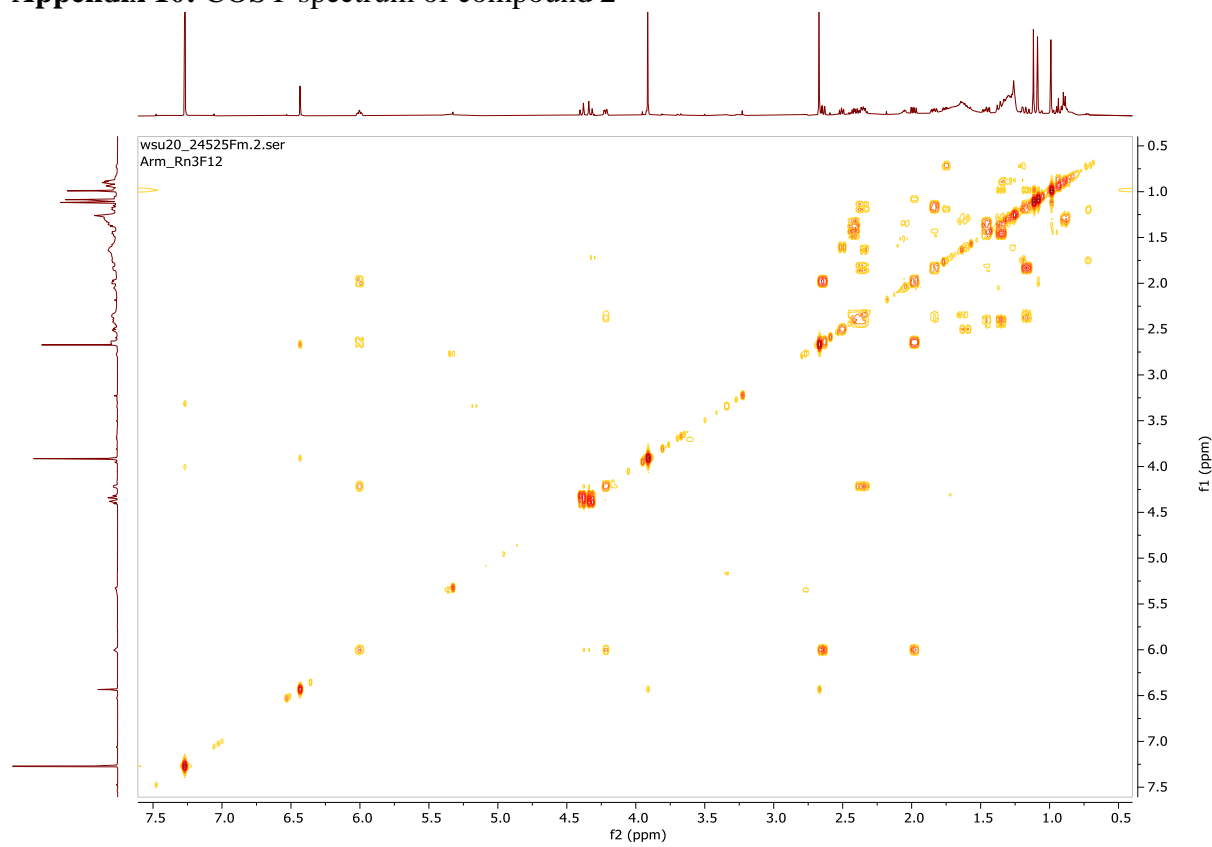
Appendix 8: HMBC spectrum of compound 2



Appendix 9: HSQC spectrum of compound 2

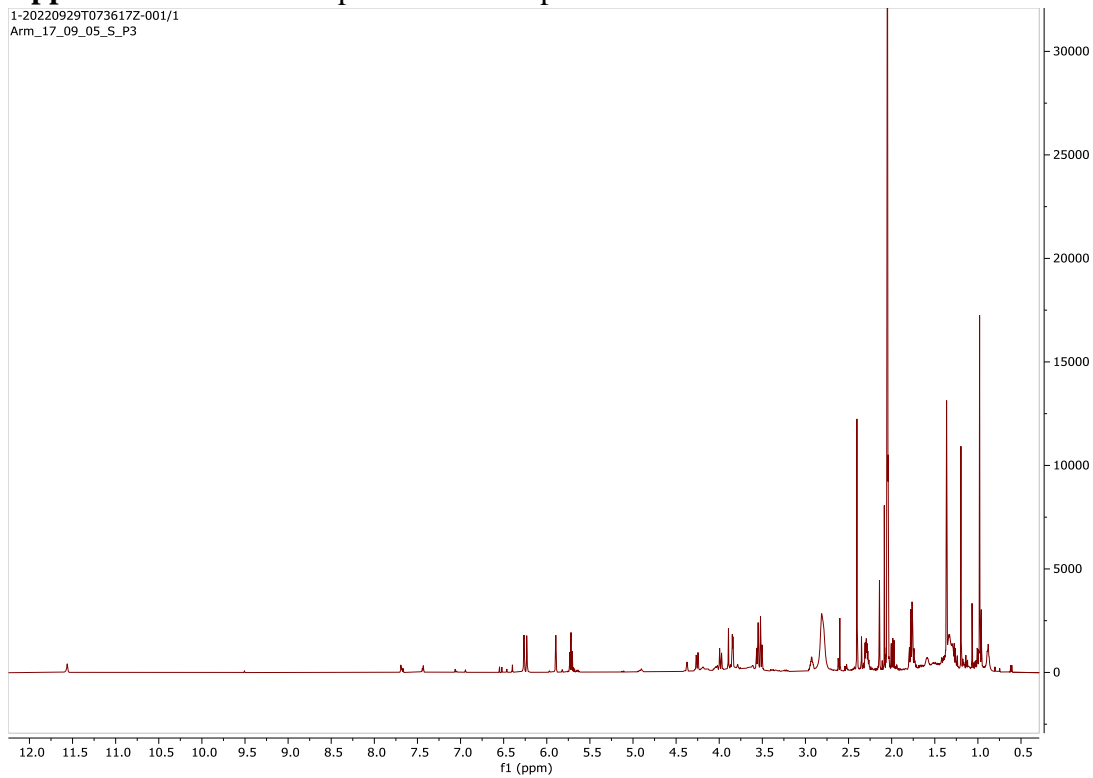


Appendix 10: COSY spectrum of compound 2



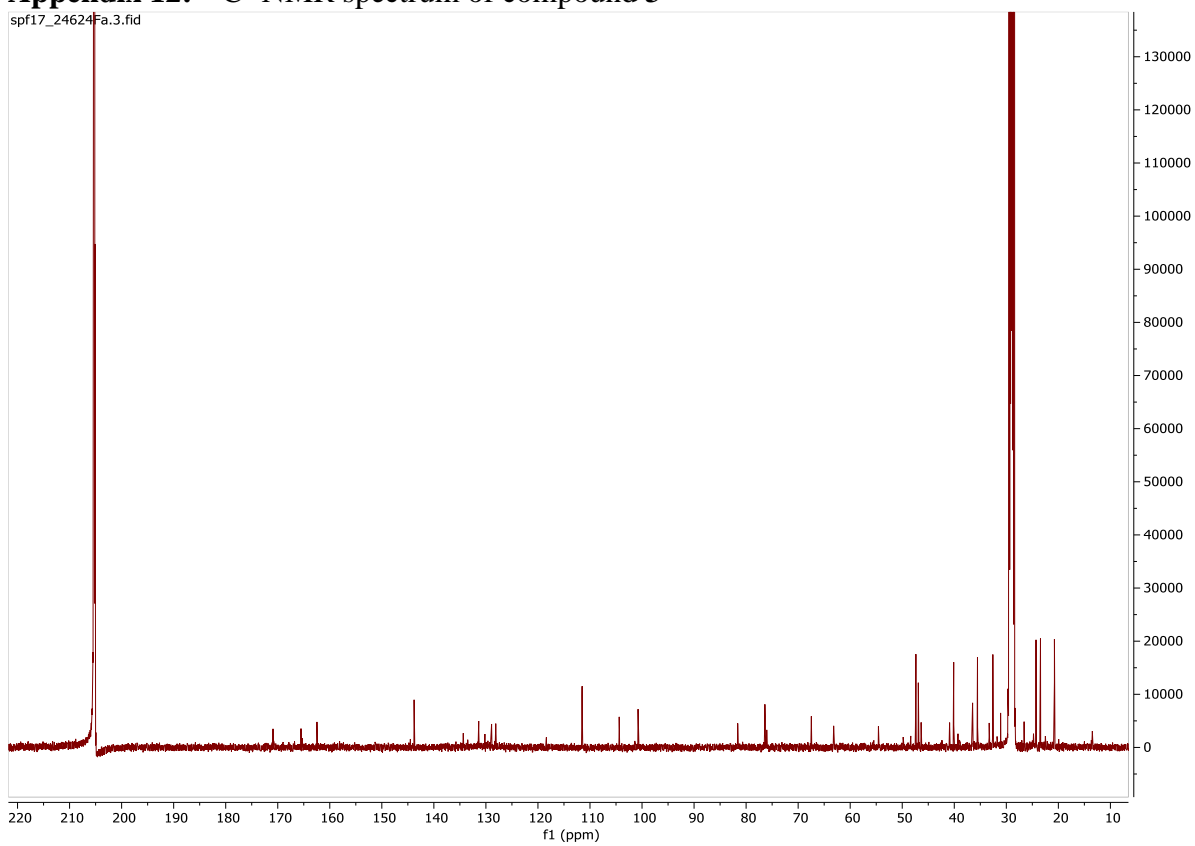
Appendix 11: ^1H -NMR spectrum of compound 3

1-20220929T073617Z-001/1
Arm_17_09_05_S_P3

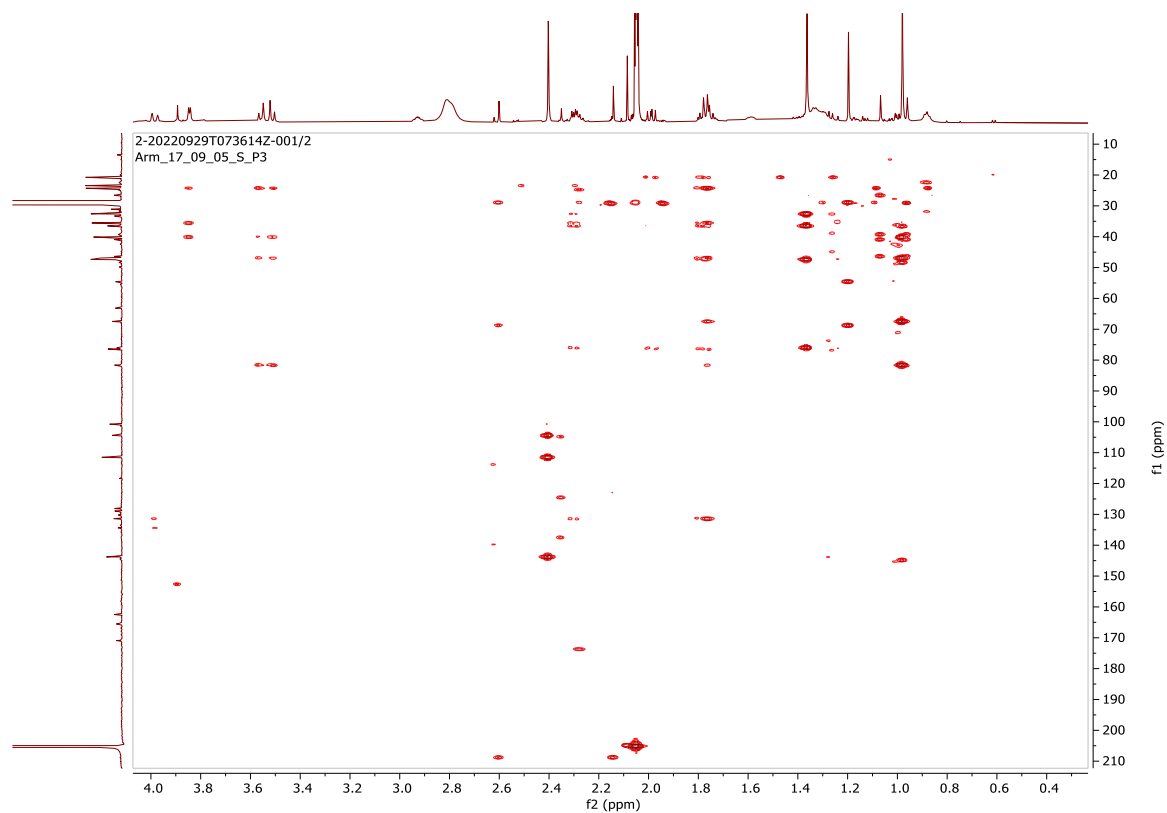


Appendix 12: ^{13}C - NMR spectrum of compound 3

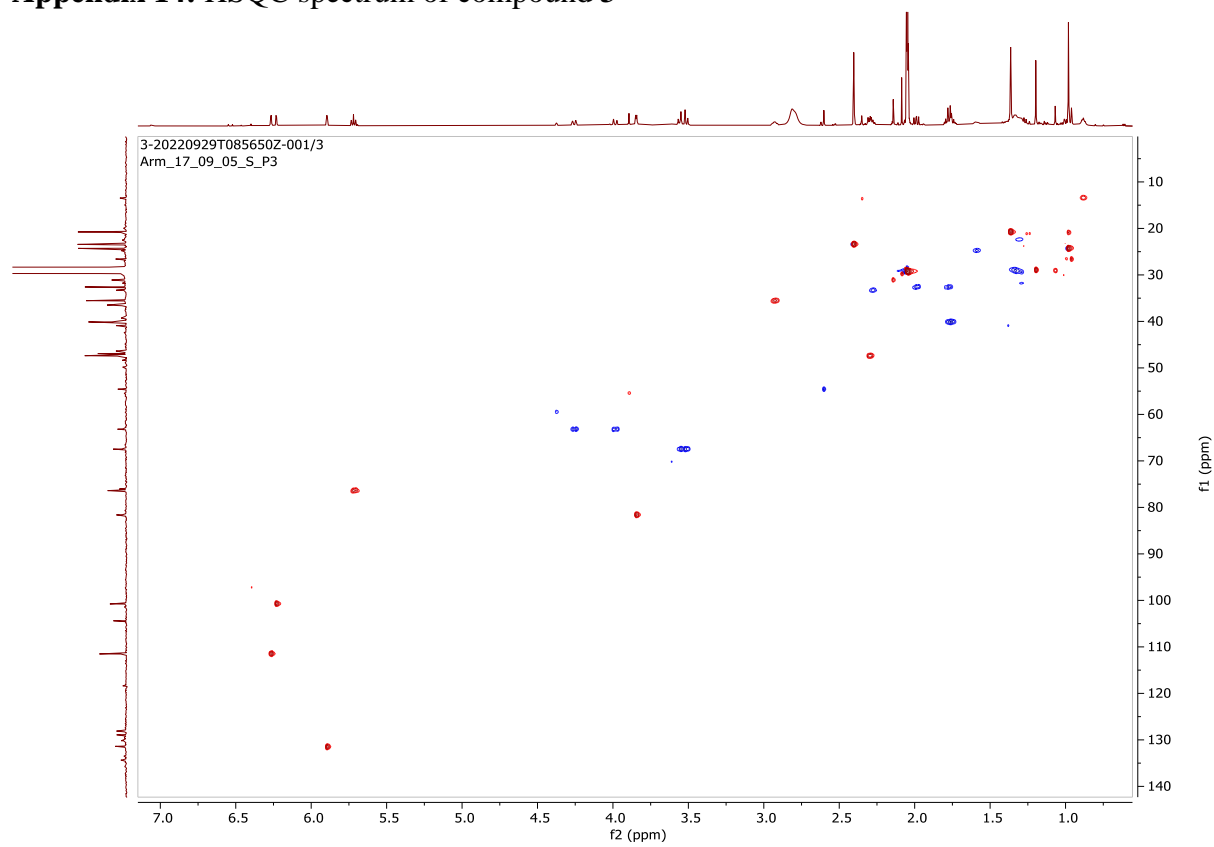
spf17_24624Fa.3.fid



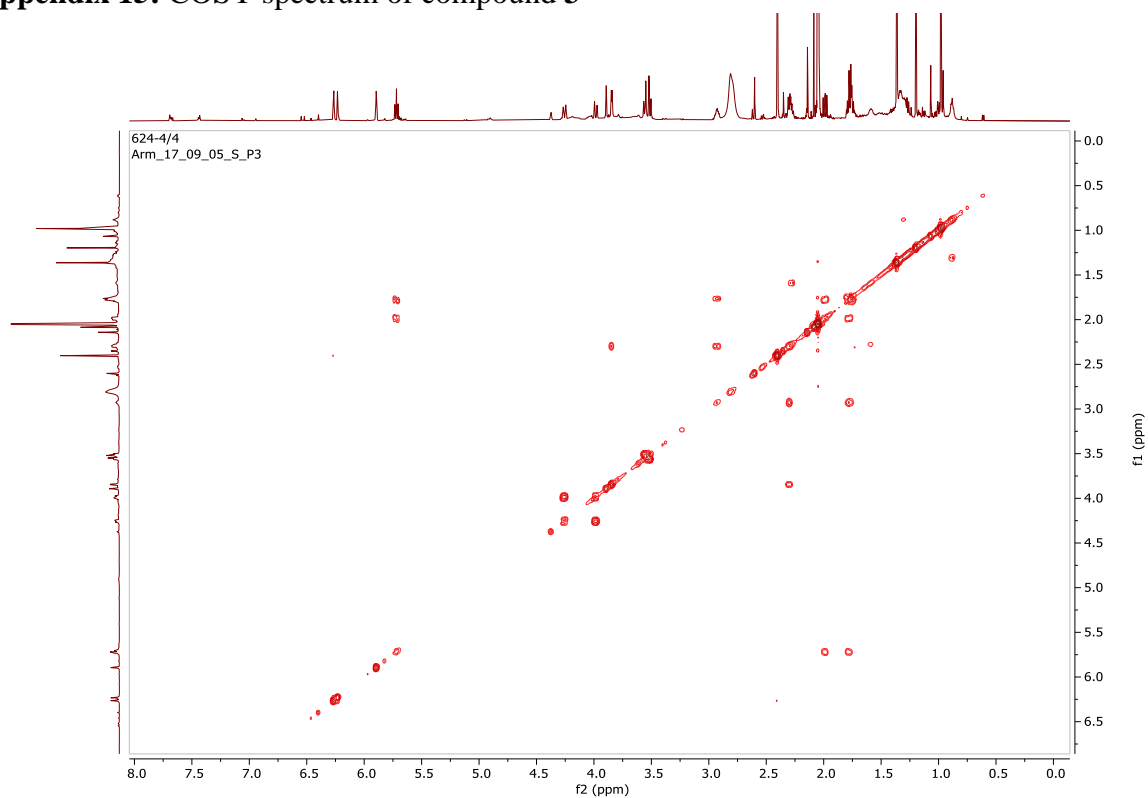
Appendix 13: HMBC spectrum of compound 3



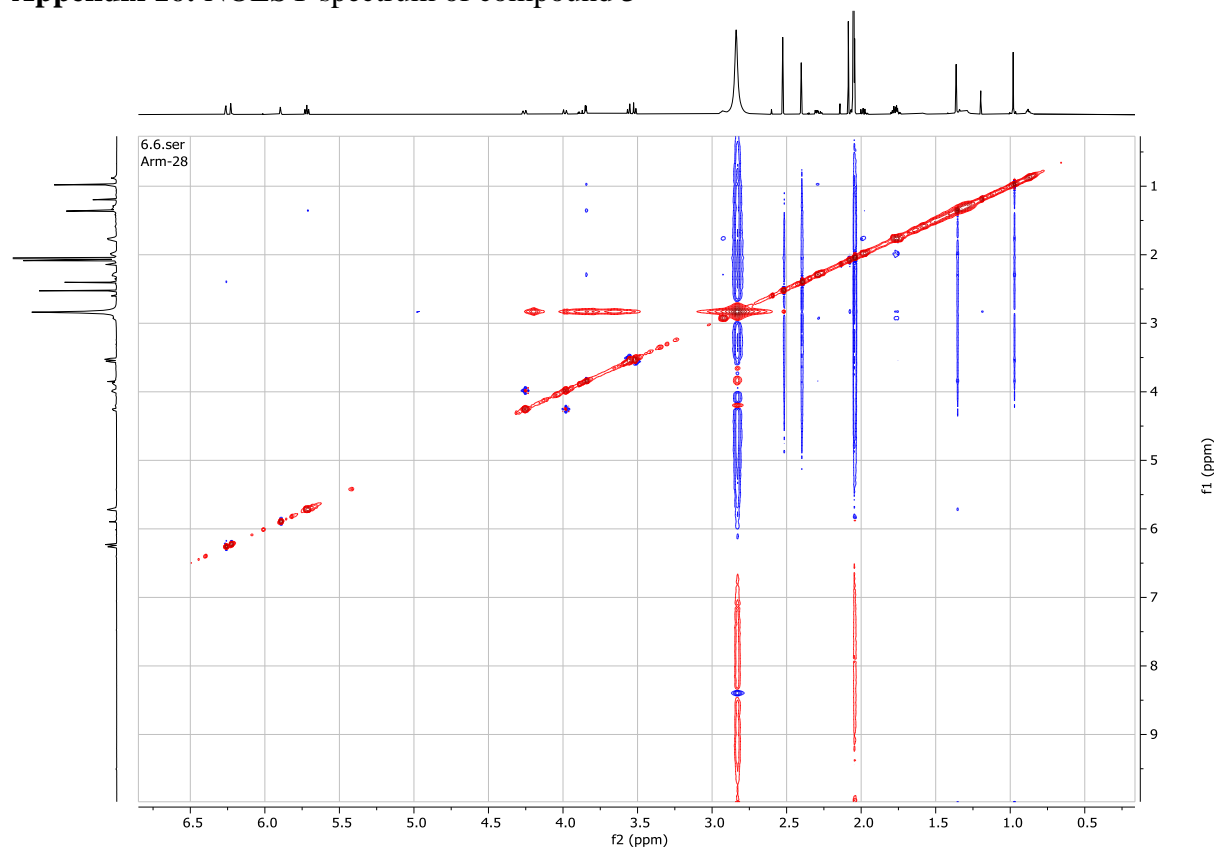
Appendix 14: HSQC spectrum of compound 3



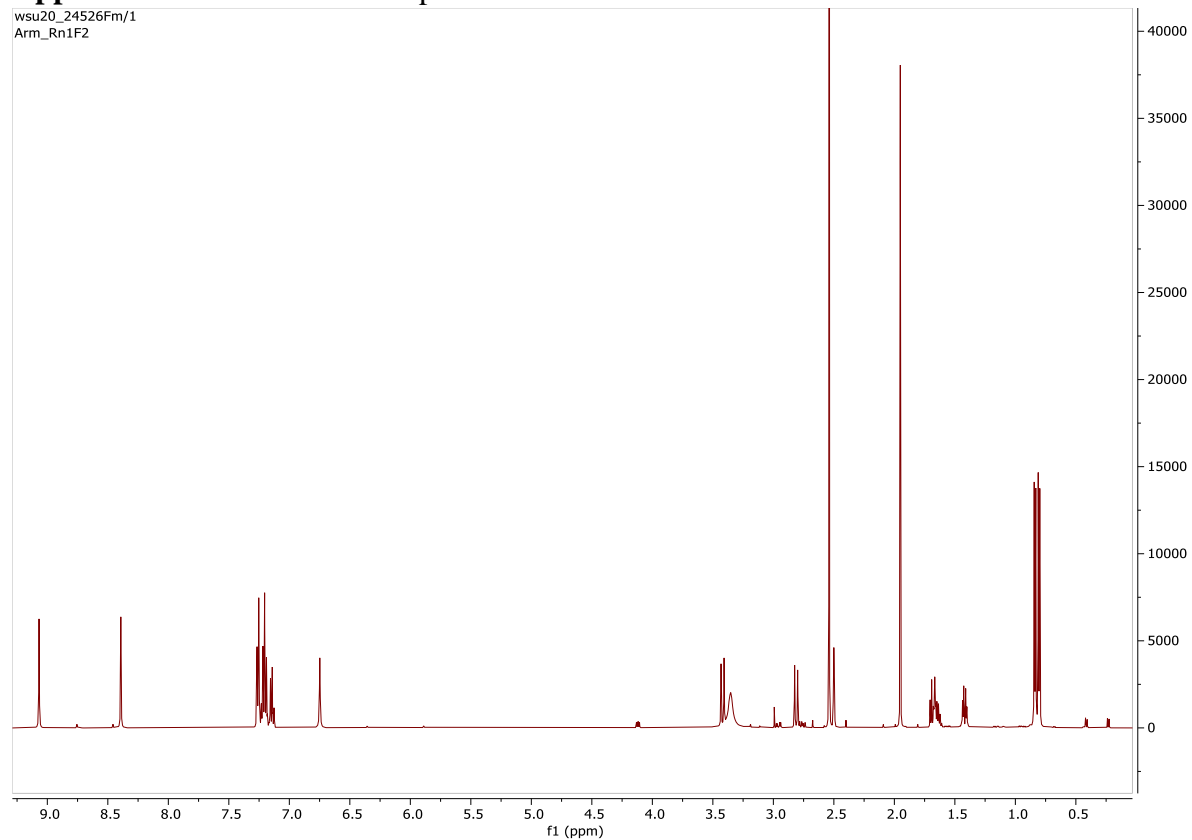
Appendix 15: COSY spectrum of compound 3



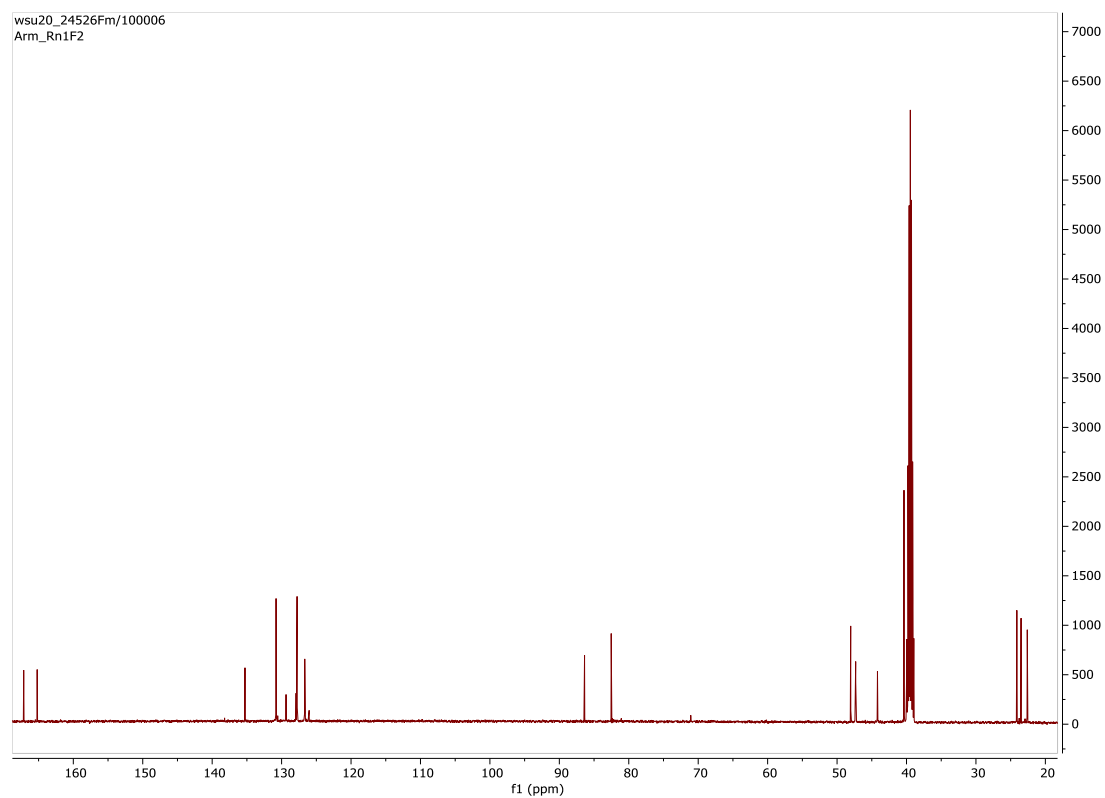
Appendix 16: NOESY spectrum of compound 3



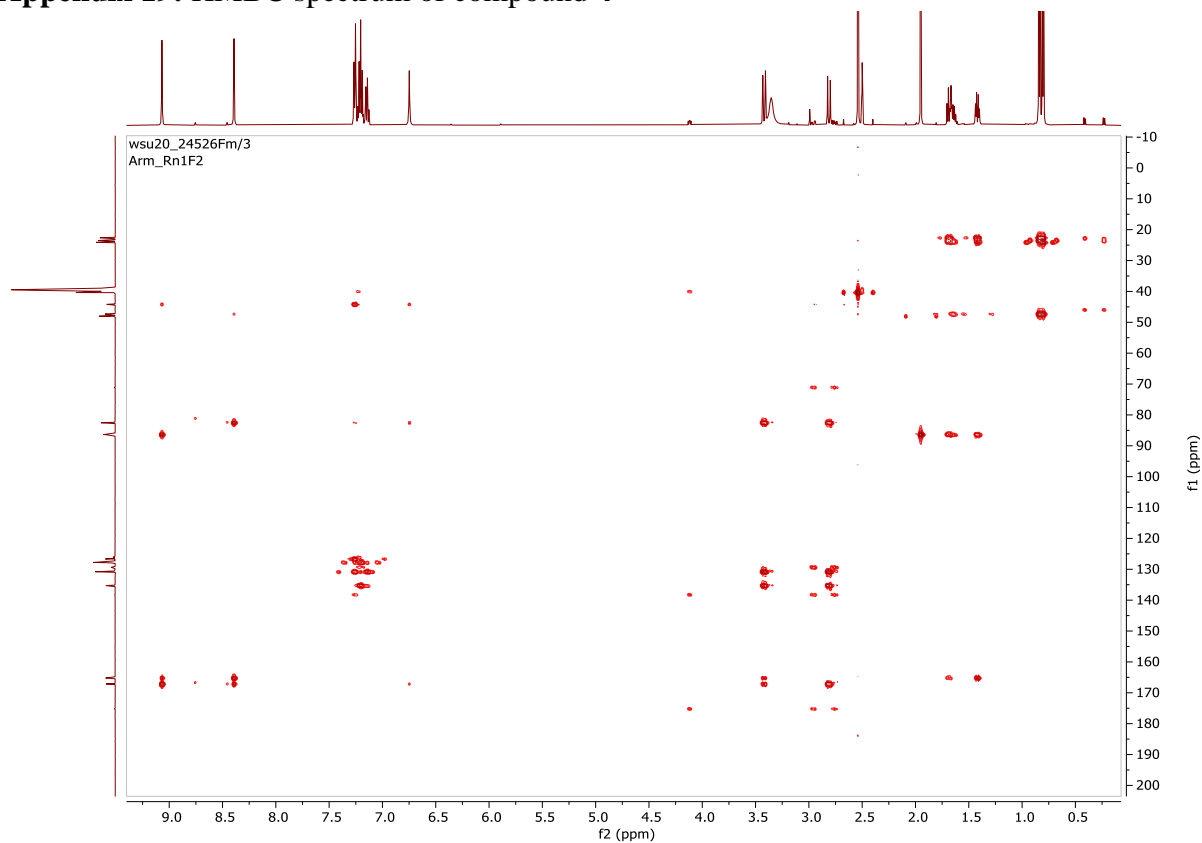
Appendix 17: ^1H -NMR of compound 4



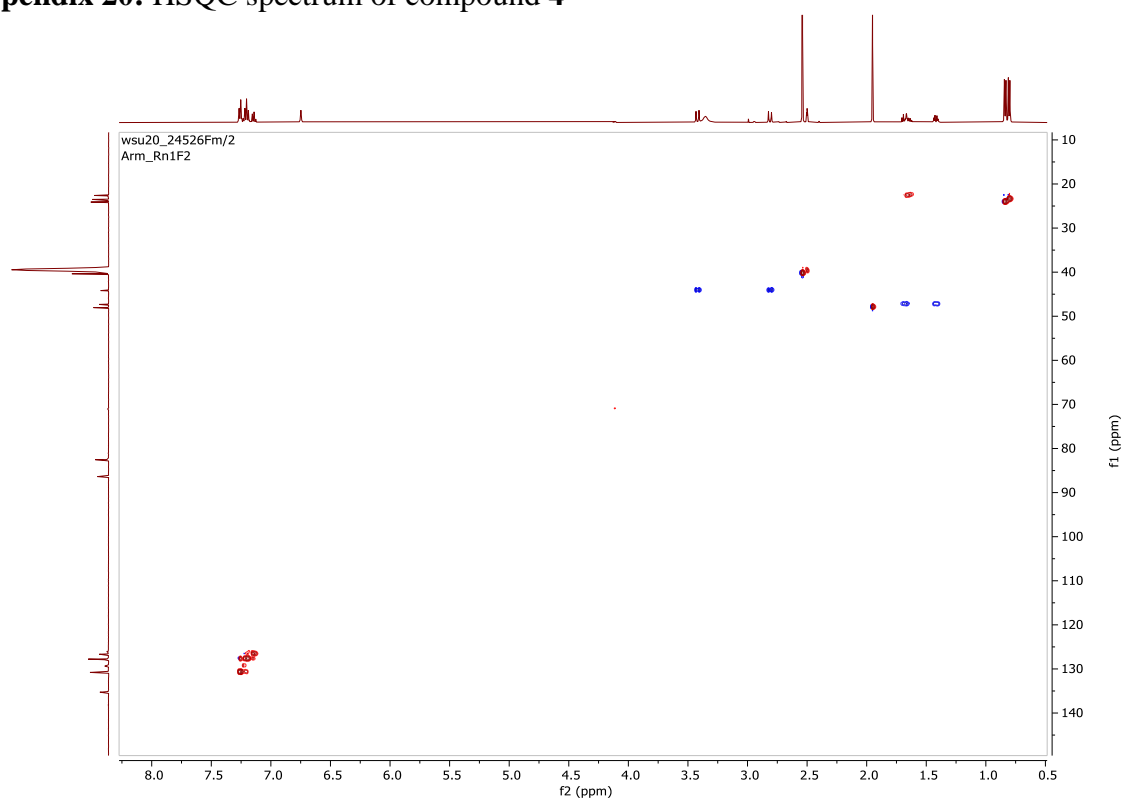
Appendix 18: ^{13}C -NMR spectrum of compound 4



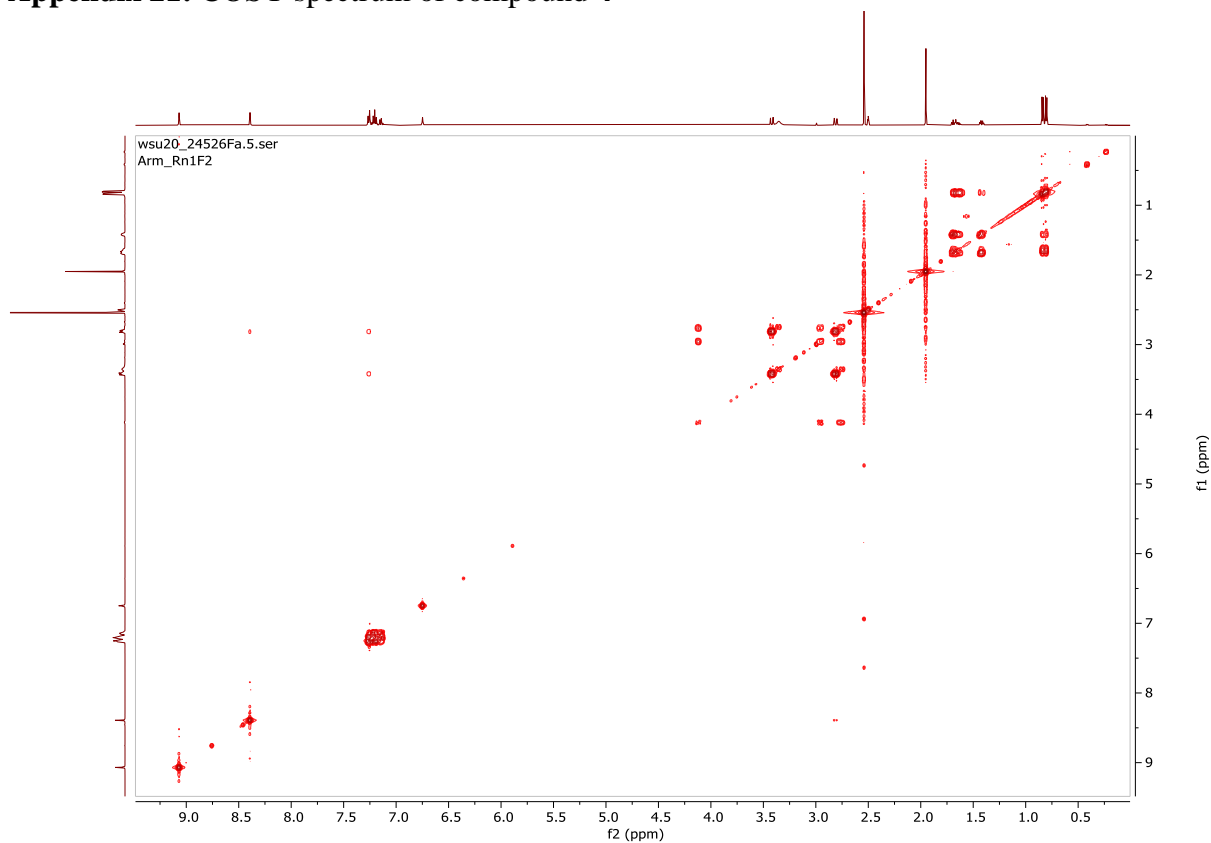
Appendix 19: HMBC spectrum of compound 4



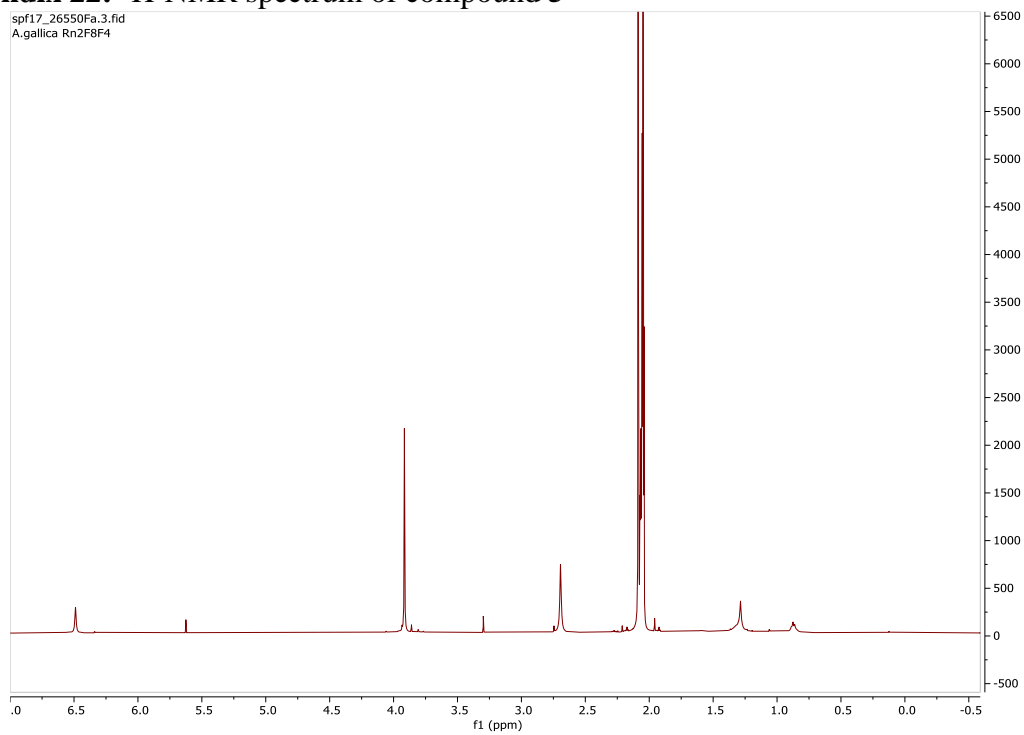
Appendix 20: HSQC spectrum of compound 4



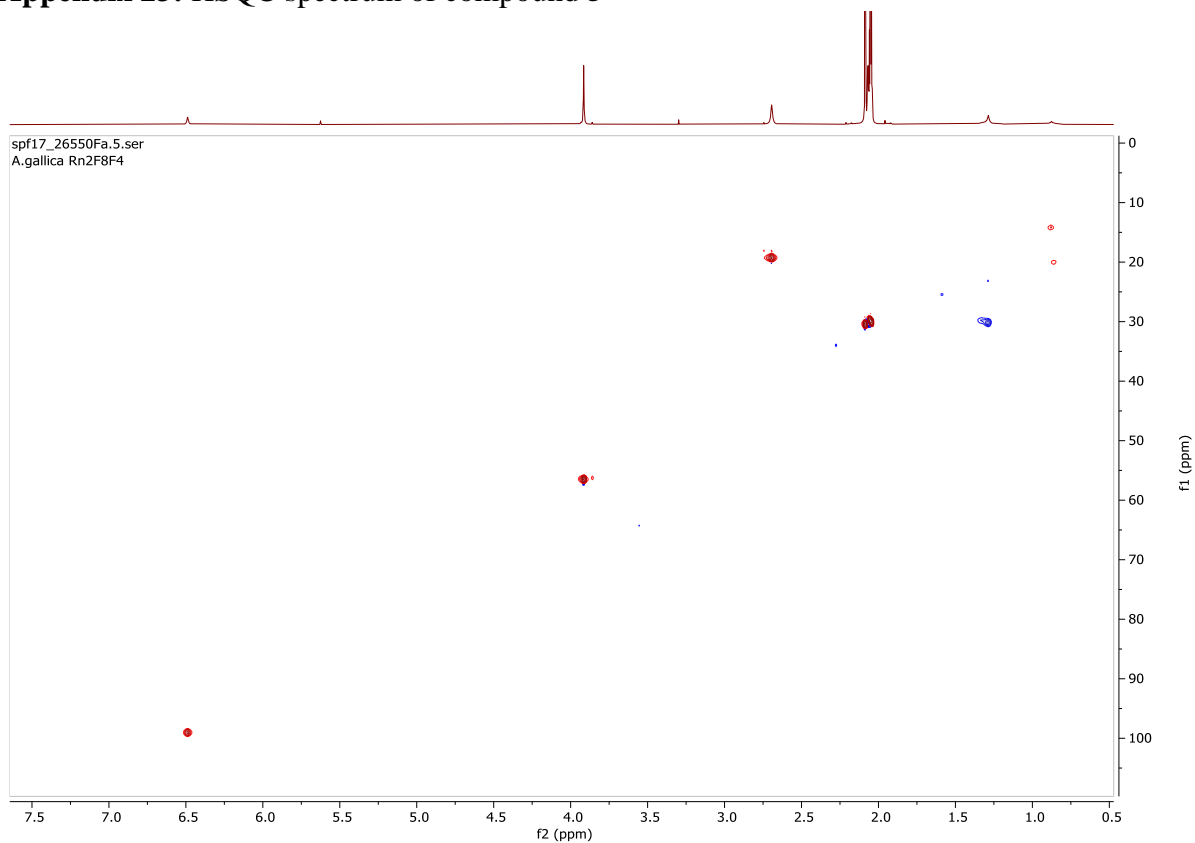
Appendix 21: COSY spectrum of compound 4



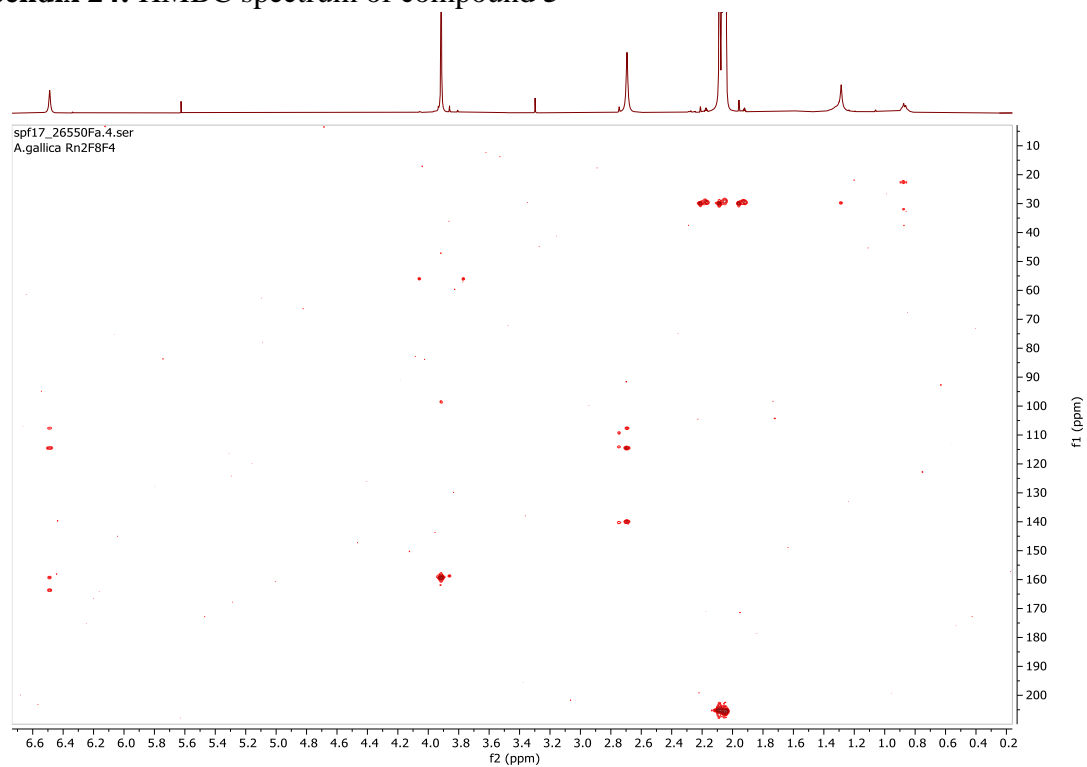
Appendix 22: ¹H-NMR spectrum of compound 5



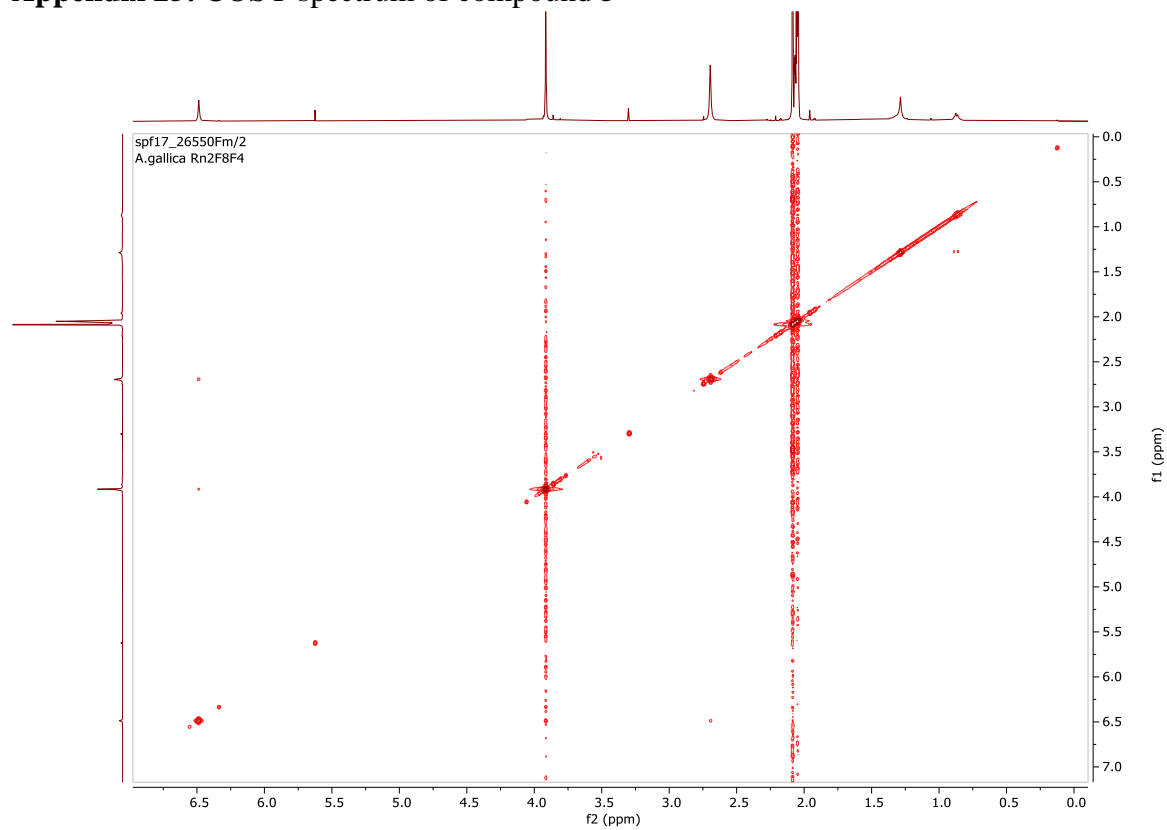
Appendix 23: HSQC spectrum of compound 5



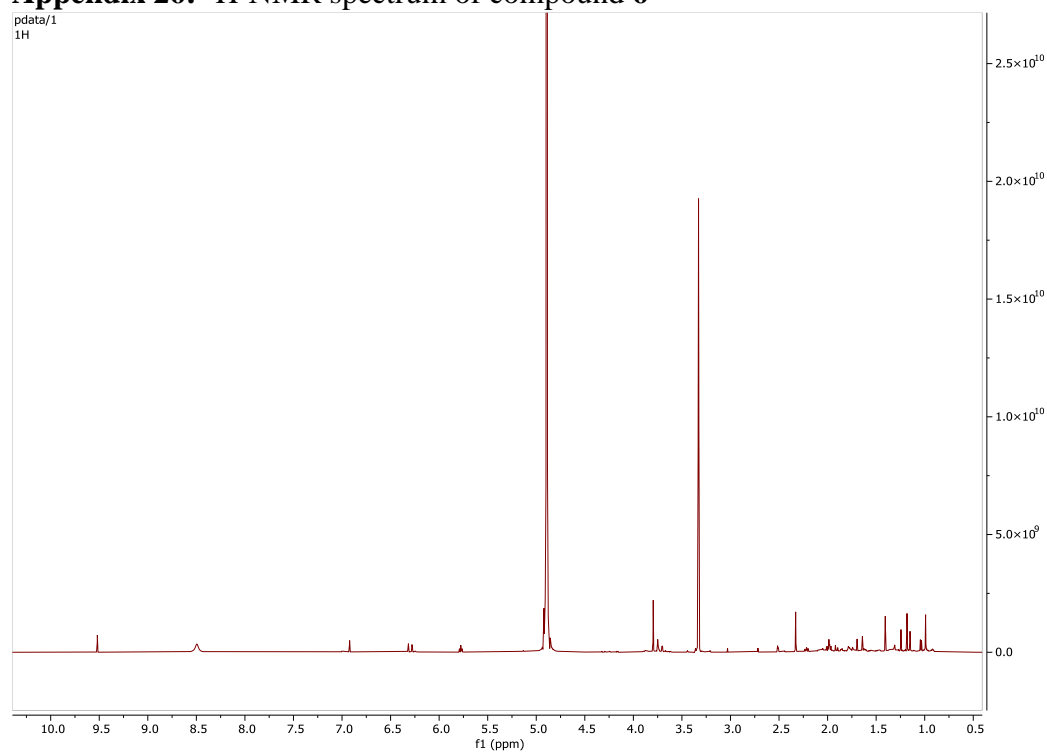
Appendix 24: HMBC spectrum of compound 5



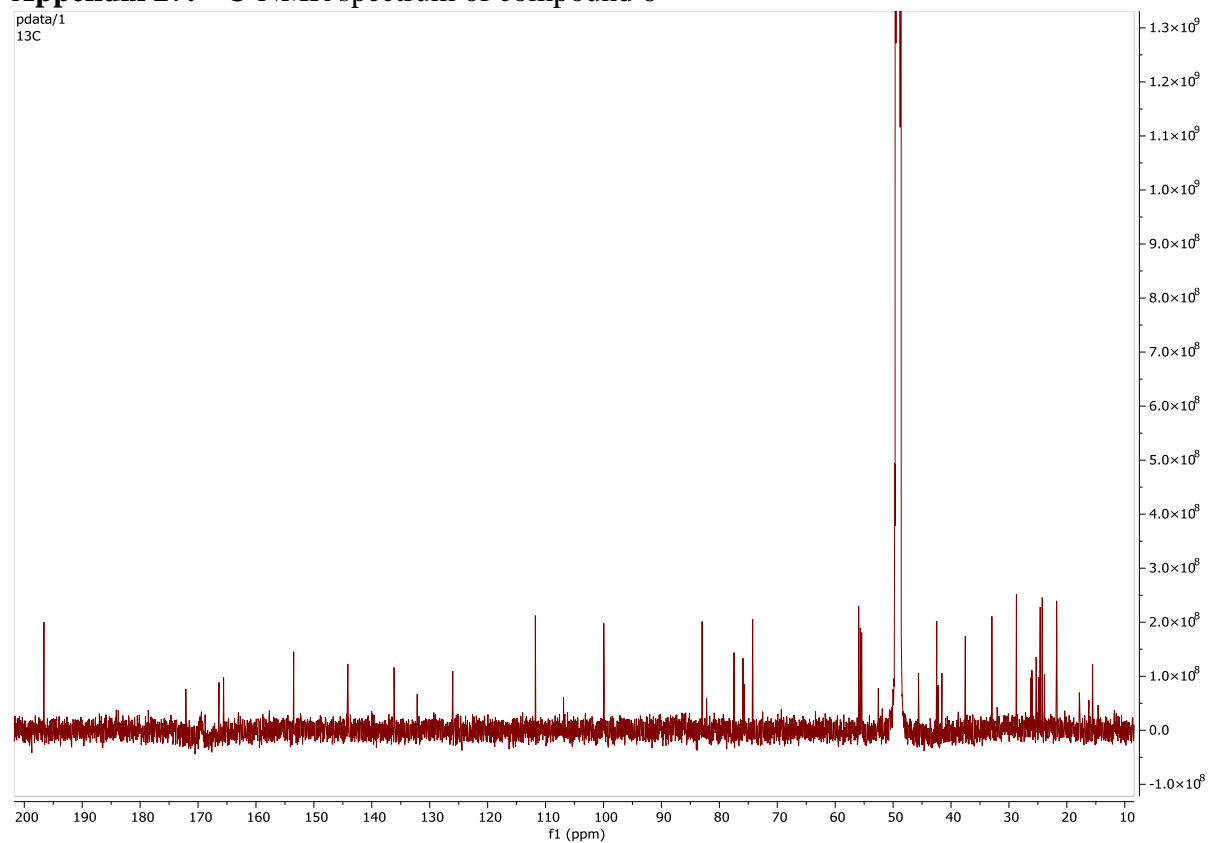
Appendix 25: COSY spectrum of compound 5



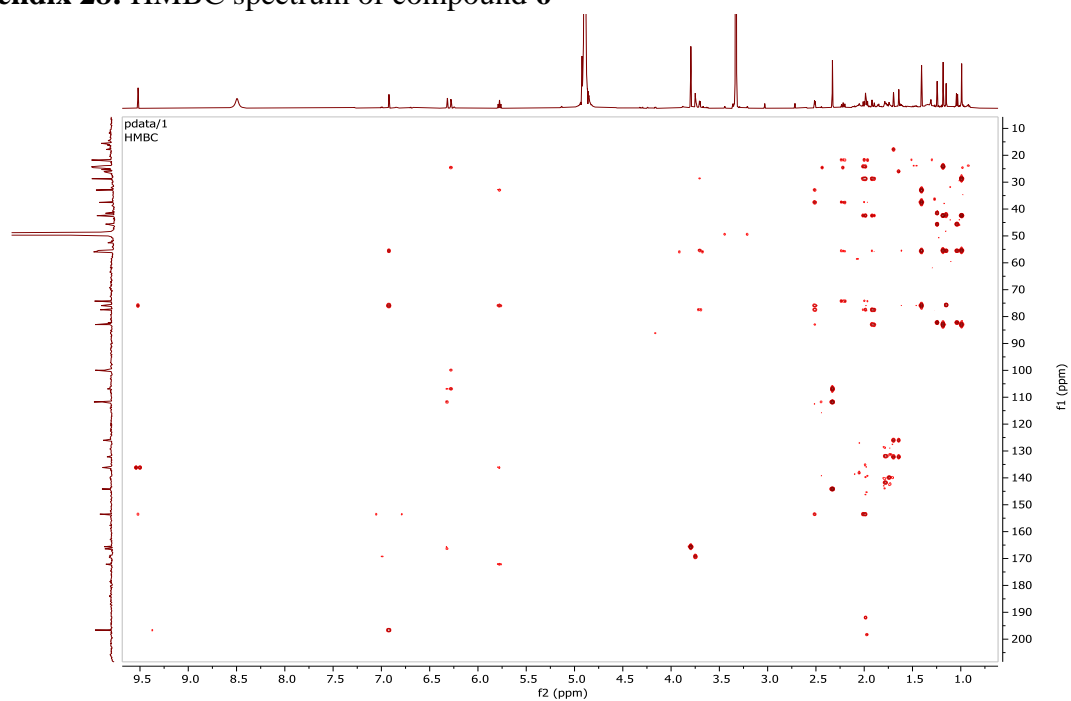
Appendix 26: ¹H-NMR spectrum of compound 6



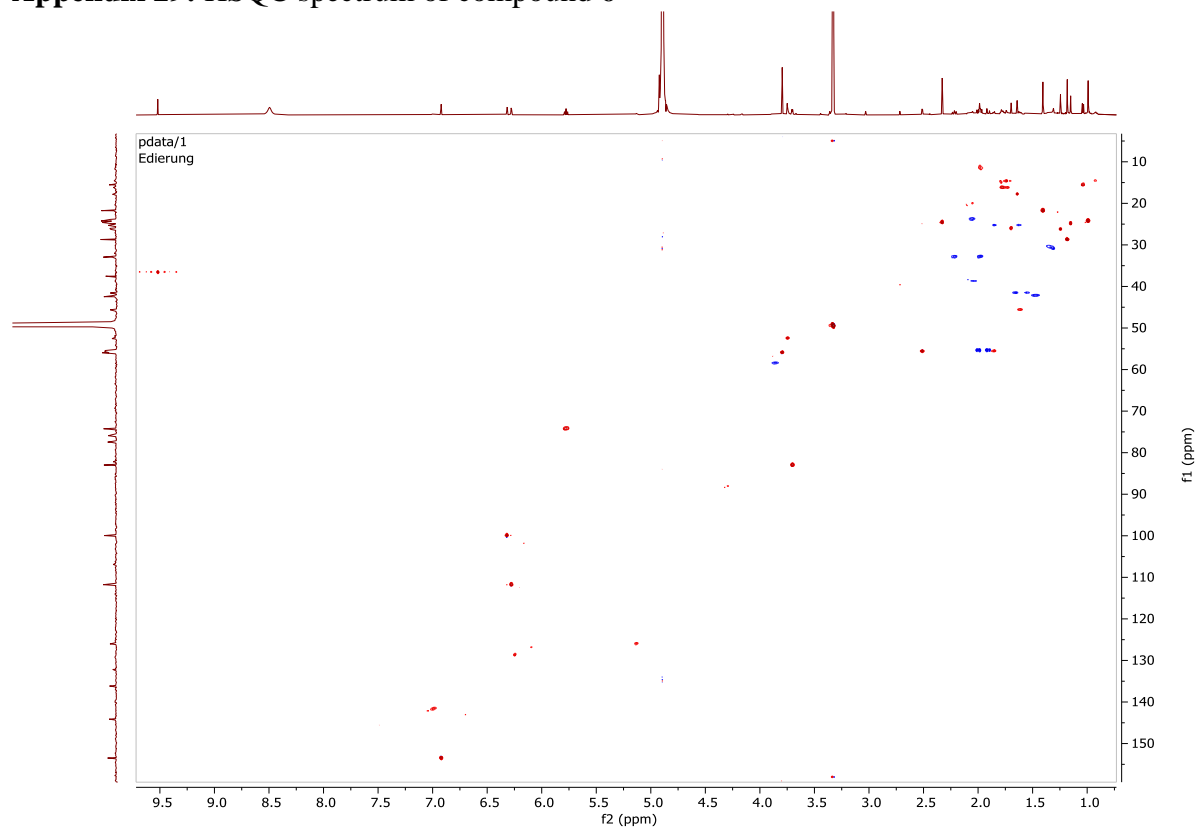
Appendix 27: ^{13}C -NMR spectrum of compound 6



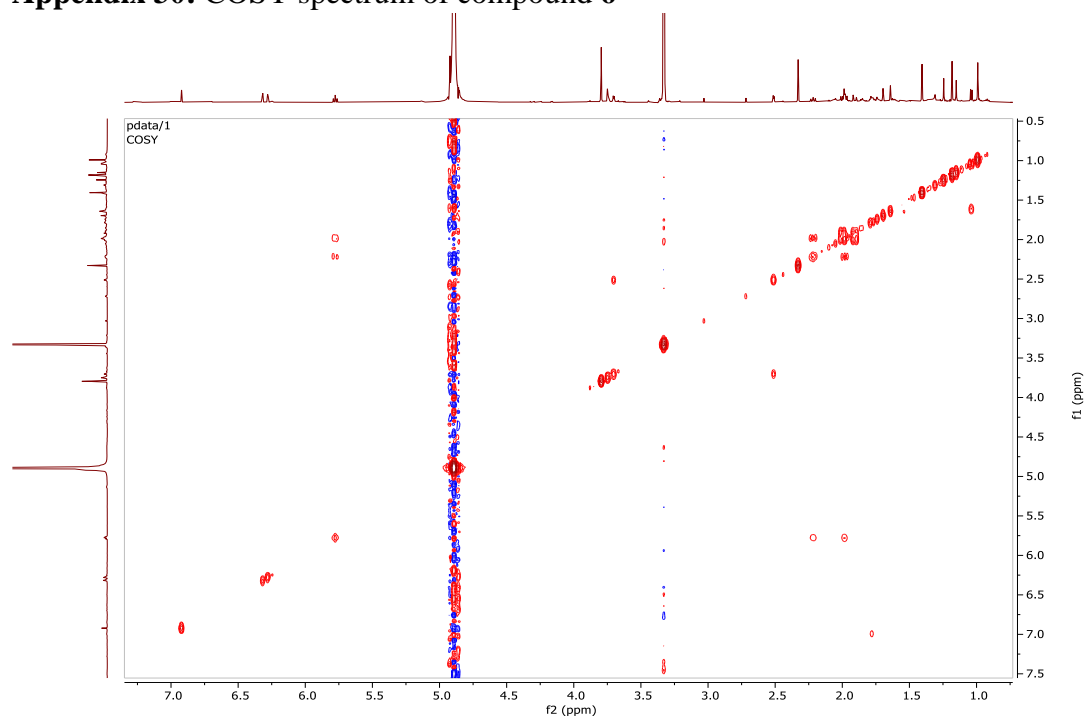
Appendix 28: HMBC spectrum of compound 6



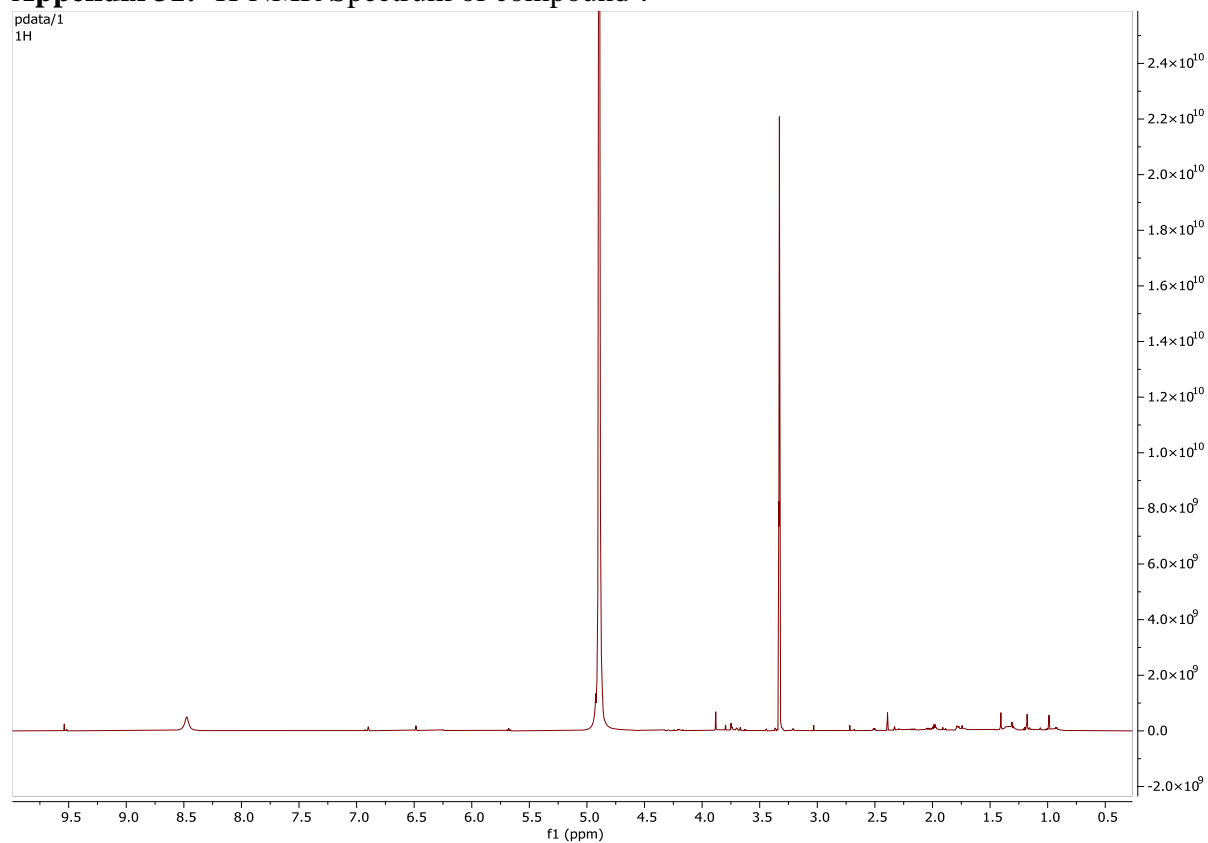
Appendix 29: HSQC spectrum of compound 6



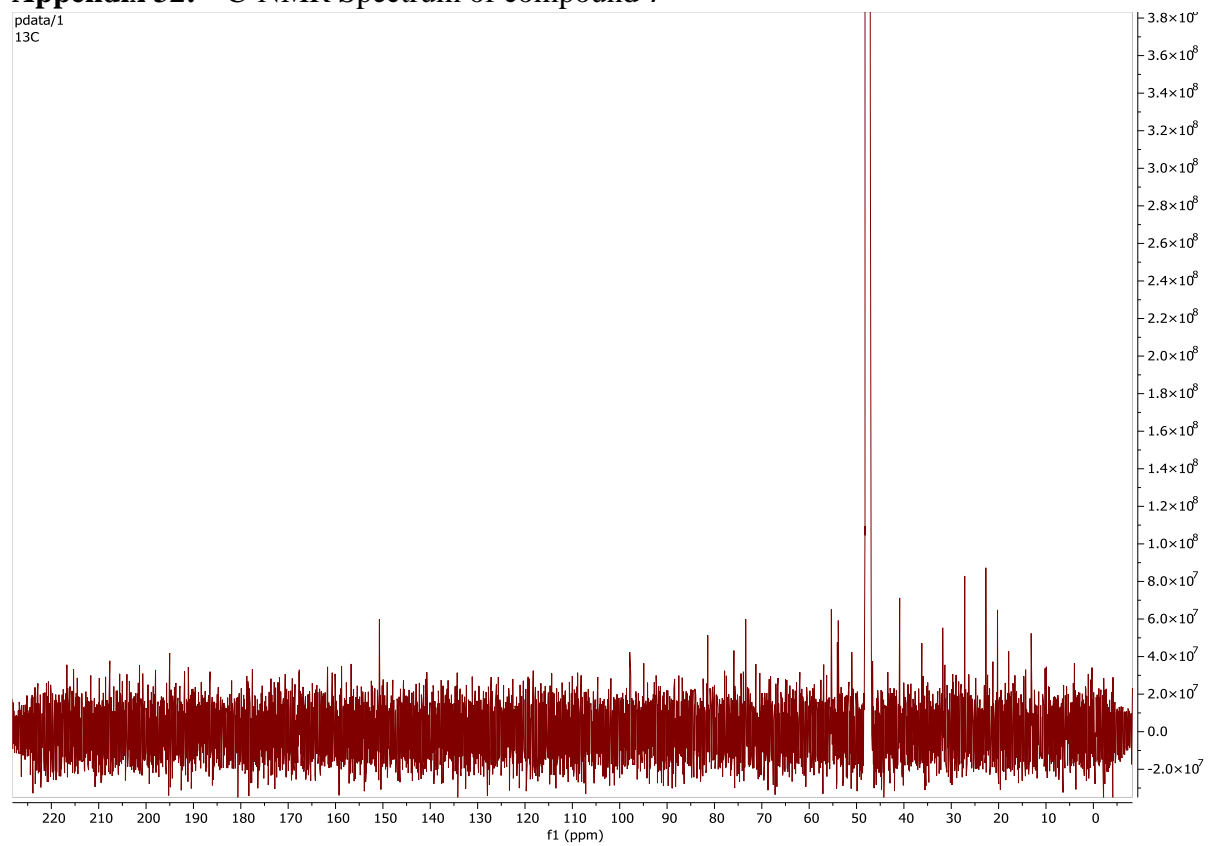
Appendix 30: COSY spectrum of compound 6



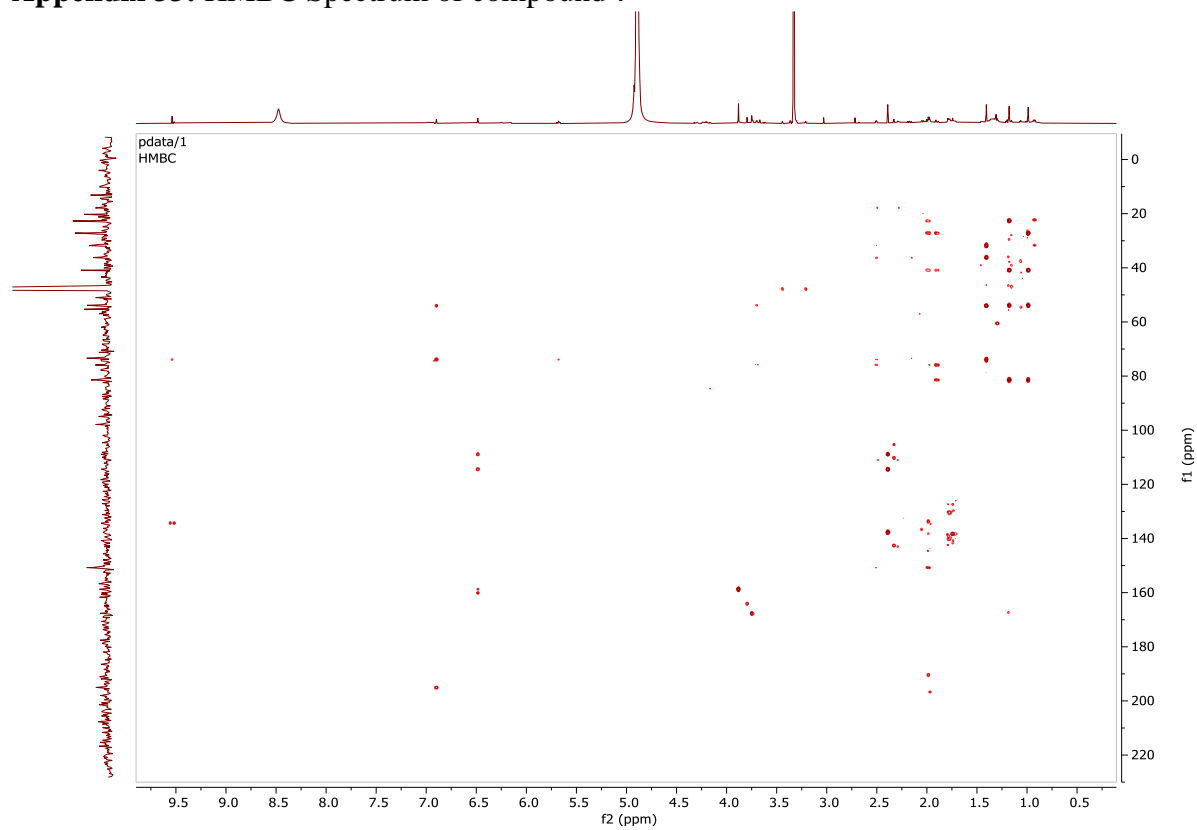
Appendix 31: ^1H -NMR Spectrum of compound 7



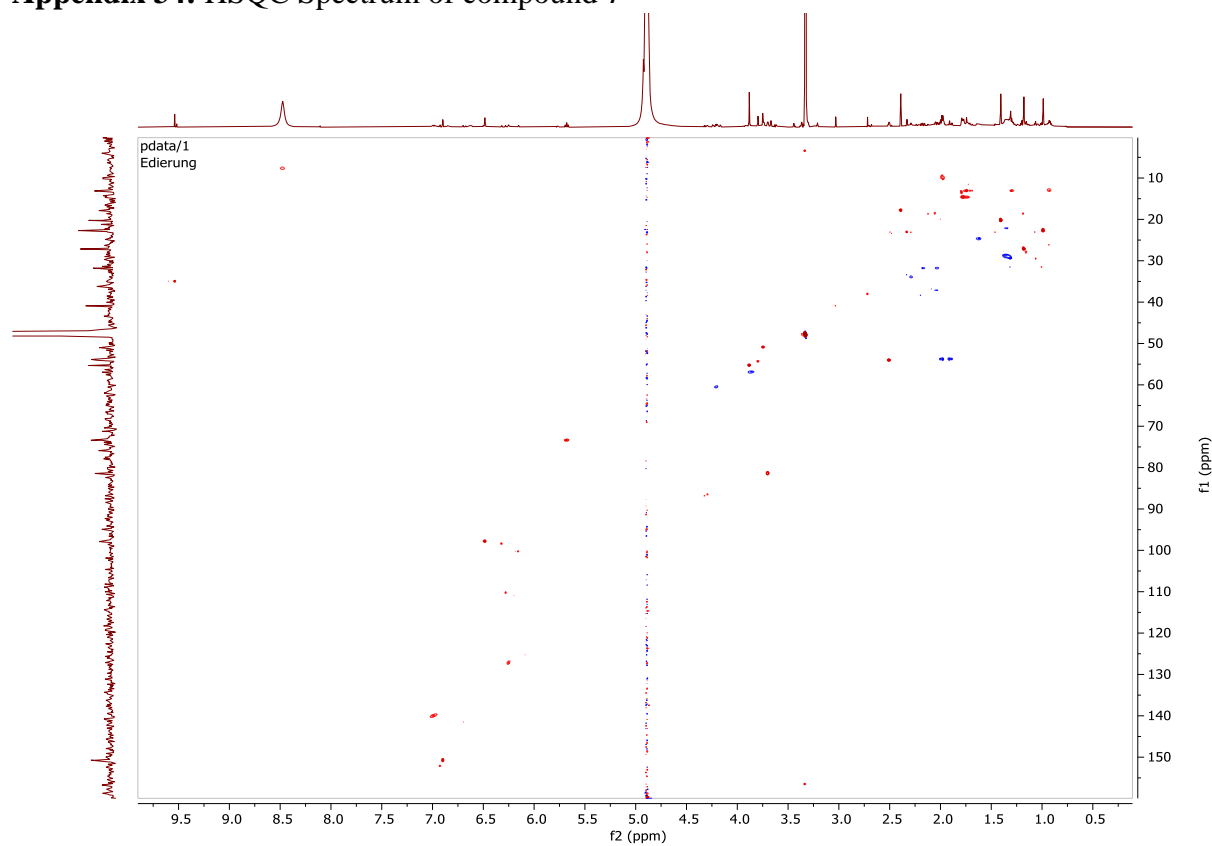
Appendix 32: ^{13}C -NMR Spectrum of compound 7



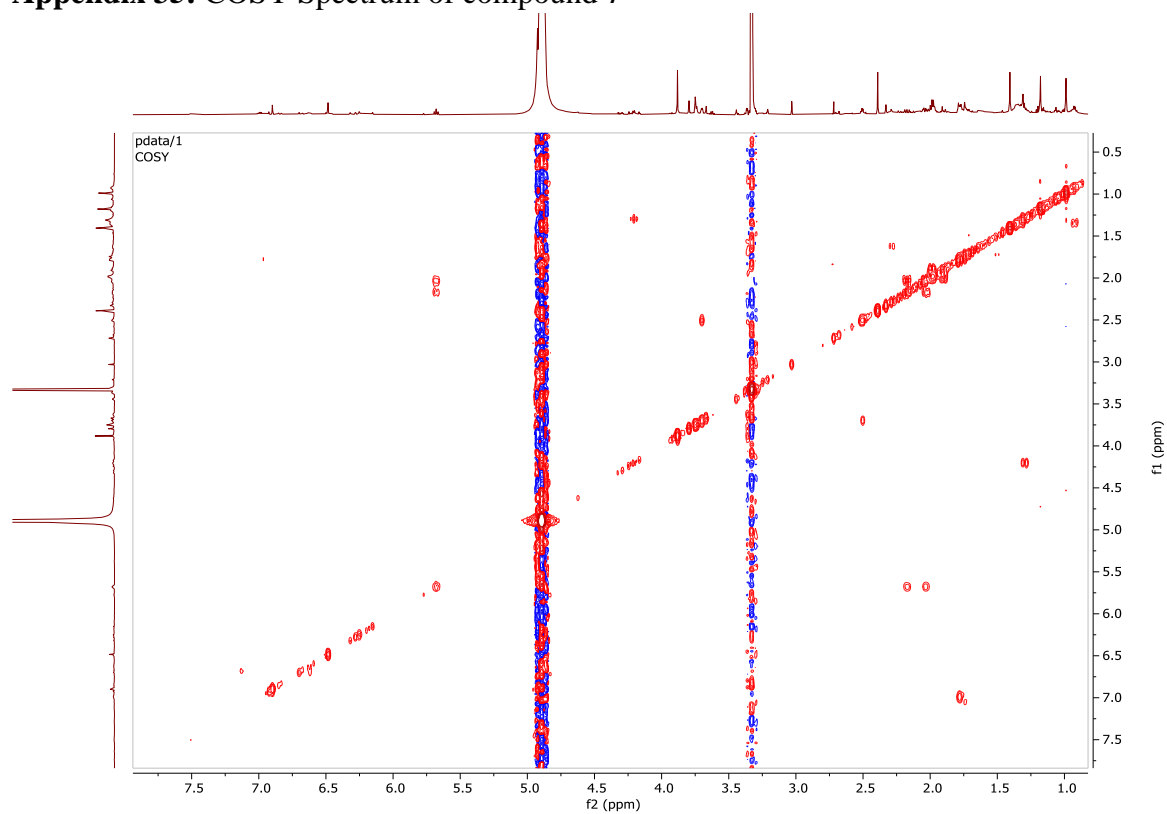
Appendix 33: HMBC Spectrum of compound 7



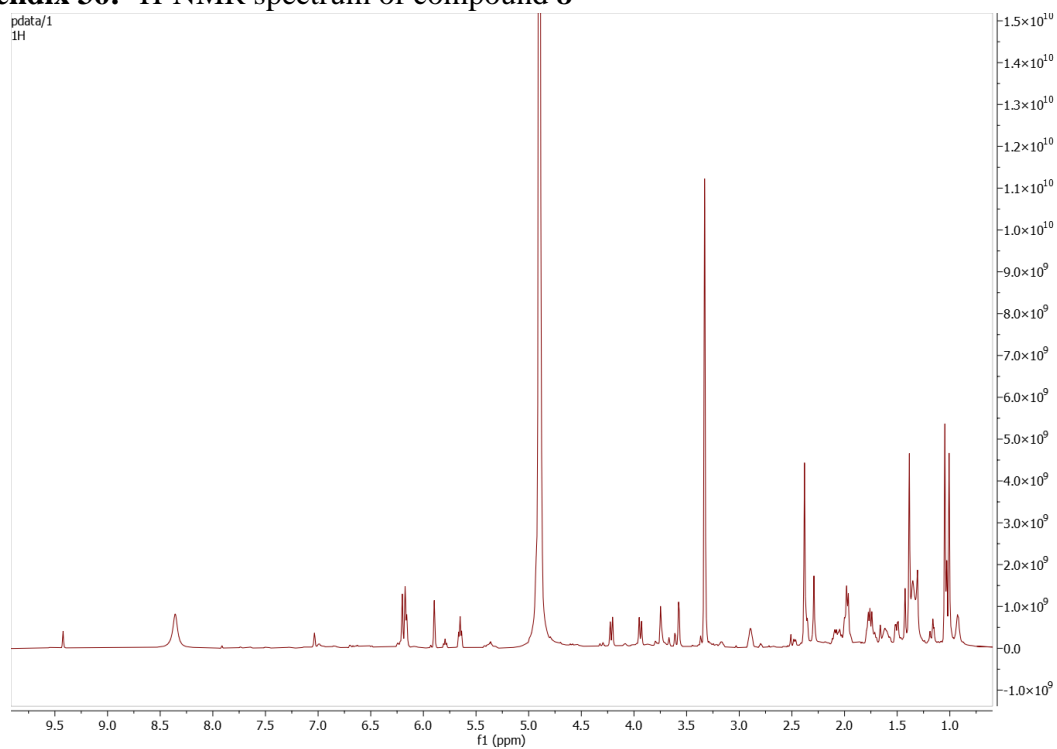
Appendix 34: HSQC Spectrum of compound 7



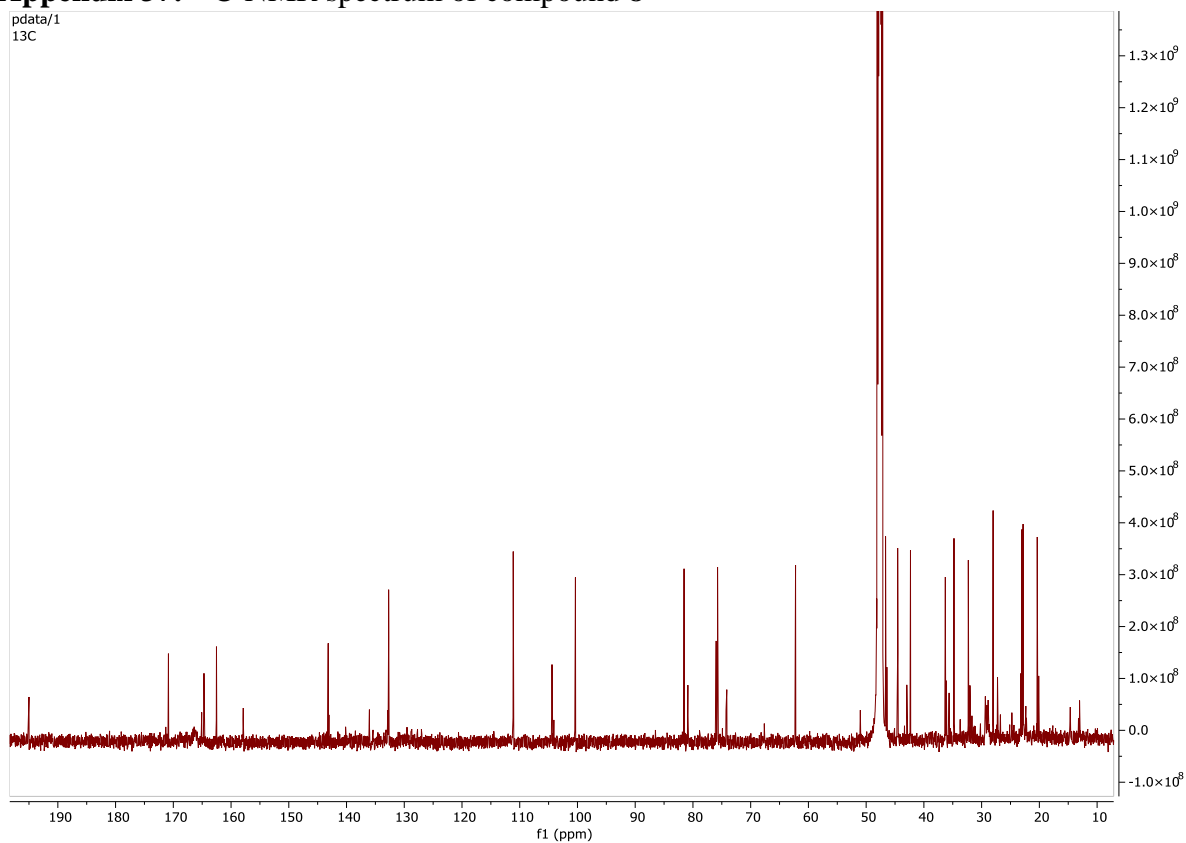
Appendix 35: COSY Spectrum of compound 7



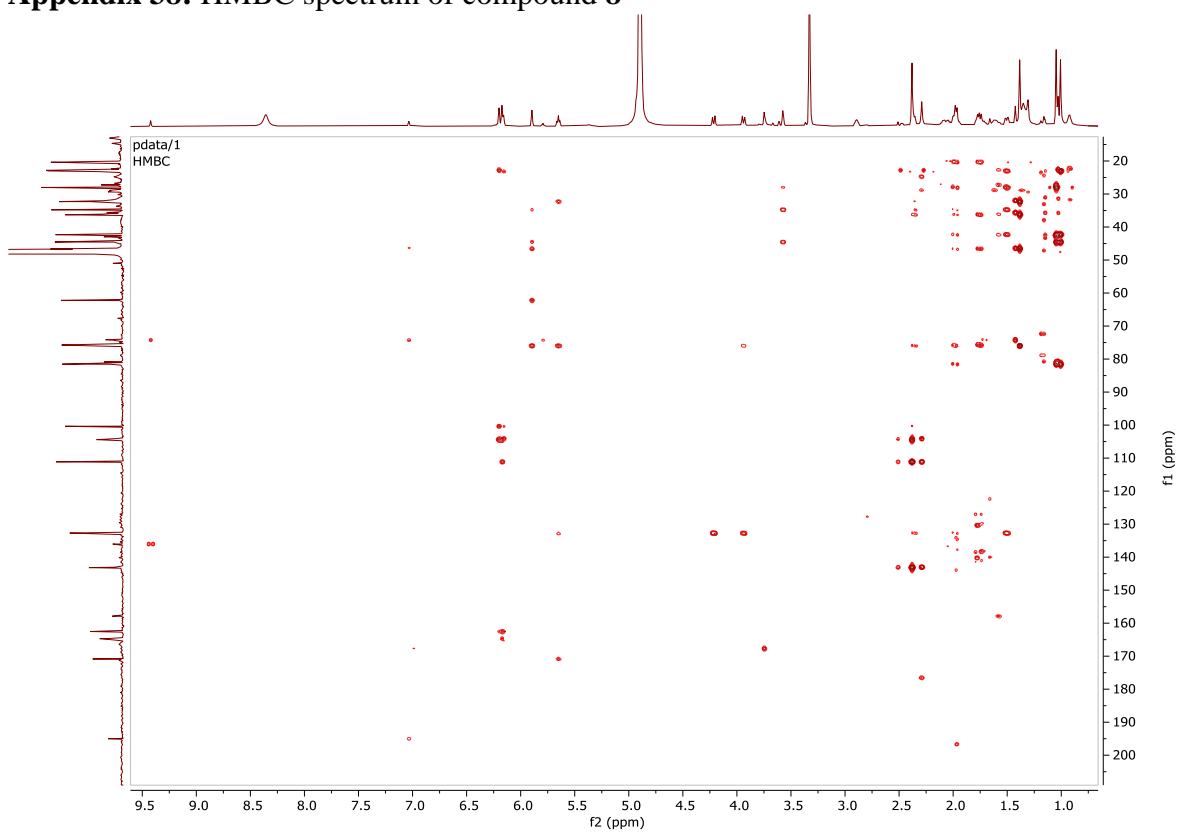
Appendix 36: ¹H-NMR spectrum of compound 8



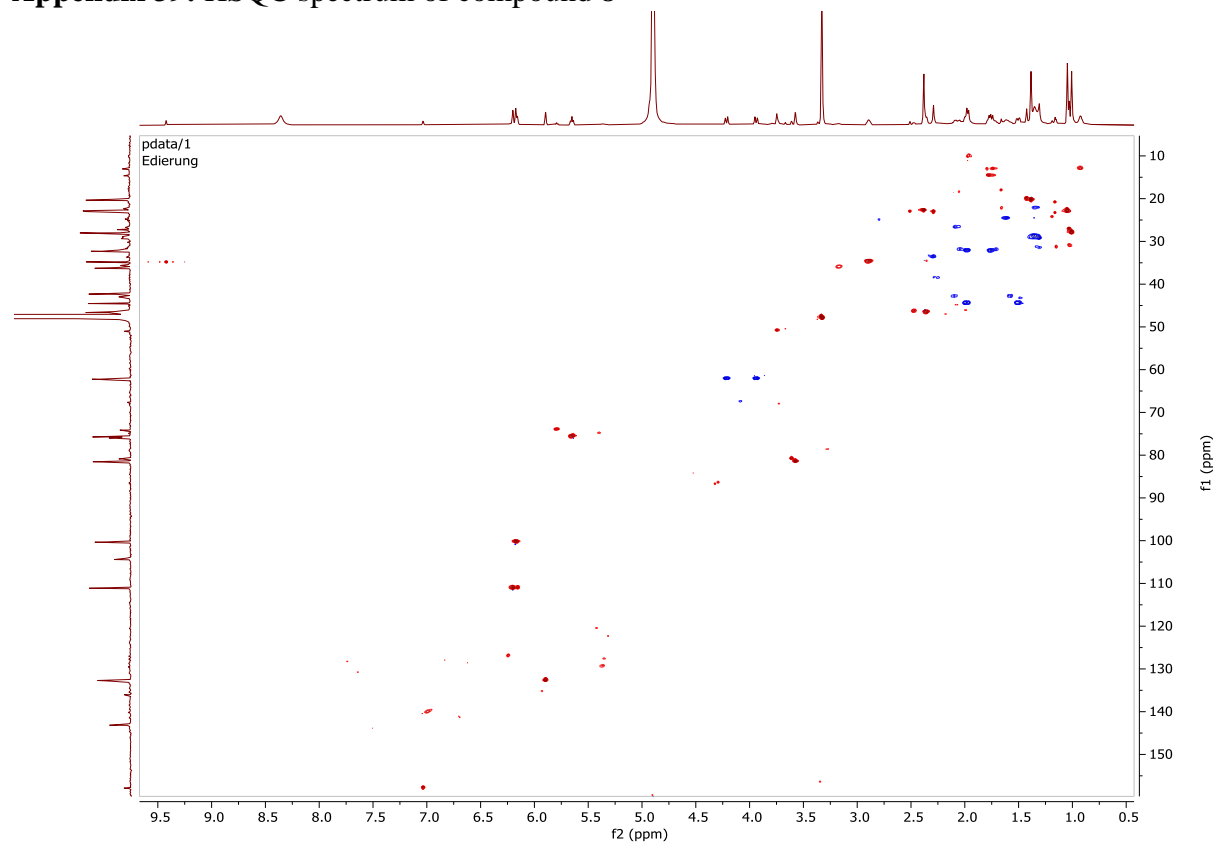
Appendix 37: ^{13}C -NMR spectrum of compound 8



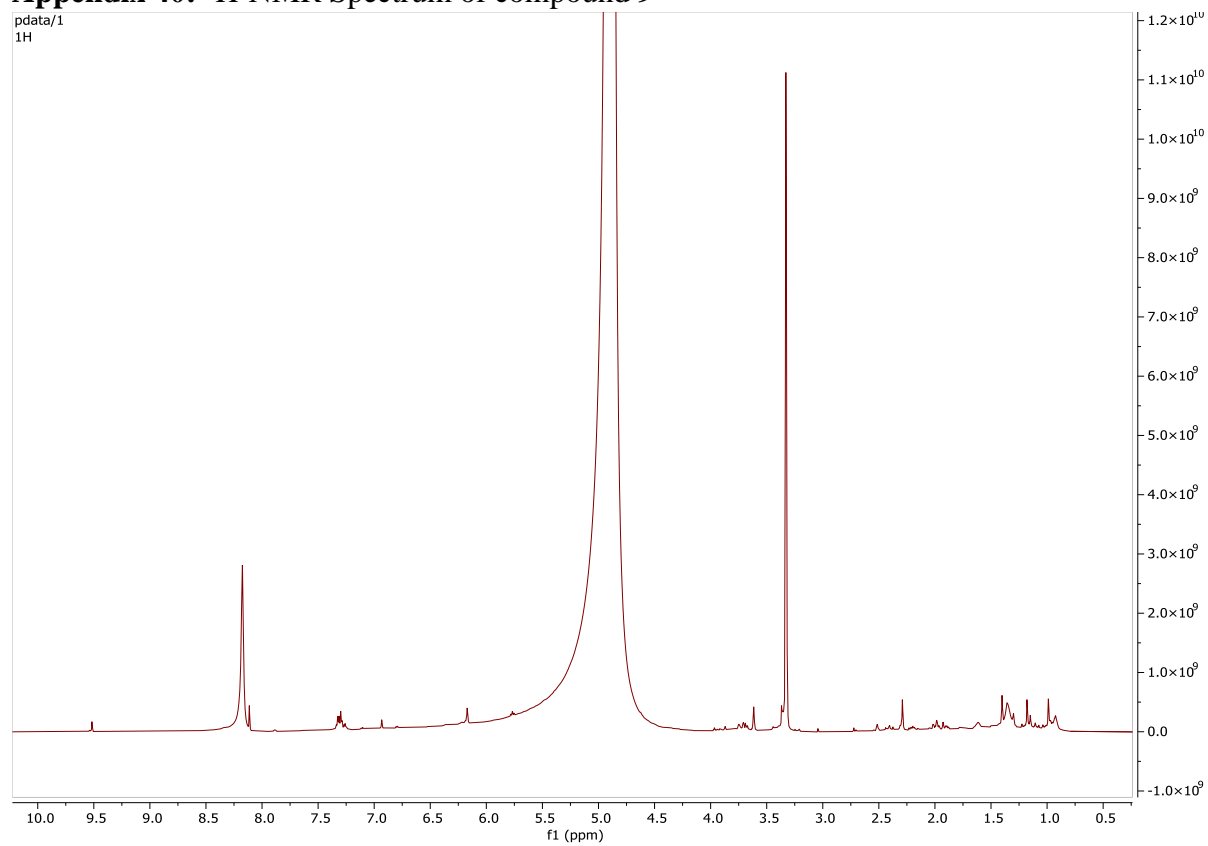
Appendix 38: HMBC spectrum of compound 8



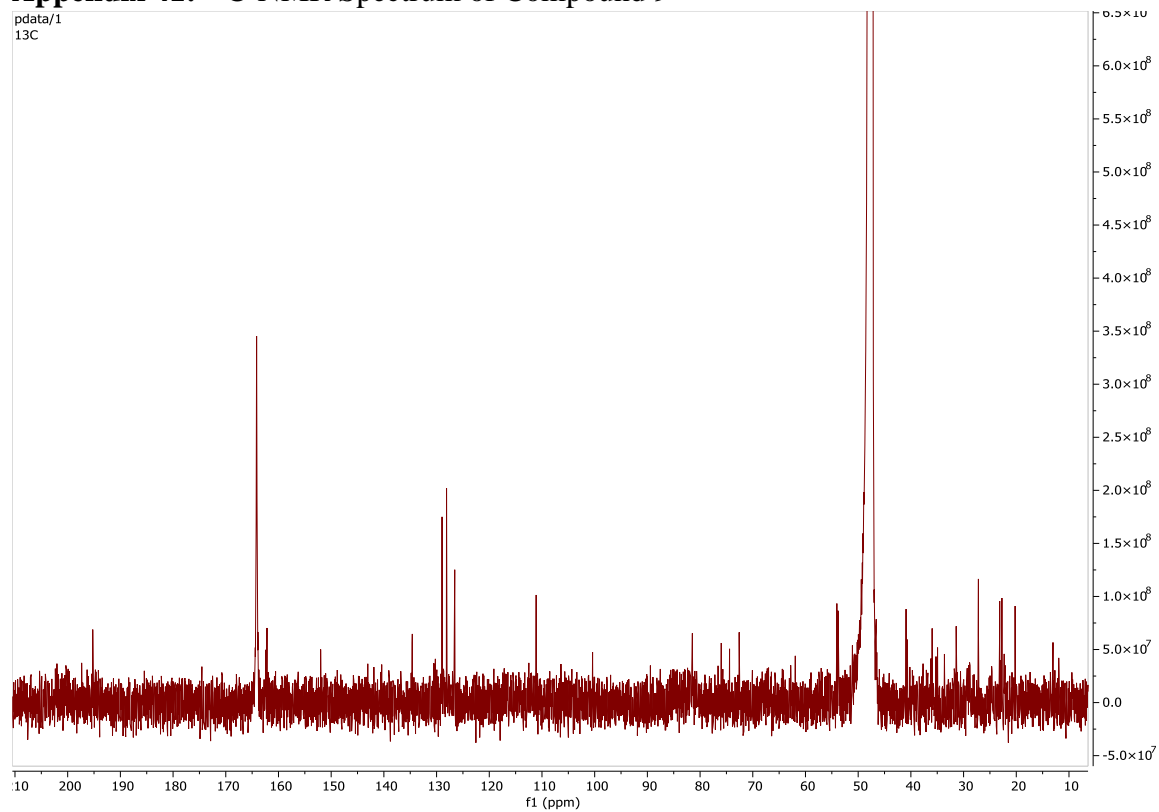
Appendix 39: HSQC spectrum of compound 8



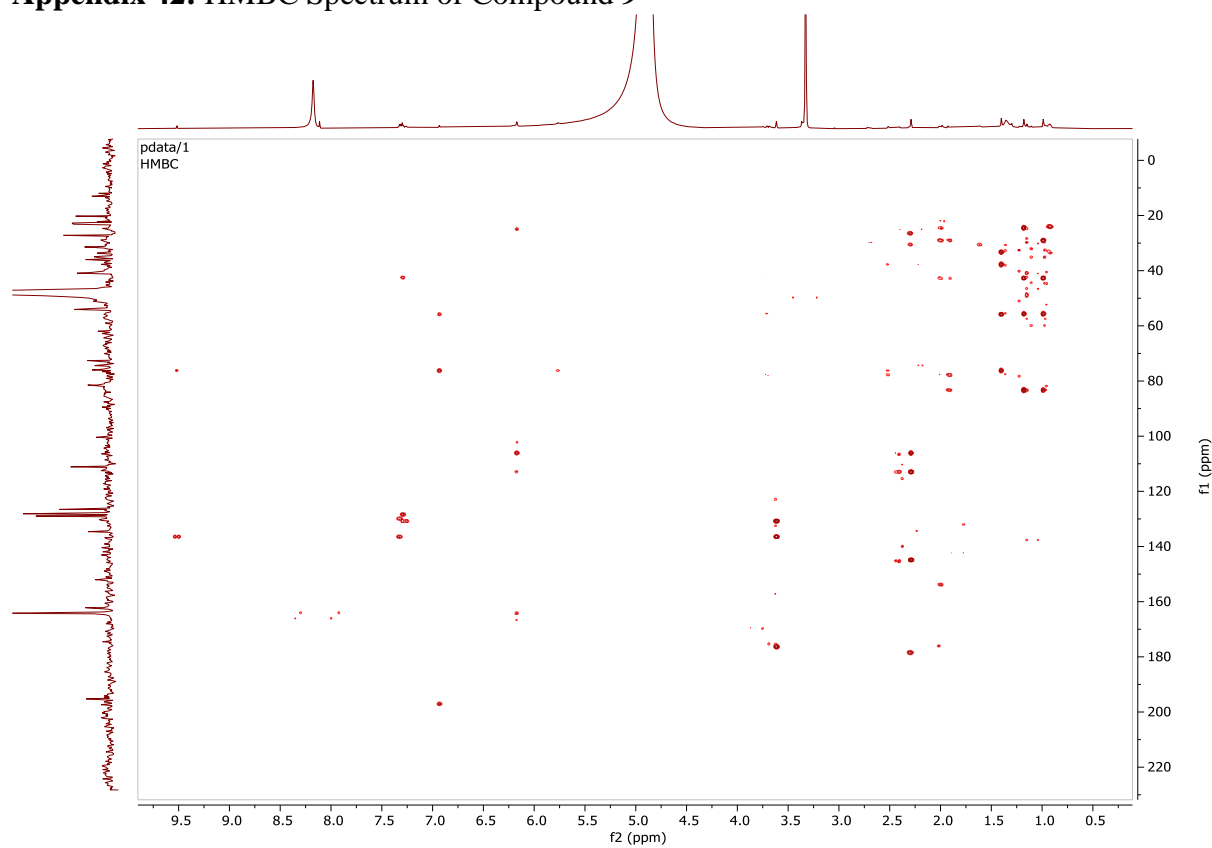
Appendix 40: ^1H -NMR Spectrum of compound 9



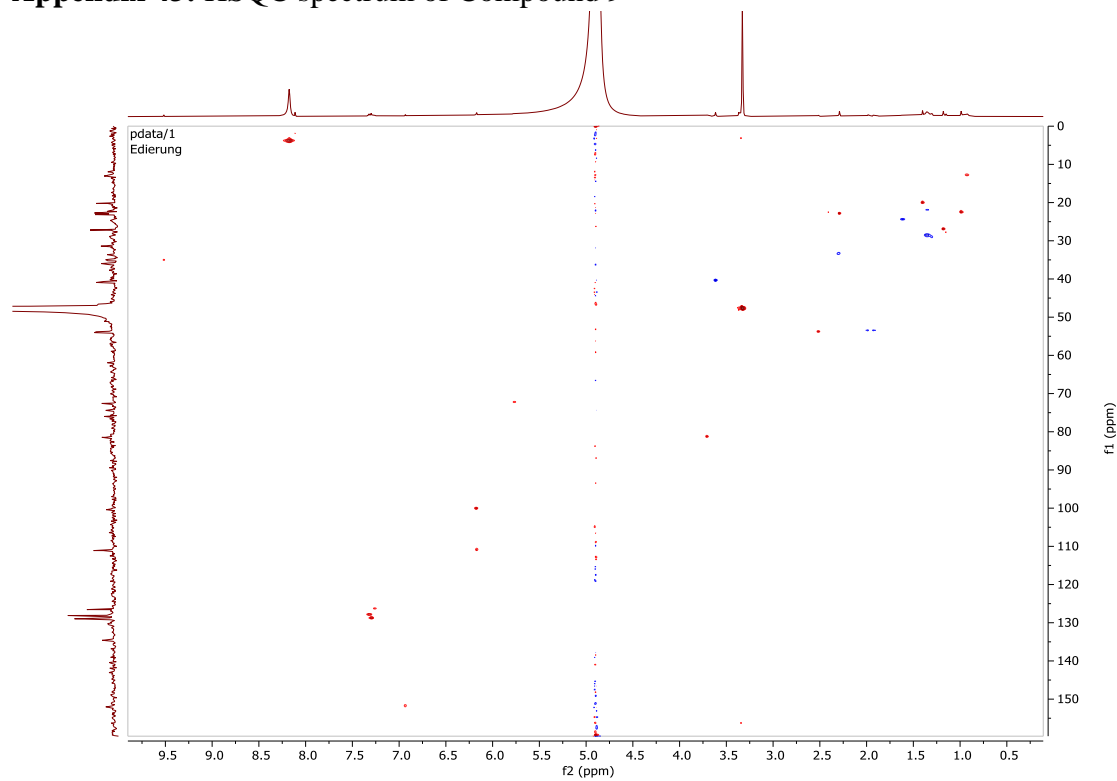
Appendix 41: ^{13}C -NMR Spectrum of Compound 9



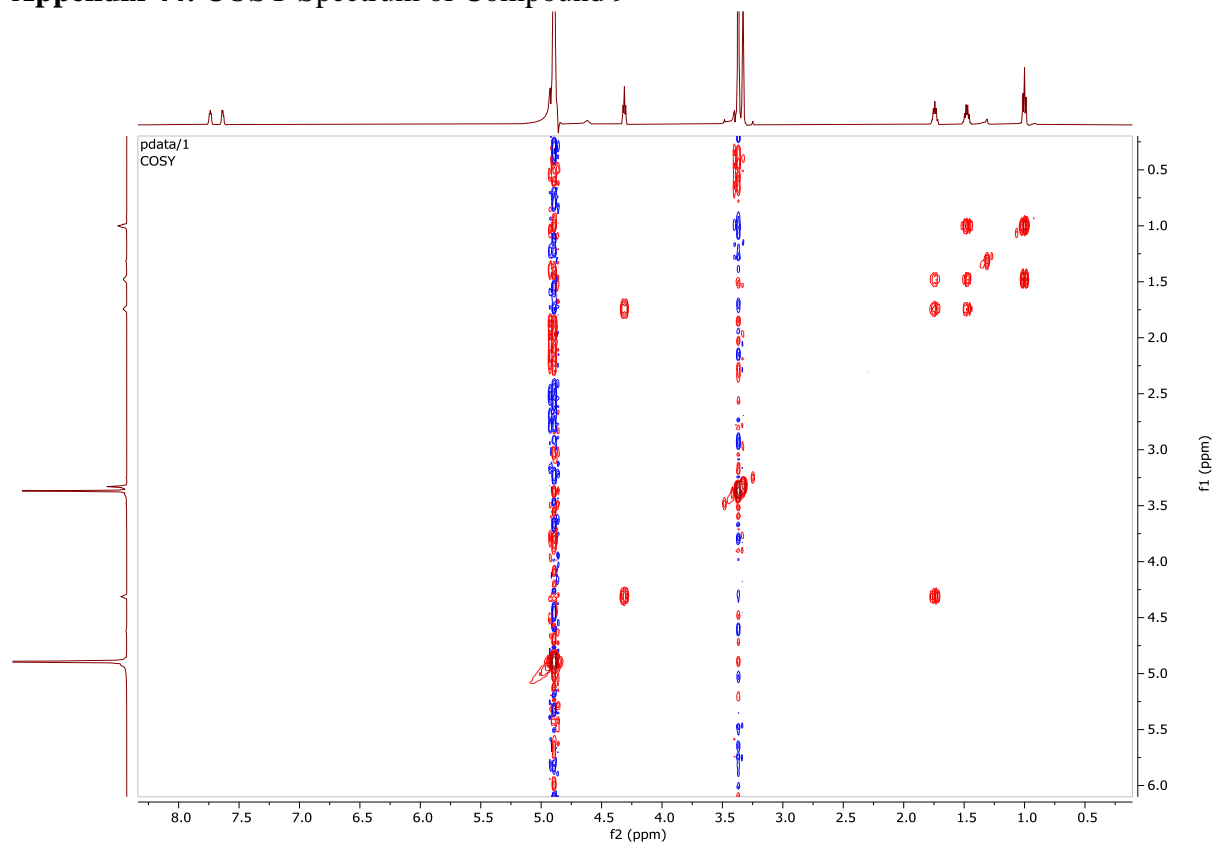
Appendix 42: HMBC Spectrum of Compound 9



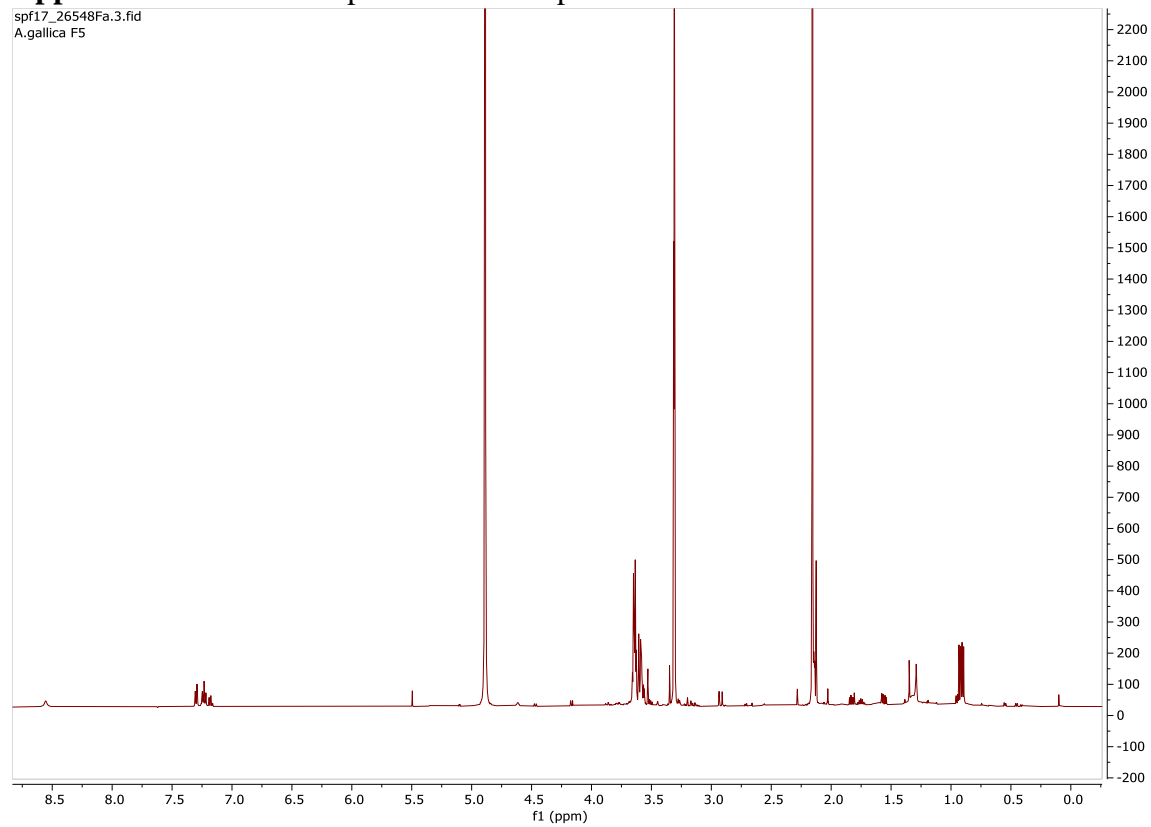
Appendix 43: HSQC spectrum of Compound 9



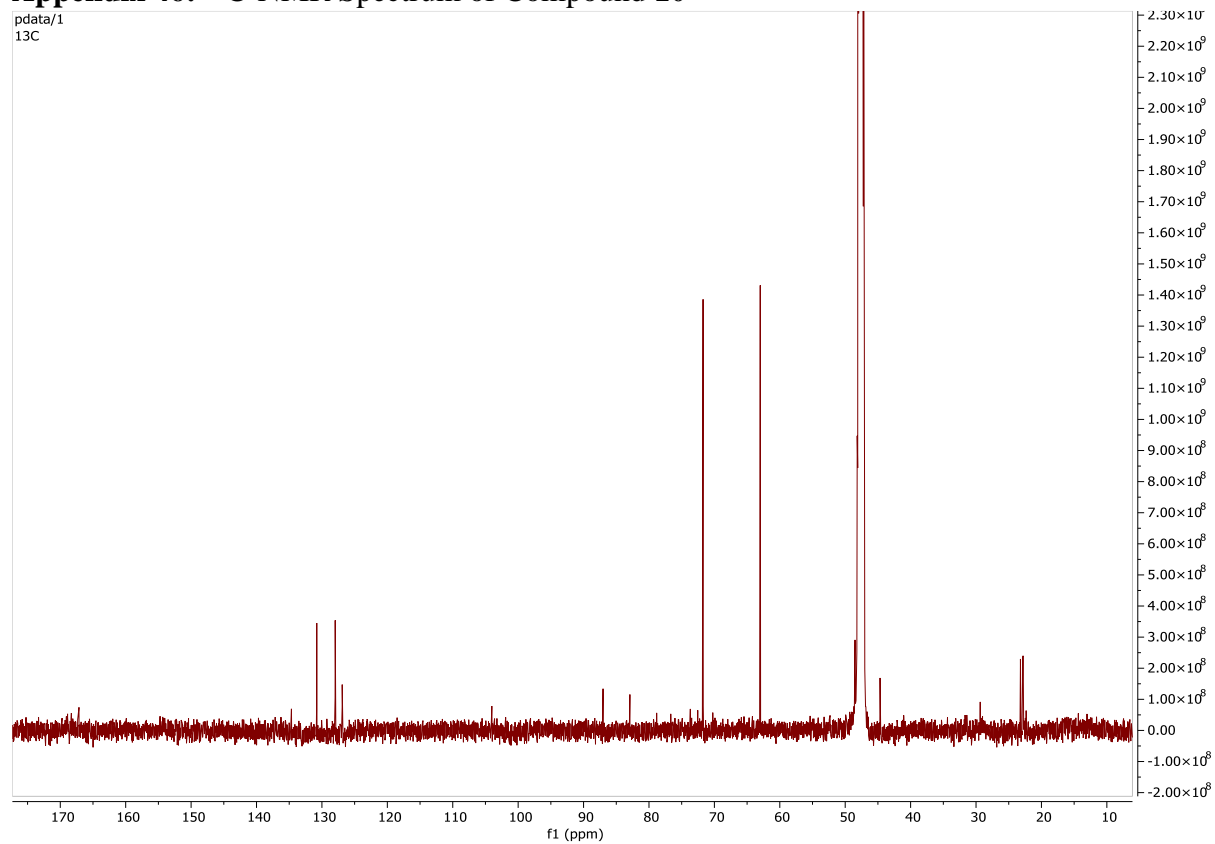
Appendix 44: COSY Spectrum of Compound 9



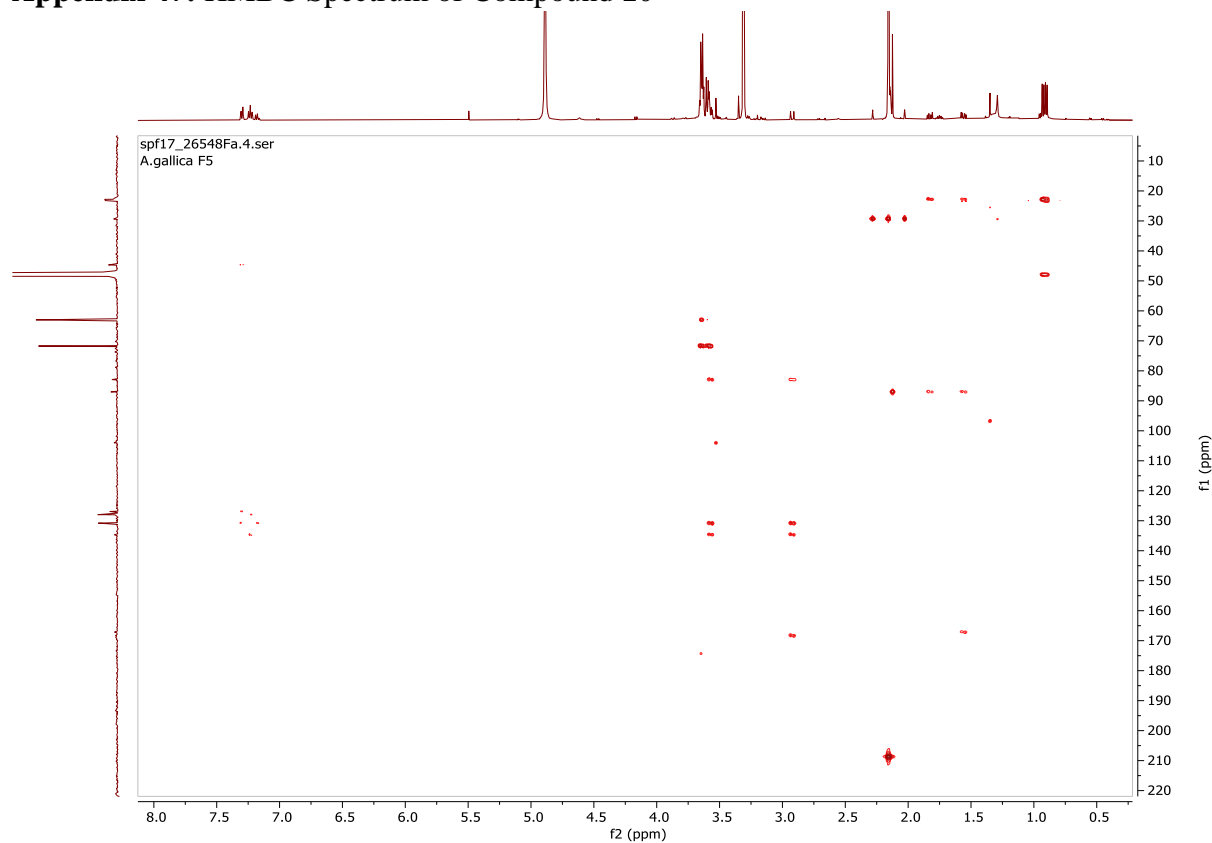
Appendix 45: ¹H-NMR Spectrum of Compound 10



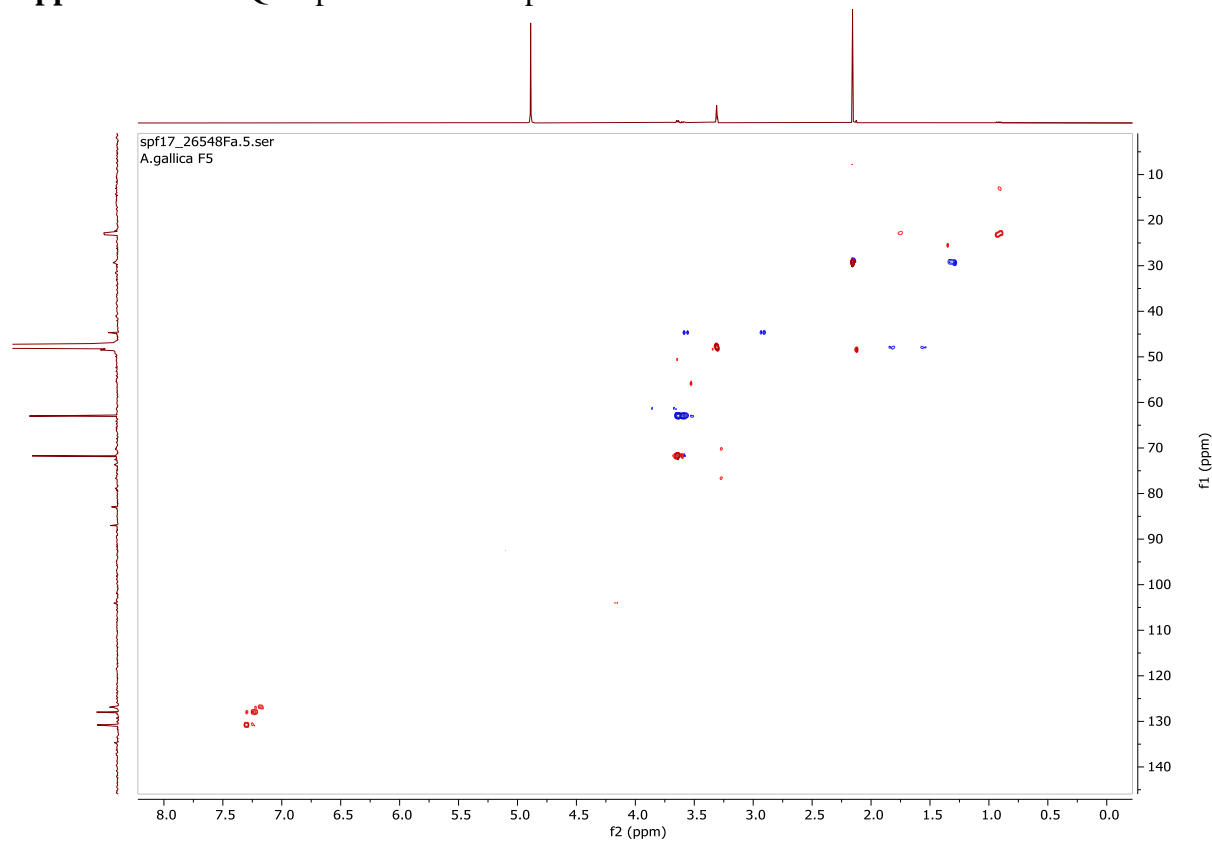
Appendix 46: ¹³C-NMR Spectrum of Compound 10



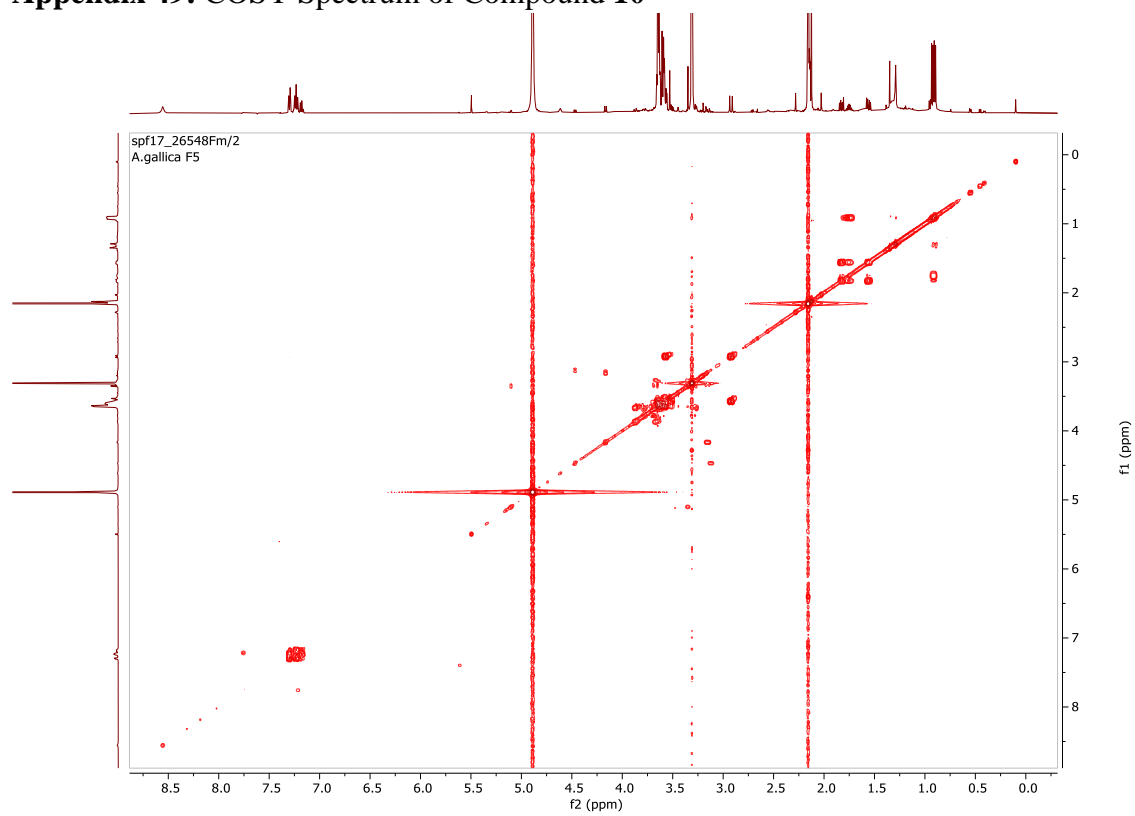
Appendix 47: HMBC Spectrum of Compound 10



Appendix 48: HSQC Spectrum of Compound 10



Appendix 49: COSY Spectrum of Compound 10



Comparison of the Secondary Metabolism of the Basidiomycetes *Armillaria mellea* and *Desarmillaria ectypa*

Jacklyne Chepkemoi,^[a] Sebastian Pfütze,^[b] Njogu M. Kimani,^[b, c] Josphat C Matasyoh,^{*,[a]} and Marc Stadler^[b]

During the course of our ongoing studies on the secondary metabolism of cultures of Basidiomycota, a new meroterpenoid named 10, 15-dihydroxydihydromelleolide (1) was isolated along with the known armillaridin (2) and anamiol (3) from cultures of the rare saprotrophic species, *Desarmillaria ectypa*. These are the first secondary metabolites that were ever isolated from the latter species. A concurrently studied strain of the common pathogenic *A. mellea* yielded other melleolides,

with 5'-O-methylmelledonal (4), melledonal C (5), 10 α -hydroxydihydromelleolide (6) and melledonal (7). The chemical structures were elucidated using 1D and 2D NMR spectroscopy and high-resolution electrospray ionization mass spectrometry (HR-ESI-MS). All compounds were studied for their antimicrobial and cytotoxic effects against a panel of microbes and mammalian cell lines, and the results are also reported.